UNCLASSIFIED

WAPD-SC-544
Reactors - Power
(TID-4500, 13th Edition)

PWR LOSS-OF-COOLANT ACCIDENT CORE MELTDOWN CALCULATIONS

L. M. Swartz
Bettis Plant

A. W. Lemmon, Jr. and L. E. Hulbert
Battelle Memorial Institute

May 1957

Contract AT-11-1-GEN-14

Information Category
Unclassified

J. E. Nolan May 2, 1957
Authorized Classifier Date

$2.25

Printed in USA. Price ~~50 cents.~~ Available from the Office of Technical Services, Department of Commerce, Washington 25, D.C.

BETTIS PLANT PITTSBURGH, PA.
Operated for the U. S. Atomic Energy Commission by
Westinghouse Electric Corporation

UNCLASSIFIED

FOREWORD

This document has been submitted to the Advisory Committee on Reactor Safeguards to the Atomic Energy Commission for use in evaluating the safety of the PWR Reactor Plant (Shippingport Atomic Power Station). As such, this information is supplemental to the PWR Hazards Summary Report, WAPD-SC-541.

LEGAL NOTICE

Distribution	No. of Copies
Aberdeen Proving Ground	3
Alco Products, Inc.	1
Argonne National Laboratory	10
Armed Forces Special Weapon Project, Washington	1
Armed Services Technical Information Agency, Dayton	5
Atlantic Fleet	1
Atomic Energy Commission, Patent Branch	1
Atomic Energy Commission, Technical Library	3
Atomics International	2
Battelle Memorial Institute	2
Bettis Plant	4
Brookhaven National Laboratory	4
Brush Beryllium Company	1
Bureau of Medicine and Surgery	1
Bureau of Ships (Code 590)	1
Chicago Patent Group	1
Combustion Engineering, Inc.	1
Consolidated Vultee Aircraft Corporation	2
Convair-General Dynamics	1
Defence Research Member	1
Department of Food Technology (MIT)	1
Department of Navy (Code 422)	2
Department of the Army, G-2	2
Division of Raw Materials, Denver	1
Dow Chemical Company (Rocky Flats)	1
Du Pont de Nemours and Company, Aiken	4
Du Pont de Nemours and Company, Wilmington	1
Frankford Arsenal	1
General Electric Company (ANPP)	2
General Electric Company, Richland	12
General Nuclear Engineering Corporation	1
Iowa State College	2
Kirtland Air Force Base	1
Knolls Atomic Power Laboratory	4
Lockheed Aircraft Corporation (Bauer)	2
Los Alamos Scientific Laboratory	4
Mallinckrodt Chemical Works	1
Massachusetts Institute of Technology (Dr. Hardy)	1
Mound Laboratory	1
National Advisory Committee for Aeronautics, Cleveland	1
National Bureau of Standards, Atomic Energy Project	1
National Bureau of Standards, (Library)	1
National Lead Company, Inc., Winchester	1
Naval Research Laboratory	3
New York Operations Office	2
New York University (Dr. Richtmyer)	1
Nuclear Development Corporation of America	1
Nuclear Metals, Inc.	1
Oak Ridge Institute of Nuclear Studies	1
Oak Ridge National Laboratory	4
Office of Naval Research	10

Distribution	No. of Copies
Phillips Petroleum Company	6
Public Health Service	2
RAND Corporation	1
Sandia Corporation	1
Signal Corps Center	1
Sylvania Electric Products, Inc.	1
Technical Operations, Incorporated	2
Union Carbide Nuclear Company (K-25 Plant)	2
United Aircraft Corporation	3
U. S. Geological Survey, Denver	1
U. S. Naval Ordnance Laboratory	2
U. S. Naval Postgraduate School	1
U. S. Naval Radiological Defense Laboratory	1
U. S. Patent Office	1
University of California Radiation Laboratory, Berkeley	2
University of California Radiation Laboratory, Livermore	2
University of Rochester, Atomic Energy Project	1
University of Rochester (Dr. Marshak)	2
Vitro Engineering Division	1
Walter Reed Army Medical Center	1
Watertown Arsenal	1
Weil, Dr. George L.	1
Westinghouse Electric Corporation	2
Technical Information Service Extension, Oak Ridge	300
Office of Technical Services, Washington	100
Manager, Pittsburgh Area Office	29
WAPD Distribution XIV	70

TABLE OF CONTENTS

LIST OF ILLUSTRATIONS

PWR LOSS OF COOLANT ACCIDENT - CORE MELTDOWN CALCULATIONS

L. M. Swartz
Bettis Plant
and
A. W. Lemmon, Jr. and L. E. Hulbert
Battelle Memorial Institute

I. ABSTRACT

This report presents the results of a study made of the possible extent of zirconium-water reaction and core meltdown following a postulated loss-of-coolant accident in the PWR plant. Zirconium-water chemical reaction and core meltdown occur in the course of the core temperature excursion which could follow a loss-of-coolant if no cooling were provided after an uncovering of the core. An analysis of the temperature excursion involves consideration of the complex relationships between core geometry, decay heating rates, water (or steam) flow through the core, and the thermodynamic and chemical properties of water, steam, and the core materials.

Parametric studies of the temperature excursion are used in evaluating the effectiveness of the PWR Safety Injection System in prevention of core chemical reaction and meltdown. Combinations of delay time in operation and rate of injection are considered.

Assuming a severe casualty has occurred, and assuming that the plant has been operating at 75 Mw net electrical output for 600 hours and that safety injection water is being supplied to the core at the maximum rate of 3000 gpm, it is concluded that no meltdown will occur except for a small amount in blanket region 1, and chemical reaction will be limited to a small amount in blanket regions 1 and 4. Delay times up to 90 seconds in operation of the Safety Injection System will not, in general, jeopardize the effectiveness of cooling of the core, but will allow a small increase in the extent of meltdown in blanket region 1, and reaction in regions 1 and 4.

For other cases studied, where less than 10% of the maximum 3000 gpm is assumed to be injected, only about 16.5 weight per cent of the Zircaloy in the core heat transfer surfaces would react.

II. SCOPE OF THIS REPORT

This report covers the calculation of the PWR core temperature excursion which would follow an uncovering of the core because of the loss of primary coolant water. If a large primary system rupture occurred in the right location a loss of primary coolant water could result.

In order to accurately define the safeguards problems associated with a loss-of-coolant accident, Bettis Plant engaged Battelle Memorial Institute to perform the necessary experimental work and detailed calculations. The results

of the calculational work were reported in a detailed report[1] which is reproduced here with the addition of introductory material and editorial changes to make this a self-contained PWR Safeguards document.

Based on the results of these calculations, conclusions are drawn as to the effectiveness of the PWR Safety Injection System in averting a core meltdown following a loss of coolant.

III. STATEMENT OF THE PROBLEM

In the event of a primary system rupture, primary coolant water is lost from the reactor to the plant container. If the rupture is large in area, and/or is located below the reactor core, essentially all of the coolant is lost from the reactor vessel, and no cooling (to remove decay heat) is available to the core unless emergency measures are taken to supply water to re-cover the core, or at least to flow through the core.

To evaluate the effectiveness of the Safety Injection System, which is designed to supply water to the core in this emergency, it was necessary to make an adequate estimate of the progress of the core temperature excursion following the loss of coolant and the thermodynamic behavior of the hot channel fuel elements of the PWR seed and blanket regions. If no cooling is available to the fuel elements, the decay heating, which continues long after the reactor is shut down, can cause the hottest portions of the PWR plate-type seed elements to reach the melting temperature of 3350°F within 5 minutes, and the hottest portions of the PWR blanket rods to reach the melting temperature within 20 minutes. These calculations have neglected the possible burnout at local hot spots, occuring due to statistical variations in fuel element dimensions, fuel loading, etc. The integrated melting of hot spots would be negligible compared to the bulk melting as may occur later. (The fission product release due to hot spot melting is expected to be of the same order of magnitude as the maximum expected activity which could be in the coolant during normal operation with defected cladding of UO_2 fuel elements.)

The rapidity of the temperature rise may be accelerated if water, or steam, is supplied to the fuel elements at certain rates, after the Zircaloy fuel elements have reached an elevated temperature of about 2000°F. An exothermic chemical reaction[2] between zirconium and water or steam could then occur causing an accelerated temperature rise in the fuel plates.

IV. REACTOR DESCRIPTION[3]

The PWR is a pressurized water nuclear reactor in which primary coolant water at 523°F and 2000 psi is circulated through the active core to remove the heat generated. The heat is transferred from the primary coolant in heat exchangers, or boilers, to generated steam which flows to a turbo-generator in a secondary loop. Figure 1 shows the PWR reactor and main coolant system.

1. Lemmon, A. W., Jr., Hulbert, L. E., and Filbert, R. B., Jr., "Analysis of the Efficacy of Cooling and the Extent of Reaction in the PWR", Battelle Memorial Institute, Columbus, Ohio (February 15, 1957).
2. For additional information on the zirconium-water reaction, the reader is referred to WAPD-SC-543, "Zirconium-Water Reaction Data and Application to PWR Loss-of-Coolant Accident", B. Lustman (May 1957).
3. For a more detailed description see WAPD-PWR-970 "Description of the Shippingport Atomic Power Station".

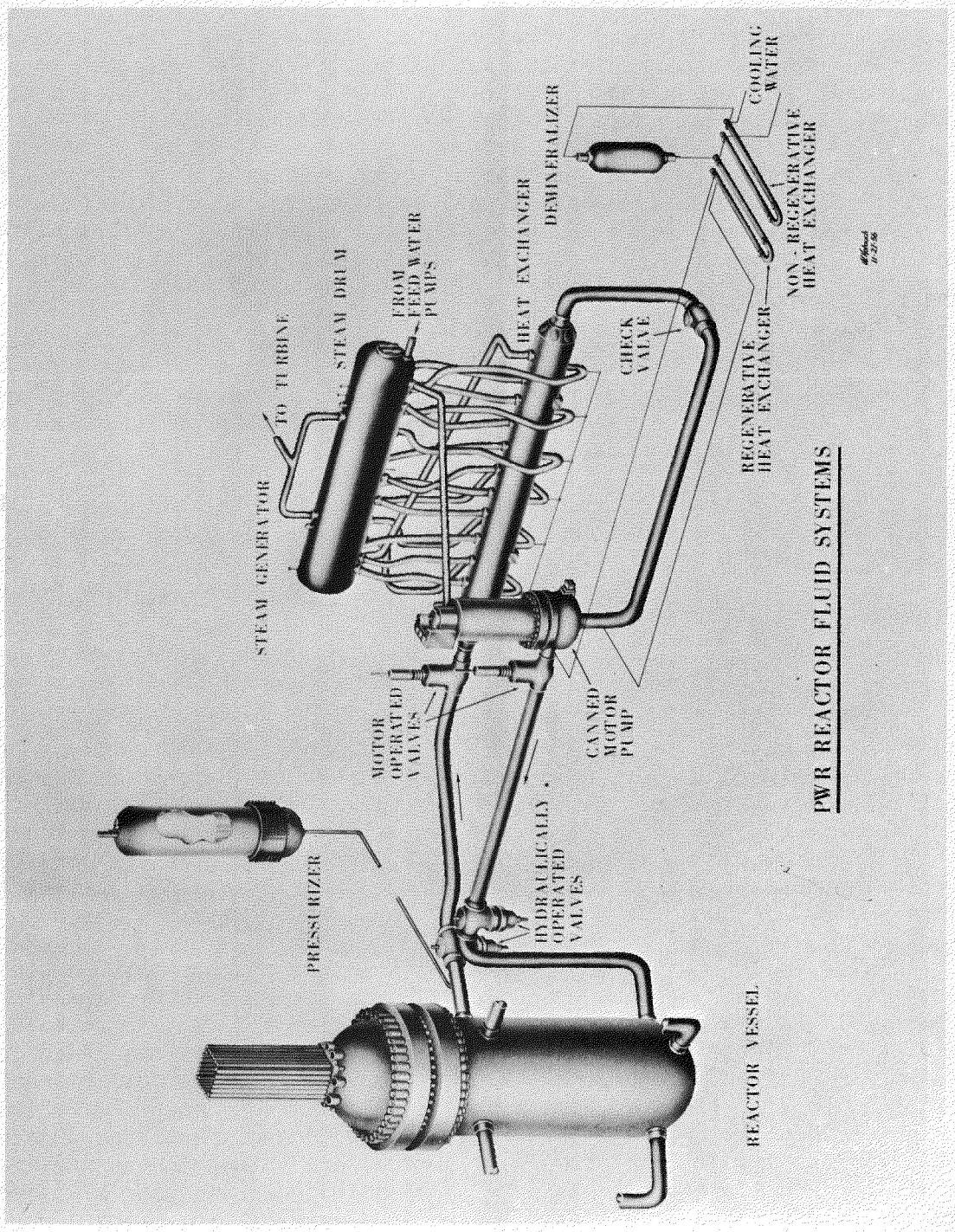

FIGURE 1
PWR REACTOR FLUID SYSTEMS

During rated operation of the plant at 60 Mw net electrical output on 3 of the 4 primary loops, the core is producing a total of 790 x 10^6 Btu/hr. On 4 loop operation the rated output is about 25% higher. Plant pressure, temperatures, and heat transfer characteristics have been selected to avoid hot channel local boiling in the core during steady state operation, and to avoid hot channel bulk boiling during operating transients.

The core is a seed and blanket type, roughly a 6' x 6' right circular cylinder. There are 32 seed assemblies, each consisting of four subassemblies. Each subassembly (see Figure 2) contains 15 fuel plates. The fuel plates contain an active fuel zone of highly enriched uranium alloyed with zirconium. The fuel is completely enclosed in a Zircaloy clad.

There are 113 blanket assemblies each containing 7 rod bundles placed end-to-end. Each bundle (see Figure 3) contains 120 rods arranged in an 11 x 11 square arrangement with one corner rod removed to allow space for an instrumentation tube. Each fuel rod (see Figure 4) contains 26 UO_2 pellets clad in an 0.030 in. thick Zircaloy tube.

Out of a total of 15.68 tons of zirconium in the PWR core, 1.11 tons are used in the seed plate cladding, with an additional 3.4 tons in the side plates and extension brackets of the seed assemblies. The blanket rod cladding and end caps contain 4.87 tons of zirconium, and the blanket shells contain 6.3 tons of zirconium.

V. SAFETY INJECTION SYSTEM DESCRIPTION

The Safety Injection System which is provided for the loss-of-coolant accident makes use of the boiler feed pumps of the secondary system to supply water to the primary loops between the stop valves on the reactor vessel outlet piping. An arrangement of valves and electrical interlocks will switch the boiler feed pumps from normal operation to Safety Injection System operation when the operator pushes a Safety Injection System button on the control panel. The operation of the system is delayed by the interlocks until the reactor coolant system pressure has dropped to 500 psi.

The Safety Injection water flows into the reactor through the outlet (upper) pipes and through the holes provided in the hold-down barrel to the core. The core hold-down barrel has two rows each drilled radially, 2 holes directed toward each of the 32 seed control-rod shrouds. Jets of safety injection water would splash against the shrouds, flowing downward into the fuel elements. In addition to cooling the seed region, it is expected (and assumed for the calculations herein) that the splashing would adequately cool the adjacent blanket regions 2 and 3 (see Figure 5), which would otherwise be the first to melt after the seed region. Although some additional splashing might be expected, resultant cooling of the low-power slower-heating blanket regions 1 and 4 has not been estimated (and no cooling assumed for the calculations herein).

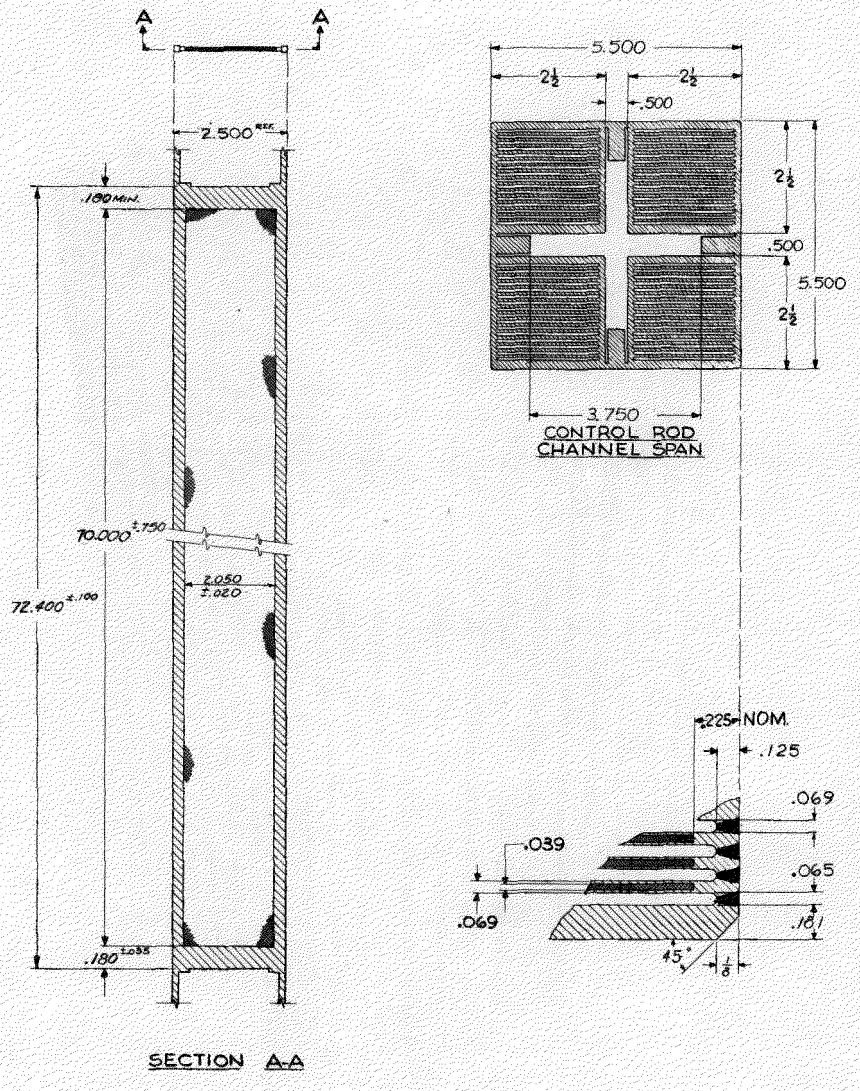

FIGURE 2
DETAILS OF SEED CLUSTER AND FUEL PLATE

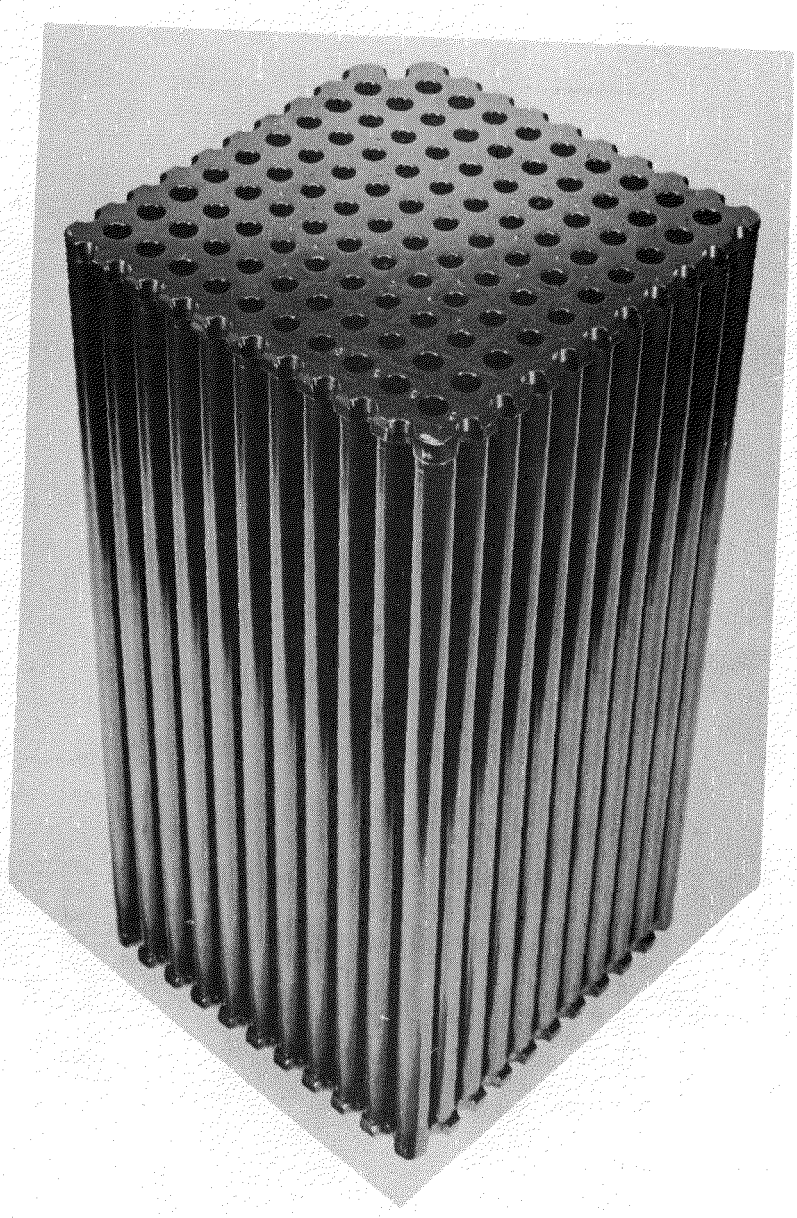

FIGURE 3
BLANKET FUEL BUNDLE

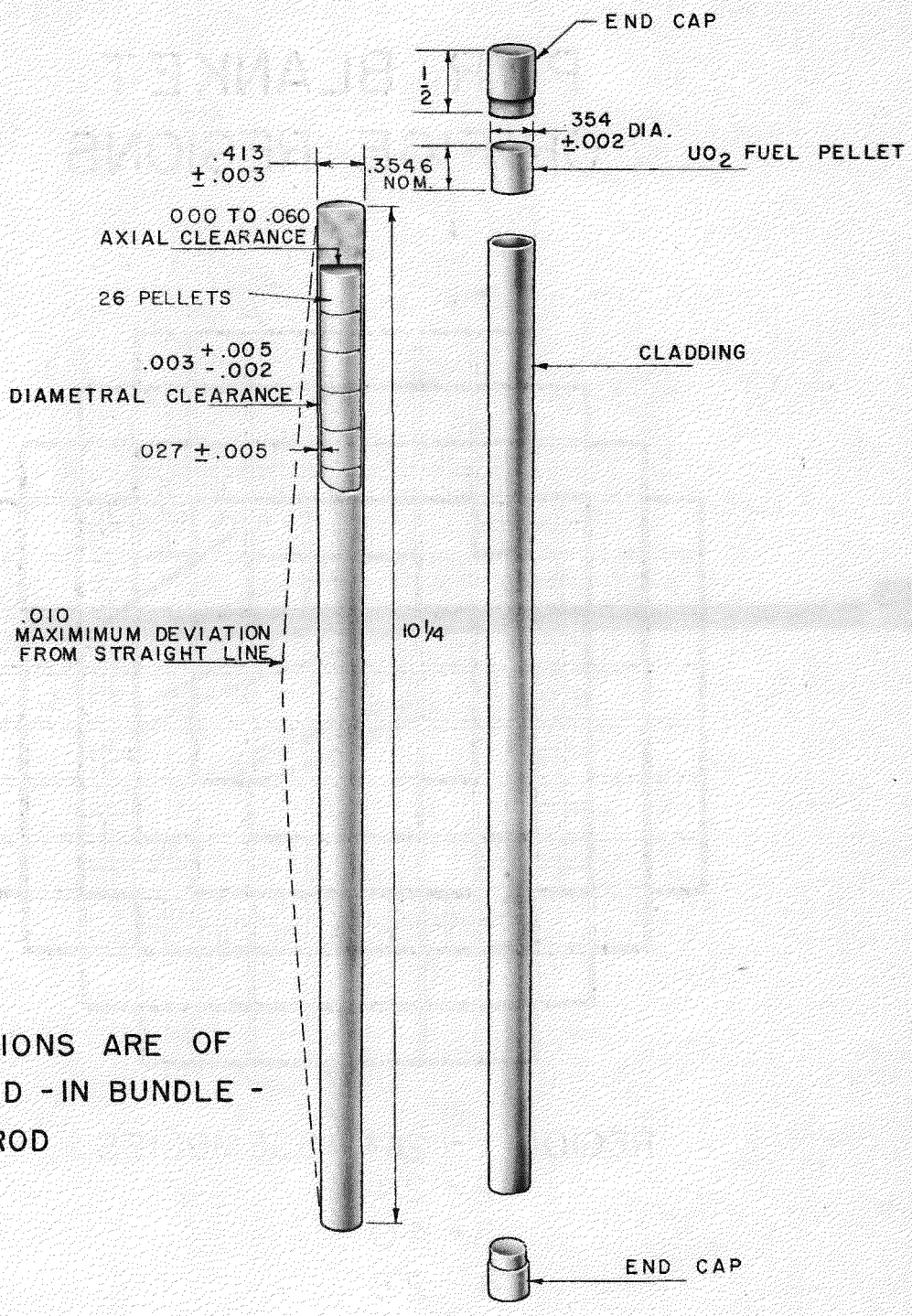

NOTE :—
DIMENSIONS ARE OF FINISHED - IN BUNDLE - FUEL ROD

PWR UO_2 FUEL ROD

FIGURE 4

PWR BLANKET ORIFICE REGIONS

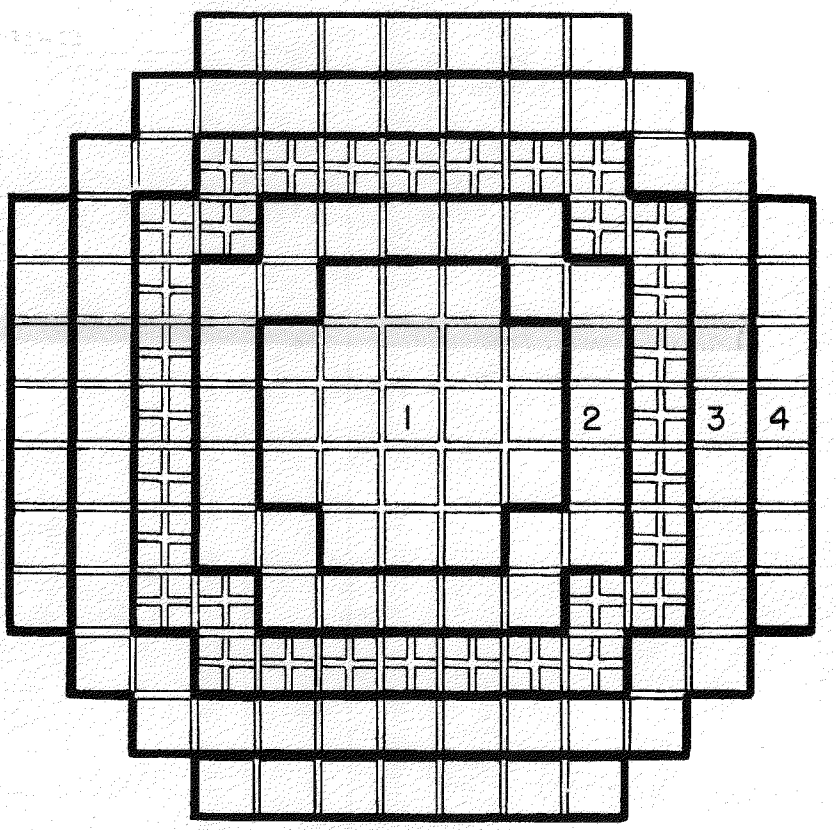

REGION 1 - 21 ASSEMBLIES
2 - 24
3 - 40
4 - 28
SEED (+) 32

FIGURE 5
SEED AND BLANKET REGIONS

VI. THE LOSS-OF-COOLANT ACCIDENT

A. Rupture and Blowdown

In the postulated loss of coolant accident it is assumed that the coolant water from the primary reactor coolant system is lost due to the rupture of some component part. The time required for the coolant to be lost from the system is, of course, dependent upon the location and size of the rupture. Dependent somewhat upon the rupture size, the coolant water would be lost more rapidly for a rupture in a low position because of a higher fluid density in the escaping fluid. However, for the selected "worst case" break, involving a pipe split equivalent in flow area to a complete shear of the 15 in. ID main coolant piping, little difference would exist for top and bottom rupture because of the extreme rapidity of blowdown, and because of the approximately equal fluid densities in those two cases. Blowdown curves for different break sizes are given in Figure 6. Although a rupture of the pressure vessel itself is not reviewed, a similar blowdown would occur, the rate of blowdown being dependent upon the size of the flow area. For sizes of pressure vessel rupture larger than the assumed "worst case" the results would be little different from those reported in the ensuing discussion, except that the core temperature would rise slightly faster.

If water is added to the pressure vessel following a large rupture in the inlet pipe near the bottom of the vessel, this water will run out through the opening, with the result that core immersion will not occur until the water level in the spherical reactor chamber of the reactor plant container rises to the core level. In the case of an elevated rupture, the added water would refill the pressure vessel before leaking out. Since the events following a large rupture below the reactor core are more difficult to control, this condition is assumed for the "worst case" studies.

B. Reactor Shut-Down Following a 15 in. ID Break

During the loss of pressure in the reactor vessel, an automatic alarm is given at 1850 psi and an automatic scram insertion of the control rods will occur when the pressure reaches approximately 1600 psi. Both the alarm and the scram will occur within 1 second of the occurrence of the assumed 15 in. ID pipe rupture. The insertion of control rods will quickly lower the fission heating rate to zero. The heating due to decay of fission products will, of course, continue at a decreasing rate. The formation of a two-phase mixture of steam and water early in this transient, is expected to cause a substantial reduction in the fission power, even before the occurrence of the scram, but no benefit of this effect is taken in the calculations.

C. Operation of the Safety Injection System

Subsequent to the occurrence of the rupture and "scram", remedial action is taken to continue to cool the core if it becomes uncovered.

Immediately after the occurrence of the low pressure scram, the operator can put the Safety Injection System into an operative arrangement by pushing the safety injection button. The system will automatically supply water to the core when the system pressure drops to 500 psi, at about 15 seconds after the occurrence of a 15 in. ID break.

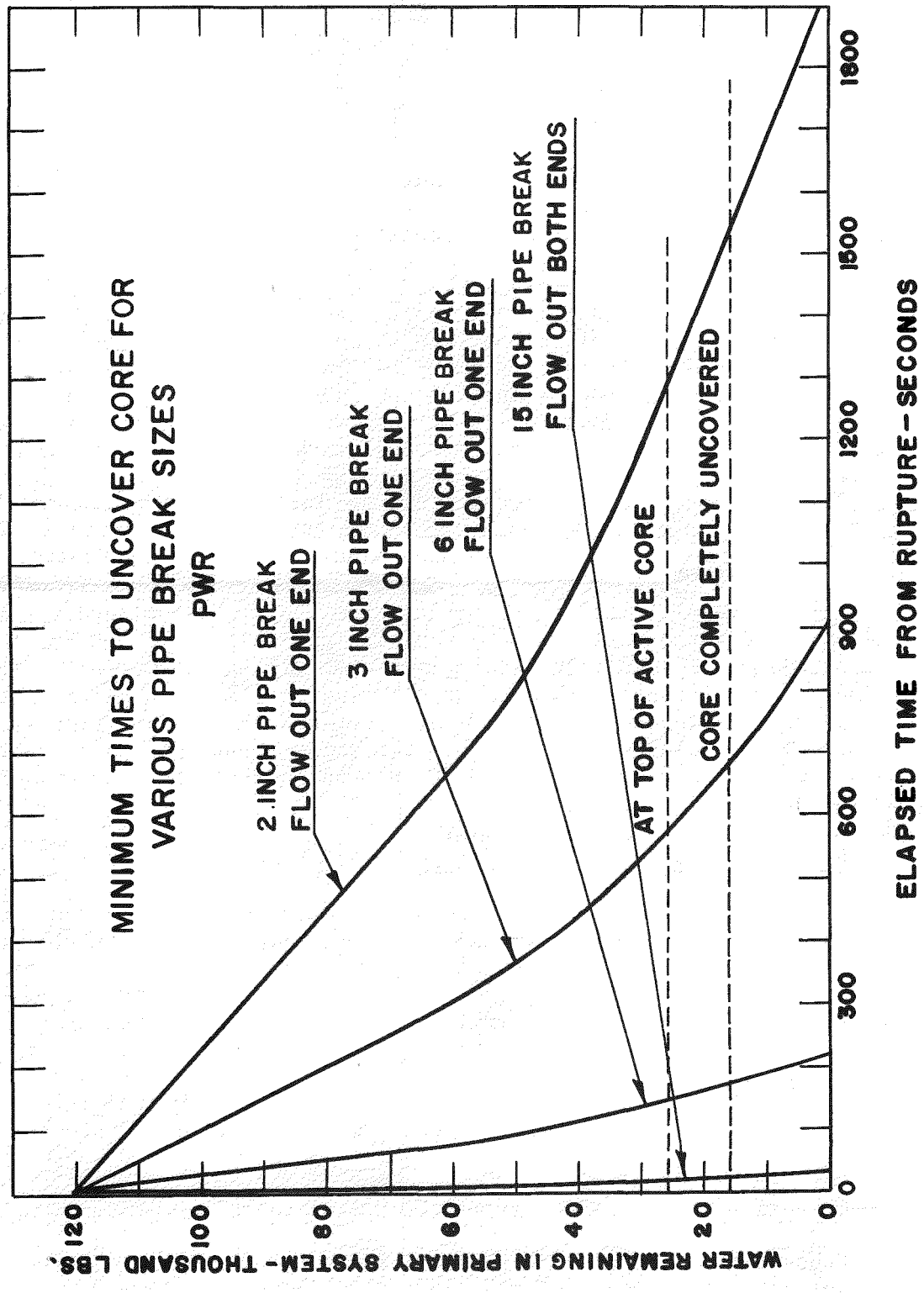

FIGURE 6
MINIMUM TIMES TO UNCOVER CORE
FOR VARIOUS PIPE BREAK SIZES

This system would supply from 1500 to 3000 gpm of boiler feed water, from the boiler feed pumps which are automatically valved over from the regular service in the secondary steam system. The water is introduced to the hot leg (upper) portion of the main coolant pipes, from where it flows downward into the pressure vessel through the outlet (upper) nozzles. The water flow is then distributed, by the holes[4] in the hold-down barrel, to provide a stream of water to strike each of the 32 control rod shrouds above the respective seed assemblies. As a result of splashing of the water from the shrouds approximately 1/2 of the water may be expected to go into the adjacent blanket assemblies (in regions 2 and 3) with the remainder flowing directly through the seed assemblies. No significant amount of water is expected to reach the majority of the assemblies in blanket regions 1 and 4 by this arrangement.

The rate of supply will vary from 1500 gpm to 3000 gpm depending upon the availability of one or both of the boiler feed pumps. Since operation at powers above 55 Mw net electrical output requires the use of two boiler feed pumps, it is assured that both boiler feed pumps will be available to the Safety Injection System when the plant is operating above this power level. However, the plant could be operating at less than 55 Mw using one boiler feed pump, the other boiler feed pump being down for maintenance. In this case only one boiler feed pump would be available to the Safety Injection System. Since the delivery of each boiler feed pump is 1500 gpm, safety injection water will be supplied at either 1500 gpm or 3000 gpm. Both cases are covered in the calculations which follow, as well as lower flow rates.

After a sufficiently long period of Safety Injection System operation, water will fill the spherical reactor chamber and back up into the pressure vessel. The water would continue to rise until it reached the level of the interconnection between the reactor chamber and the auxiliary chamber, at which level the excess water will spill over into the auxiliary chamber as it is added (see Figure 8). The level of this spill over point is 8 in. below the top of the active core, and will be reached in 25 min with two boiler feed pumps operating and 50 min with one boiler feed pump in operation.

D. Core Temperature Excursion

During normal operation of the reactor, large temperature differences exist between the interior and exterior of the fuel elements because of the high rates of heat generation. These temperature differences are particularly high for the blanket rods because of their greater thickness and lower thermal conductivity.

4. These holes are located in two rows of 32 each; the bottom row of holes, 1-1/8 in. diameter, are located 6 in. below the centerline of the pressure vessel outlet nozzles, and the second row, 1-3/4 in. in diameter are located 12 in. higher and staggered with respect to the bottom row of holes to avoid any interference of the streams issuing from the upper and lower holes. (See Figure 7)

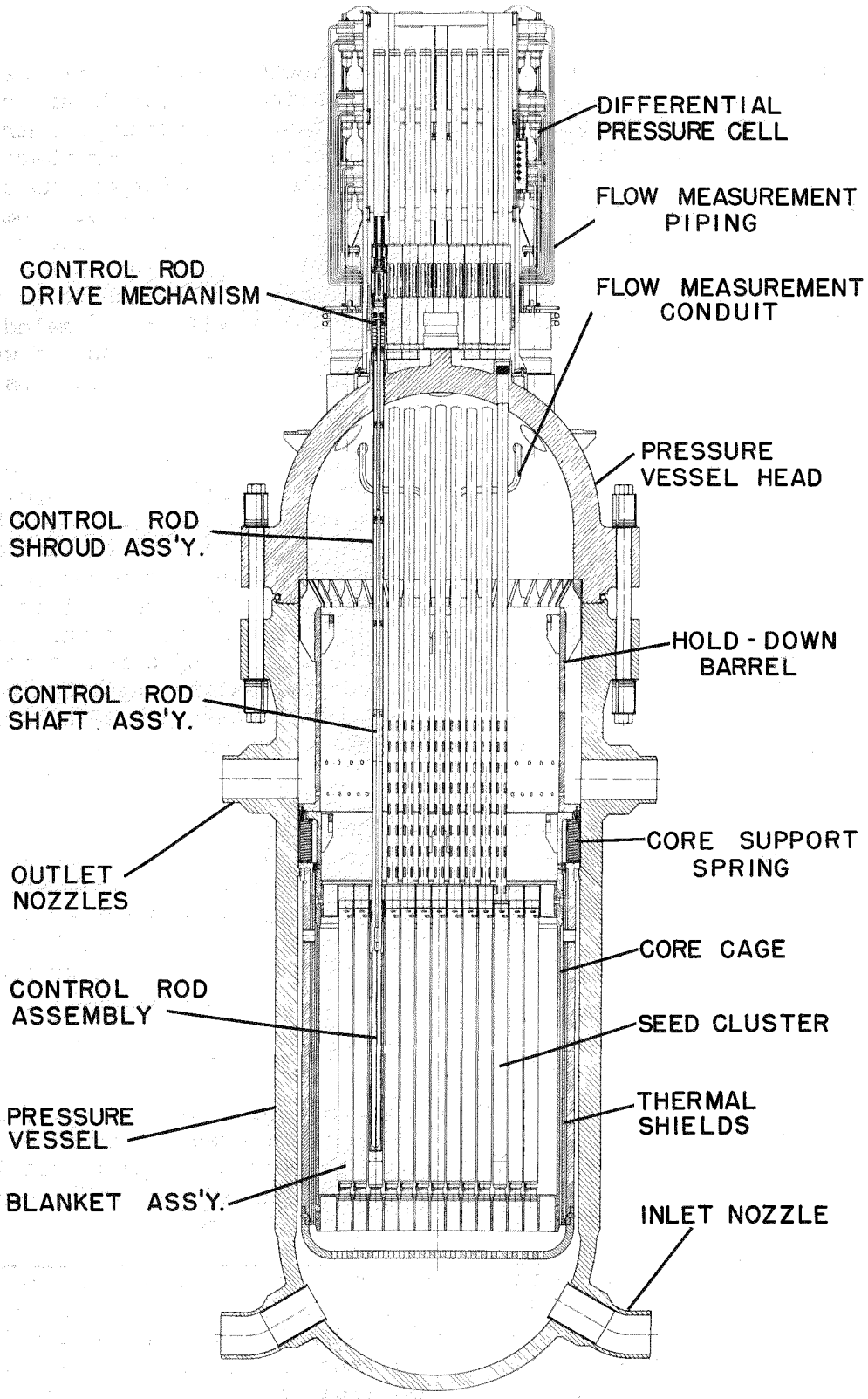

FIGURE 7
LONGITUDINAL SECTION THROUGH REACTOR VESSEL AND CORE

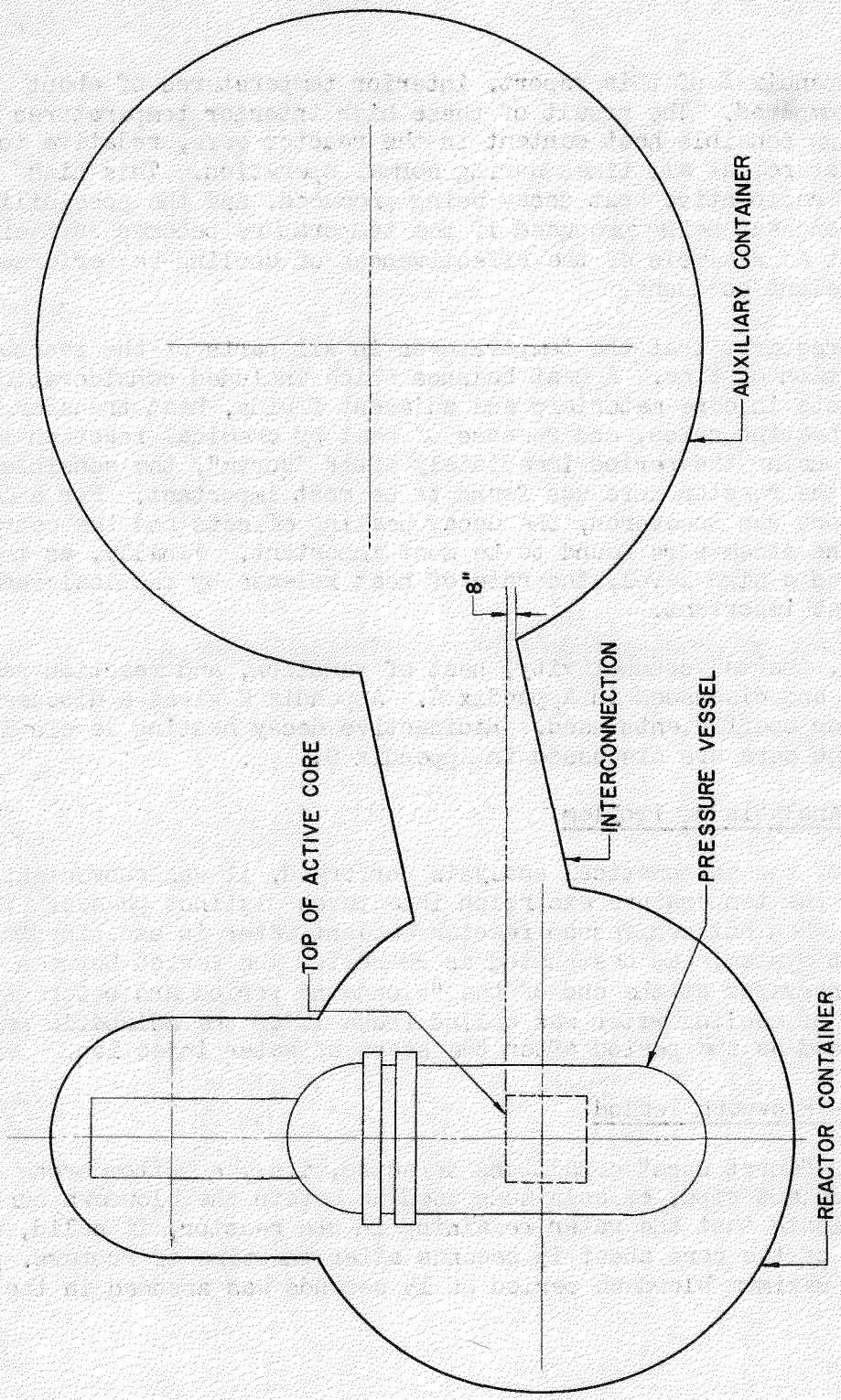

FIGURE 8
INTERCONNECTION BETWEEN PWR AUXILIARY AND REACTOR CHAMBERS

As indicated in Appendix E of this report, interior temperatures of about 3000°F have been computed. The result of these high interior temperatures is that there is a high sensible heat content in the reactor core, relative to the coolant temperature, at all times during normal operation. This high sensible heat, the radioactive heat decay being produced, and the possibility of chemical reaction heat being produced if the temperature becomes sufficiently high, required that an analysis of the effectiveness of cooling be performed for the loss-of-coolant accident.

The analysis requires that the temperatures in all parts of the reactor core be known as a function of time. A heat balance which included consideration of sensible heat effects in core materials and adjacent fluids, heat transfer rates, radioactive decay heating rates, and release of heat by chemical reaction was found necessary. During the period immediately after "scram", the sensible heat contained in the reactor core was found to be most important. For a long period after the core was uncovered, the decay heating effects and the convective heat transfer to the steam were found to be most important. Finally, as the temperatures reached a high level, the rate of heat release by chemical reaction was found to be most important.

Heat capacity, thermal conductivity, heat of reaction, and reaction rate data are tabulated and discussed in Appendix A. Appendix C gives a discussion of the heat transfer coefficients used. Radioactive decay heating levels in various parts of the core are discussed in Appendix D.

E. Mathematical Analysis of Problem

For purposes of the mathematical analysis performed, it was convenient to divide arbitrarily the temperature excursion into three distinct phases. The "blowdown" period, when hot compressed reactor coolant water is escaping from the Reactor Coolant System, was designated as Phase I. The period between the time the core is uncovered at the end of the "blowdown" period and before the start of injection of cooling water was called Phase II or the adiabatic period. Phase III was defined as the period after the start of water injection.

1. Phase I - Blowdown Period

Under the "worst case" conditions selected, i.e., a bottom break of a 15 in. ID main coolant pipe, calculations used to obtain the blowdown curves (see Figure 6) indicate that the water remaining in the reactor, if solid, would fall below the top of the core about 15 seconds after the time of rupture. To be conservative, a maximum blowdown period of 15 seconds was assumed in the calculations.

Using the temperature distribution for a blanket rod in region 2 as computed by the methods discussed in Appendix E, an analytical solution was obtained for rod temperatures as a function of the axial and radial positions in the rod, and as a function of time, as described in Appendix F. An analytical approximation of the axial distribution of decay heating was used. This distribution is compared with the steady state axial distribution of heat generation in Figure F-2.

The type of solution which was possible for this period required that constant values for heat-transfer coefficients, thermal conductivities, etc., be used. Consequently, the initial solution was based on average values for these quantities which were considered to be those most representative. Subsequently, more conservative values were used for additional solutions. The conditions for the cases computed are summarized in Table F-1.

In general, all solutions indicated that the temperature difference between blanket rod surface and centerline at 15 seconds after scram would be small, i.e., a maximum value of the order of 200°F, so that for subsequent periods an average value could be used for the radial temperature and thus only the axial temperature variation needed to be considered. This approximation greatly reduced the complexity of the subsequent calculations.

2. Phase II - Adiabatic Period

From 15 sec after scram, when the core would become uncovered, until such time as the safety injection water or other cooling water would be added, the reactor core would be essentially in an adiabatic condition. Radiation from the ends (top and bottom) of the core would be small, as would any heat losses by natural convection of steam through the core. Even for long periods, with no cooling water added, the supply of steam available would be too small to permit any significant contribution to heating by chemical reaction. Thus, radioactive decay would contribute heat to the system, but the losses would be insignificant. However, the heat produced by radioactive decay would be sufficiently high to cause melting of the hotter portions of the seed plates in about 200 sec and melting of the hotter portions of the blanket rods in 1100 sec, as shown in Table 1. Details of calculations made for Phase II are given in Appendix G. Since this phase can be considered as a special case of the Phase III, it will be treated further after the method of solution of that case is discussed.

3. Phase III - Heating and Reaction after Water Addition

At some time in the Phase II period, water is assumed to be supplied to the core by the Safety Injection System, or other means, and heat removal by the fluid will occur. Depending upon the rate of supply of the water and the temperature of the plate (or rod) when the water is introduced, chemical reaction could occur. To permit the simultaneous evaluation of heat transfer, chemical

reaction, radioactive decay heating, and system point-to-point temperature, a heat balance was written. This heat balance was written in differential form for a radial cross-section of a blanket rod and its associated fluid. Heating effects due to radioactive decay and chemical reaction were included, as was heat transfer by conduction and convection. Radiation heat transfer was considered to be of negligible benefit to the centers of the plates because the individual rods (and plates) were essentially perfectly shielded. Similarly, edgewise conduction was considered to be of negligible benefit. Check calculations, not appearing in this report, were made verifying the assumptions on radiation and edgewise conduction.

It should be noted that the introduction of liquid water cannot be guaranteed to enter every fuel assembly. It was assumed, for the cases investigated where only small amounts of liquid water were available, that the water injected is vaporized by coming in contact with hot metal anywhere in the reactor and that the steam generated flows through the coolant channels in the same distribution as the water in normal reactor operation.

Since an analytical solution of this complex system of equations was considered impossible, it was programmed for solution on the IBM 650 digital computer. Details of the methods used are given in Appendix H.

Essentially, the solution was performed in the following manner. To initiate the computation of a case, a heat flux level representative of the particular blanket rod (or seed plate) of interest, a steam rate, and an axial temperature profile for a chosen time from a Phase II calculation were selected. Using the values given, the machine computed for 31 equally spaced points on each blanket rod (or seed plate) the temperatures for the next time interval. Each solution for the next time interval was based on the previous temperature profile. In addition to the rod (or plate) temperature, the fluid temperature, the mole-fraction of the gas reacted, and the amount of reaction on the rod at each point along the length were computed and tabulated. The cumulative amount of hydrogen produced was also recorded.

Computations were continued until chemical reaction ceased, either by having the rod (or plate) cool to an inactive temperature level, or by having the cladding of one portion of the rod melt and the remainder of the rod cool to an inactive temperature. The occurrence of one or the other of the above results depends upon the heat flux level and the rate of supply of steam chosen for the particular case. A comparison of the results for a series of these cases led to the stated conclusions as to the effectiveness of the Safety Injection System in avoiding fuel element melting.

For the computation of Phase II, the same program was utilized, but modified to prohibit convective heat transfer and chemical reaction. Results of these computations are reported along with those of Phase III.

4. Over-all Conditions Computed

It became evident early in this work that the prediction of the occurrences in the reactor core after loss of coolant must be based on representative conditions. This was because any computation for each blanket rod and seed plate for an over-all assumed condition would have been too time-consuming. Since a knowledge of the "worst" conditions were desired, representative rods (or plates) could be used, providing the flux level chosen was sufficiently high. As a result of these considerations, a blanket rod having an average flux 1.44 times the average for the region was chosen to represent each region. A seed plate having an average flux 1.15 times the average flux for the seed region was also chosen. In addition, the axial variation in heat generation equivalent to that which occurs during reactor operation is assumed. For the seed the peak-to-average ratio is taken to be 2.0, and for the blanket it is taken to be 1.77. These calculations have neglected the possible burnout at local hot spots, occurring due to statistical variations in fuel element dimensions, fuel loading, etc. The integrated melting of hot spots would be negligible compared to the bulk melting as may occur later. (The fission product release due to hot spot melting is expected to be of the same order of magnitude as the maximum expected activity which could be in the coolant during normal operation with defected cladding of UO_2 elements.)

For the Phase II calculations, the stepwise machine computation was started at 15 sec and the temperature as a function of time was computed. The calculation was continued until the melting temperature was reached. The time to reach melting temperature for these cases providing base values on which to compare the results for other conditions. For Phase III, a series of delay times and constant rates of steam supply were assumed in an effort to find the necessary steam supply rates to turn back the temperature excursion without a significant amount of reaction. It was assumed further that the water would be supplied to the individual blanket rods and seed plates in the form of steam and in the same proportion as the coolant during normal operating conditions. Two other steam flow assumptions were used to evaluate the extent of chemical reaction and core meltdown. A strictly "worst case" situation would occur if steam were supplied to each point of the core surfaces at a rate which would just support the maximum rate of chemical reaction, which depends partly upon the temperature of the core metal. This is known as the "stoichiometric case", reported in Case 2 of Table 1. Certain aspects of the assumption of a stoichiometric rate of steam supply are considered unreasonably pessimistic for various reasons. Specifically, it is virtually impossible to match the supply of steam to each point of the core surface to the rates indicated for the temperatures, which vary widely over the length of a plate (or rod) due to the variable axial distribution of heat flux. It was felt that a more reasonable, yet conservative, evaluation of the situation would be obtained by assuming that 1/3 of the decay heat as produced would be used to generate steam by boiling of the water outside of the fuel assembly shells, which might flow back from the loop piping into the spaces between assemblies and within the core cage. It is assumed that no effective core cooling is provided to all fuel elements except by the convective transfer due to steam flowing through the reactor channels, that is, the Safety Injection System is not assumed to be in operation. This case was based on the fact

that 39 of the 120 rods in each blanket fuel rod bundle are in the outer row. These rods, in the outer row will radiate possibly all their decay heat to the cooler blanket assembly shell, if these shells are kept in contact with water in the spaces between assemblies. At the same time radiation from the inner rods to the shell would be negligible because these rods would be well shielded. Since the Zircaloy heats up moreslowly for this case, as compared to the "stoichiometric" case, the metal remains a longer time at high temperatures before melting occurs, and a more extensive zirconium-water reaction occurs. Therefore, if the total amount of zirconium-water reaction (or the resulting heat or hydrogen release) is the basis of comparison, this case is worse than the "stoichiometric case". The "1/3 decay heat" case has therefore been selected as a basis for evaluating the worst case situation. Extensive calculations based on the "1/3 decay heat" case are summarized in Table 1 as case 3.

Since the heat of vaporization of water would involve a complicated discontinuity in the computer calculation, it did not prove feasible to consider the effect of the addition of water, rather than steam, to the elements computed. The cooling effects on the fuel elements reached by safety injection water would therefore be greatly increased. The results reported in Table 1 are therefore conservative in this respect.

F. Cases Calculated and Results Obtained

The conditions computed and the results obtained are summarized in Table 1. All cases assumed the decay heat generation rates which would be applied after 600 hours of operation at about 75 Mw net electrical output of the plant. The assumed rate of steam flow and the time delay in supplying the steam were varied in an effort to answer the following questions:

(1) What is the maximum extent of core meltdown, zirconium-water reaction, hydrogen production, and heat release that could occur?

(2) What is the minimum amount of steam which must be supplied to cool the core and prevent chemical reaction?

(3) What delay time for the addition of safety injection water would cause a worst condition than would be caused by not adding water?

(4) Are the rates and location of cooling water addition by the Safety Injection System sufficient to prevent core meltdown and significant chemical reaction?

The heating process is a delicate balance between the release of heat by radioactive decay, the carrying away of heat by the steam, and at the higher temperatures, the heat generated by chemical reaction. Fortunately, the chemical reaction is somewhat self-retarding. The reaction product, ZrO_2, which builds up on the rod or plate surface, interferes with the supply of reagent to the point of action.

An additional amount of reaction would take place, however, if it is assumed zirconium leaves the core and falls into a steam-water environment in the bottom plenum chamber of the reactor vessel. Experimental results for chemical reaction of Zircaloy droplets falling through steam or water indicate that only about 12 w/o of the Zircaloy will be reacted for the limited distance of fall and the droplet size expected in the PWR.

Results, indicating the amount of reaction and extent of melting over time, are presented in Figures 9 through 26 for the "1/3 decay heat" case. The power history assumed, as stated earlier, are 600 hours at full power of 75 Mw net electrical output.

A summation of hydrogen generated, for the whole core, is shown in Figure 19 where it was assumed that the behavior of all rods (or plates) in each region is represented by the one rod (or plate) computed for each region, for the 1/3 decay heat case. The extent of reaction, shown at 3700 sec, amounts to about 16.5% on the average for all regions. It was assumed, for analyses of energy and fission product release, that the seed side plates would receive enough heat by conduction from the melting fuel plate to react chemically in the same manner as the adjacent fuel plates. The amounts of Zircaloy in the field of action, 4.51 tons in the seed and 4.87 tons in the blanket, would produce 67.5 lb-moles of H_2 on the basis of a 16.5% reaction.

The above assumption that the seed side plates would come into the reaction is conservative. Even a small amount of heat transfer, by radiation or boiling of water between assemblies, from the side plates would prevent extensive chemical reaction in these plates. If it had been assumed that the seed side plates do not enter the chemical reaction, the total extent of reaction would be about 20% less, resulting in a total hydrogen production of about 54 lb-moles instead of 67.5 lb-moles.

Information obtained from the stepwise machine calculations is used to develop additional results; in particular, those needed to evaluate the design of the reactor plant container surrounding the reactor pressure vessel. Figures 19 through 26 indicate the quantities of reaction products and energy released as a function of time for the "1/3 decay heat" case.

To obtain these curves, use was made of the data which gave the amount of reaction and amount of meltdown occurring in the core as a function of time. From the information on mole-fraction of the gas stream reacted, the steam input rate, and the temperature of the existing gas stream, it was possible to determine the hydrogen and steam flow in the exit gas stream. Then, by using the calculated amounts of zirconium melted as a function of time it was possible to compute the hydrogen generated by the additional 12% reaction of the molten zirconium in the steam-water environment of the bottom plenum chamber of the reactor vessel.

For this purpose, it was considered that a pool of water existed in the bottom of the reactor vessel at all times, that 12% of the Zircaloy reacted upon falling into this pool, and that the hydrogen and steam produced in the reaction and in cooling the reaction system to the boiling point of the water, 281°F, produced steam and hydrogen at 281°F. (At an assumed plant container pressure of approximately 35 psig, the boiling point is 281°F) Summing the products of reaction and the energy released from these two sources led to the composite curves shown. Figures 20, 21, 22 and 23 show the rates while Figures 19, 24, 25, and 26 show the integrated quantities as a function of time.

The peaks on the rate curves are a direct result of the fashion in which core reaction and meltdown occur when no safety injection water is added. This can be seen by inspection of the reaction and melting times in Table 1. Figures 19, 24, 25, and 26 give the cumulative gas release, energy release, and temperatures in the steam-hydrogen mixture issuing from the core. This information was necessary for the evaluation of the pressures within the reactor plant container due to the heat released from the zirconium-water reaction and from combustion of hydrogen. This data was also used to assess the possibility of the hydrogen-air-steam mixture burning or detonating in the plant container. These evaluations are reported in WAPD-SC-545, "Hydrogen Flammability Data and Application to PWR Loss-of-Coolant Accident", May, 1957.

G. Effectiveness of the Safety Injection System

The consequences of any loss-of-coolant accident are, of course, dependent upon the rupture size, location, and reactor power level, as well as the rate of supply and distribution of the water from the Safety Injection System.

As indicated in Figure 1 and Figure 8 only a small fraction of the primary system piping is located at levels below the active core. All valves, pumps, and boilers, as well as the taps for pressurizer lines and other fluid systems are so located that failures of these components would not lead to loss of safety injection water from the pressure vessel until the core is re-immersed.

Other things being equal the relatively small fraction of the primary system piping which is below the level of the core makes the probability of the "worst case" (bottom) break correspondingly small.

Moreover, the "worst case" discussion assumes that the Safety Injection System is not in operation to supply water flow through the reactor channels.

The "worst case" discussed below, is therefore not a plausible case, but it is included to provide an estimate of the "worst case" results which might occur if the Safety Injection System does not operate.

1. Worst Case Break

Examination of Table 1 shows that 3000 gpm maximum capacity of the Safety Injection System for cooling of the PWR core after a loss-of-coolant accident

following a "worst case" break and 600 full power hours at about 75 Mw is vastly in excess of the amount required if it were distributed to the core in proportion to the decay heat generation. However, due to difficulties in obtaining the proper distribution, some excess is needed to assure that more than the minimum requirement of water will be supplied to the assemblies in the seed and in blanket regions 2 and 3. A small amount of reaction would begin in regions 1 and 4 of the blanket before all assemblies are immersed, because no significant amount of water is expected to splash onto the majority of the assemblies in these two regions.

With 3000 gpm supplied, immersion of the core to within 8 in. of the top is expected at 1500 seconds. The level is expected to reach the midline of the core at 1260 seconds, at which time boiling in the channels of regions 1 and 4 would provide cooling for the hotter portions of the rods in those regions. It is indicated in Table 1, for the "1/3 decay heat" case, that the axial hot spot of the hottest (radially) rods in region 1 would begin melting in 1162 seconds. Therefore, some reaction could be expected in regions 1 and 4. At the most, the reaction could not involve more than 4.8 w/o of the Zircaloy-2 cladding in region 1 and 1.0 w/o of the cladding in region 4 if all the rods in the system were equivalent to the rod computed. Since this is not the case, a lower amount of reaction would be expected.

It should be noted that in region 1 the 4.8 w/o of reaction is not uniformly distributed over the length of a rod, and that only approximately 2-1/2% of the length of a rod would have the cladding completely melted away, thereby exposing the UO_2 fuel in that portion of the rod, and resulting in a corresponding release of the fission products to the pressure vessel and through the rupture to the plant container. No melting would occur in region 4 because the assemblies in region 4 would be cooled by re-immersion before the melting point is reached.

If a delay up to 1-1/2 minutes in the initiation of operation of the Safety Injection System is assumed, the extent of reaction in region 1 is increased from 4.8% to 6.7% and the extent of melting in region 1 is increased from 2-1/2% to 8-1/2%. The reaction in region 4 is increased from 1.0% to 1.4%, with no melting occurring.

Finally, it should be recognized that many of the assumed conditions used in performing the analysis were conservative, i.e., led to results which are worse than can be expected in any loss-of-coolant accident. Thus, any Safety Injection System which, as a minimum meets the requirements imposed by these results, may be considered to have a design factor of safety inherently included.

2. Effectiveness Under Other Assumed Conditions

All of the preceding conclusions were based on the assumption of the worst combination of power level, rupture size, and rupture location. Any variation of these would, of course, result in a reduced amount of reaction and meltdown. Also, a smaller leak, or a rupture at other locations is much more probable. The effects of such variations from the worst case study are discussed separately in the following sections.

a. Smaller Rupture Sizes

All of the calculations described herein assume the rupture is a pipe split equivalent in flow area to a 15 in. ID pipe shear. (Since the primary coolant system piping is made of stainless steel, a ductile material, a brittle shear is not believed to be possible.) If the rupture were assumed to be of smaller size, the core would remain covered for a much longer period, as indicated by the curves of Figure 6. As a result, the rate of decay heat production would be lower when the core became uncovered, causing slower initial heating of the core than calculated herein as Phase II.

Equivalent effects would occur should a rupture occur in one of the many auxiliary connections to the main coolant loops. The largest effective area of such a rupture could be no greater than the flow area of the auxiliary line involved. The largest connecting pipe is the 6 in. schedule 160 surge and pressure relief system line. All others are 3 in. schedule 160 or smaller.

b. Elevated Rupture Locations

After a rupture of the Reactor Coolant System above the elevation of the top of the active core, the Safety Injection System could quickly flood the reactor vessel and cover the core, preventing any significant core meltdown or zirconium-water reaction regardless of the size of rupture. If the safety injection water is supplied at 3000 gpm, the core would be completely immersed in 2-1/2 minutes, or in 5 minutes of only one 1500 gpm boiler feed pump is available. Even with only one boiler feed pump operating, and a rupture in one reactor outlet line permitting 750 gpm of the safety injection water to escape without entering the reactor vessel, the core would be completely immersed within 10 minutes, well before any significant chemical reaction or core meltdown should occur. The seed region and blanket regions 2 and 3 are calculated to be adequately cooled by the flow of safety injection water during the filling of the reactor vessel, and regions 1 and 4 would not reach melting (if left uncovered) until about 20 minutes. Therefore, it is concluded the core can be adequately protected by the Safety Injection System in case of rupture above the level of the core.

All auxiliary pipe connections to the main coolant system are either above the elevation of the top of the active core, or outboard of an elevated portion of the reactor piping (that passes from the reactor chamber to the boiler chambers). As a result, safety injection water would collect in the reactor vessel, covering the core before it could flow out the rupture, within the safe time limits mentioned above.

c. Lower Powers

If it is postulated that the reactor plant has been operating for 600 hours at the design requirement power of 60 Mw net electrical output on 3 loops, the decay heating would be 80% of the assumed 75 Mw used in the preceding discussions. In that case, with the design injection rate of 3000 gpm, no melting and only a small amount of surface reaction would occur after a rupture of the reactor coolant system below the level of the core.

A somewhat worse situation would exist if one boiler feed pump is, for any reason, not available to the Safety Injection System. Reactor operation with only one boiler feed pump will be limited to power levels corresponding to the capacity of the secondary system on one feed pump, or about 55 Mw. This is only about 73% of the power assumed in the calculations. The appropriate reduction in decay heating extends the time to beginning of melt by a factor of about 1-1/2. Thus, instead of 1162 seconds for region 1 to reach melting it would be about 1700 seconds calculated on the "worst case" basis. A comparison of this time with the 42 minutes required to fill the core to midline with one boiler feed pump, indicates that melting in region 1 could continue for about 14 minutes. About 44% of the rod cladding would melt in region 1, again based on the assumptions that all rods behave like the one calculated (heat generation rate 1.44 times that of the average blanket rod). Some difficulty is also encountered in region 4 where melting would begin in about 2350 seconds (calculated on the "worst case" basis). Melting would continue for about 3 minutes (until the core is submerged) with a melting of about 1/10 of the rod cladding in region 4. The total melting of clads in regions 1 and 4 represent about 11% of the total rod cladding in all blanket regions. It should be emphasized again, here, that this represents essentially an extremely unlikely condition, i.e., a boiler feed pump out of service for maintenance, followed by a rupture accident, of 4 inch equivalent diameter or larger, and located below the level of the core on the reactor side of the main stop valves. Although only one boiler feed pump is required during plant operation below 55 Mw net electrical output, it will be normal procedure to operate both boiler feed pumps at plant loads above about 30 Mw net. When operating below 30 Mw with one boiler feed pump, the operator may bring the second pump on the line almost instantaneously (if the pump is not out of service for maintenance) by closing a switch located on the control console.

TABLE 1

SUMMARY OF CASES COMPUTED AND RESULTS WHEN SAFETY INJECTION WATER IS ADDED TO PWR CORE

Case No.	Total Injection Water Added to Reactor Core gal/min.	Region Considered in Calculations	% of Total Water Added to Each Reg.	Steam Flow Rate to Each Element lb mole/sec	Time Measured After Scram, sec (Time at Scram = 0 sec)			Amount of Zr Present Which is Melted[G] w/o	Chemical Reaction Occurring per Region		
					Time Water First Introduced	Time to Reach Melting Temp.	Time Melting Completed		Total Solid Phase Reaction At End of Melting w/o Zircaloy	Liquid Phase Reaction in Droplet, w/o Zircaloy	Total Reaction w/o Zircaloy
1	0	Seed	---	0	---	204.8	---[E]	---[E]	0	---[E]	---[E]
		Blanket Reg.2	---	0	---	1111.0	---[E]	---[E]	0	---[E]	---[E]
2	Stoichiometric[A]	Seed	---	Variable[A]	25.8(44.8)	90.4	---[F]	---[F]	---[F]	---[F]	---[F]
		Blanket Reg.2	---	Variable[A]	25.8	575.0	---[F]	---	---	---	---
3	1/3 Decay Heat[B]	Seed	47.3	Variable[B]	24.8	95.1	151.1[H]	52	1.8	12	8
		Blanket Reg.1	7.2	Variable[B]	25.0[C]	1162.0	~2800	59	21	12	28
		Blanket Reg.2	15.6	Variable[B]	25.0	610.0	~1550	57	18	12	25
		Blanket Reg.3	23.6	Variable[B]	25.0[C]	670.0	~1650	57	19	12	26
		Blanket Reg.4	6.3	Variable[B]	25.0[C]	1567.0	~4600	60	23	12	30
4	25	Blanket Reg.2	15.6	9.4×10^{-6}	25.0	651.0	<1650	<25	<18	12	<21
5	50	Seed	47.3	8×10^{-5}	24.8	99.7	118.8	35	1.2	12	5.4
	50	Seed	47.3	8×10^{-5}	46.8	97.8	---	---	---	---	---
	50	Blanket Reg.2	15.6	1.88×10^{-5}	160.0	cools	No melting	0	5	0	5
	50	Blanket Reg.2	15.6	1.88×10^{-5}	451.0	642.0	~ 800	<30	<18	12	<22
	50	Blanket Reg.2	15.6	1.88×10^{-5}	691.0	732.1	~1030	<48	<18	12	<24
	50	Blanket Reg.2	15.6	1.88×10^{-5}	1108.0	1109.23	~1350	~56	~11	12	~18
6	100	Seed	47.3	1.6×10^{-4}	46.8	cools	No melting	0	0.3	0	0.3
7	150	Seed	47.3	2.4×10^{-4}	89.8	105.1	---	<20	<1	12	<3.4
	150	Seed	47.3	2.4×10^{-4}	126.8	129.63	144.23	42	1.1	12	6.1
8	250	Seed	47.3	4×10^{-4}	89.8	cools	No melting	0	0.3	0	0.3
	250	Seed	47.3	4×10^{-4}	126.8	129.9	---	<40	<1	12	<5.8

Notes for Table 1:

(A) Only the amount of steam which would react chemically was added to the element at any time, i.e., no steam leaving reactor. Flow through the seed was essentially zero until 50 sec and increased to 1.46×10^{-5} lb moles/sec at 116.7 sec. Flow through blanket region 2 was essentially zero until 200 sec and increased to 5.86×10^{-6} lb moles/sec at 575 sec.

(B) Steam equivalent to 1/3 the decay heat for each element is considered to flow past that element. Flow past each element is as follows:

(1) Seed: 6.82×10^{-5} lb moles/sec at 24.8 sec and 3.40×10^{-5} lb moles/sec at 200 sec.

(2) Blanket (Region 1): 6.51×10^{-6} lb moles/sec at 25.0 sec and 2.05×10^{-6} lb moles/sec at 1200 sec.

(3) Blanket (Region 2): 1.24×10^{-5} lb moles/sec at 25.0 sec and 4.66×10^{-6} lb moles/sec at 600 sec.

(4) Blanket (Region 3): 1.13×10^{-5} lb moles/sec at 25.0 sec and 4.23×10^{-6} lb moles/sec at 600 sec.

(5) Blanket (Region 4): 4.88×10^{-6} lb moles/sec at 25.0 sec and 13.5×10^{-6} lb moles/sec at 2000 sec.

(C) The axial temperature distribution at 25.0 sec was computed only for Blanket Region 2. This same distribution was assumed for the initial temperatures for the Phase III calculations for the other blanket regions. Blanket Region 3 should be essentially equivalent to Blanket Region 2. Also, since Blanket Regions 1 and 4 are lower power regions, the temperatures should be lower than those used. Therefore, any error introduced by this assumption is on the conservative side.

(D) Last point on rod reaches melting temperatures at time given but cools below melting point again at 193.26 sec.

(E) These cases were not computed beyond the time the melting point was reached. Based on the assumptions used, no reaction would occur in the core but all Zircaloy cladding would be expected to melt from radioactive decay heating. If water were present in the bottom of the reactor vessel, 12 w/o of the Zircaloy would be expected to react as melting occurred.

(F) These cases were not computed beyond the time the melting point was reached. However, since net heating rates are faster than any other cases computed and overall behavior is similar to the 1/3 decay heat cases chemical reaction (in solid phase) would be less than in the corresponding 1/3 decay heat case. Extent of melting is unknown but might be somewhat above the corresponding 1/3 decay heat cases.

(G) Values given indicate per cent of length of rod or plate from which the Zircaloy cladding has completely melted. For purposes of further computations based on the per cent melted values, it was considered that the active Zircaloy in the seed was 4.51 tons and in the blanket, 4.87 tons. These values were obtained from WAPD-PWR-RD-127.

(H) At 151.1 sec, melting is completed for the last complete section which melts. Partial melting of an additional section occurs after this time. Approximately 1/2 of this additional section becomes molten at 234.1 sec before it begins to resolidify.

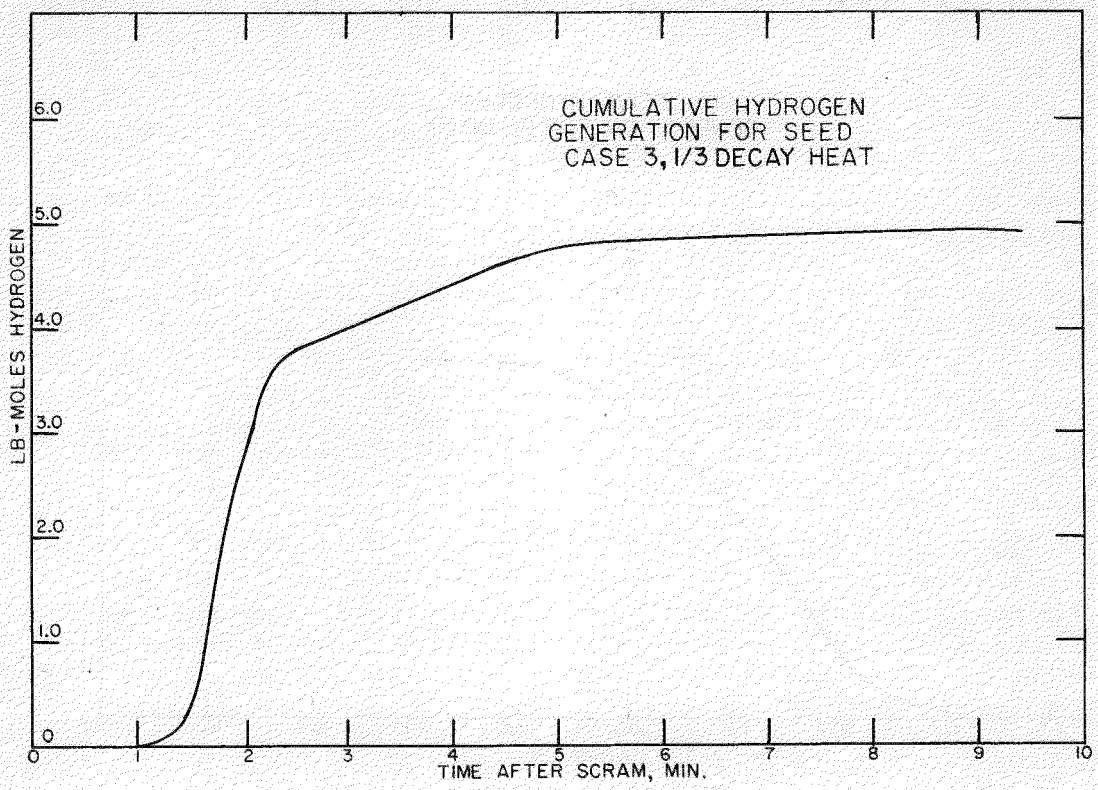

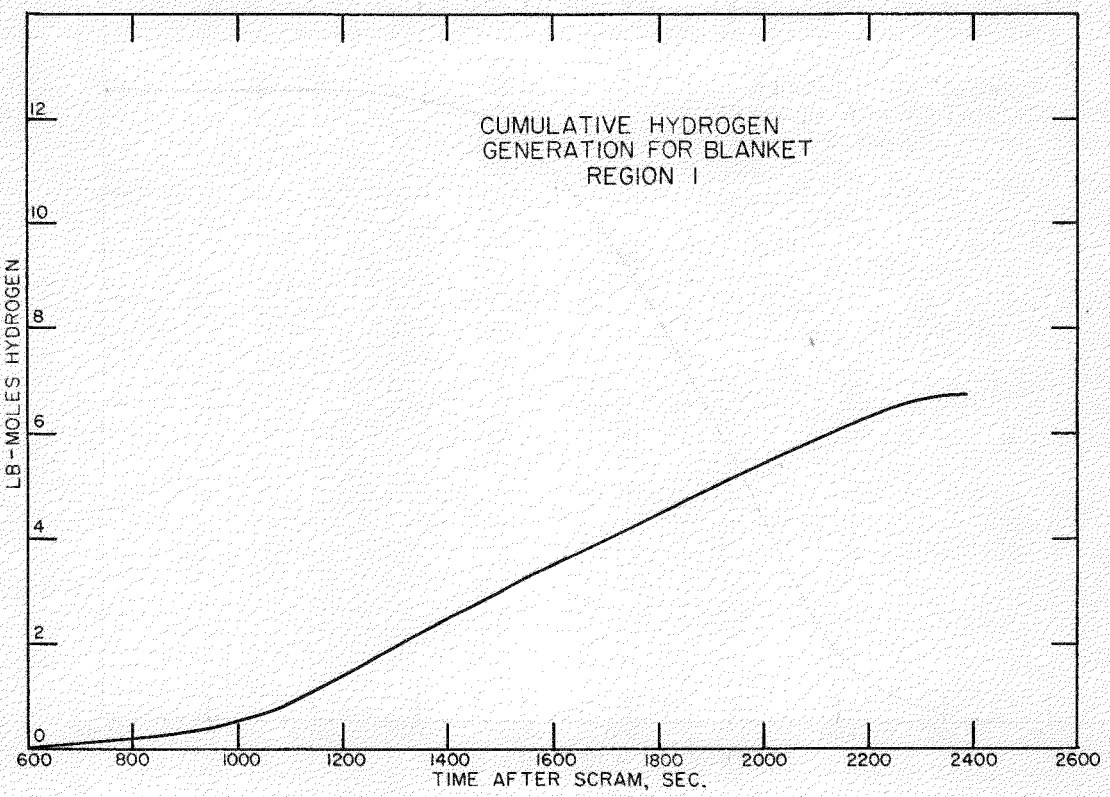

FIGURE 9 CUMULATIVE HYDROGEN GENERATION FOR SEED

FIGURE 10 CUMULATIVE HYDROGEN GENERATION FOR BLANKET REGION 1

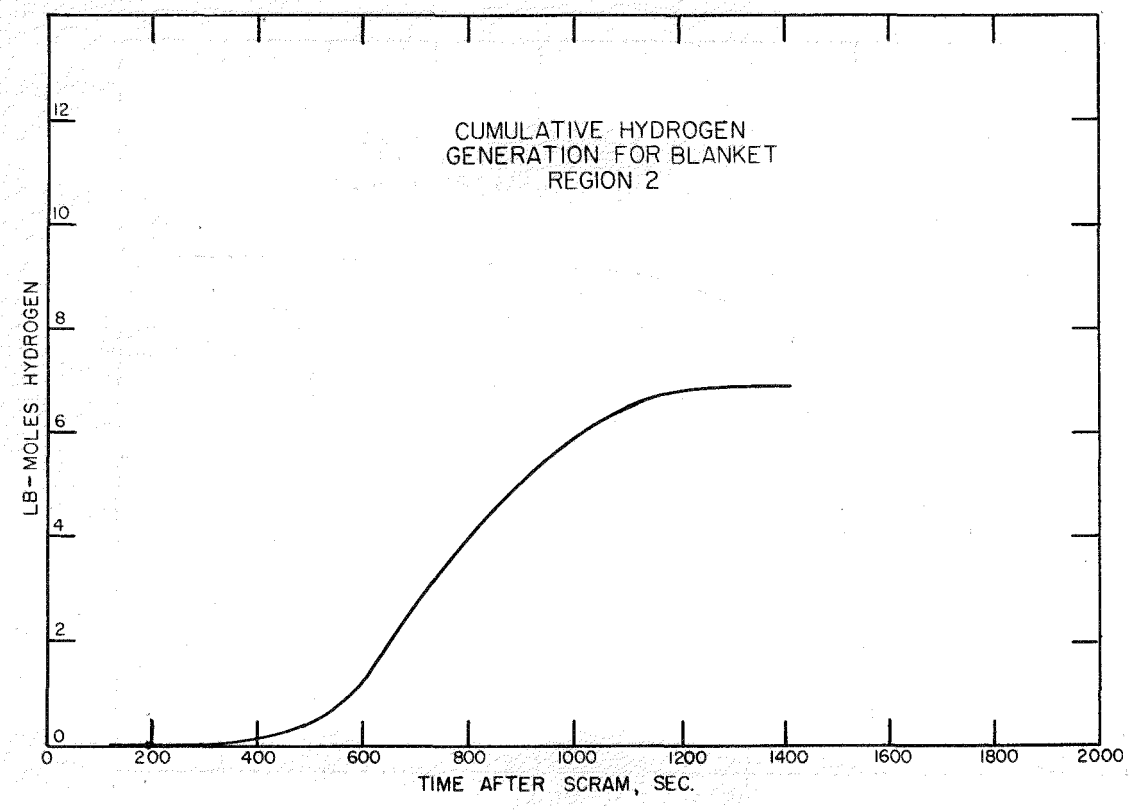

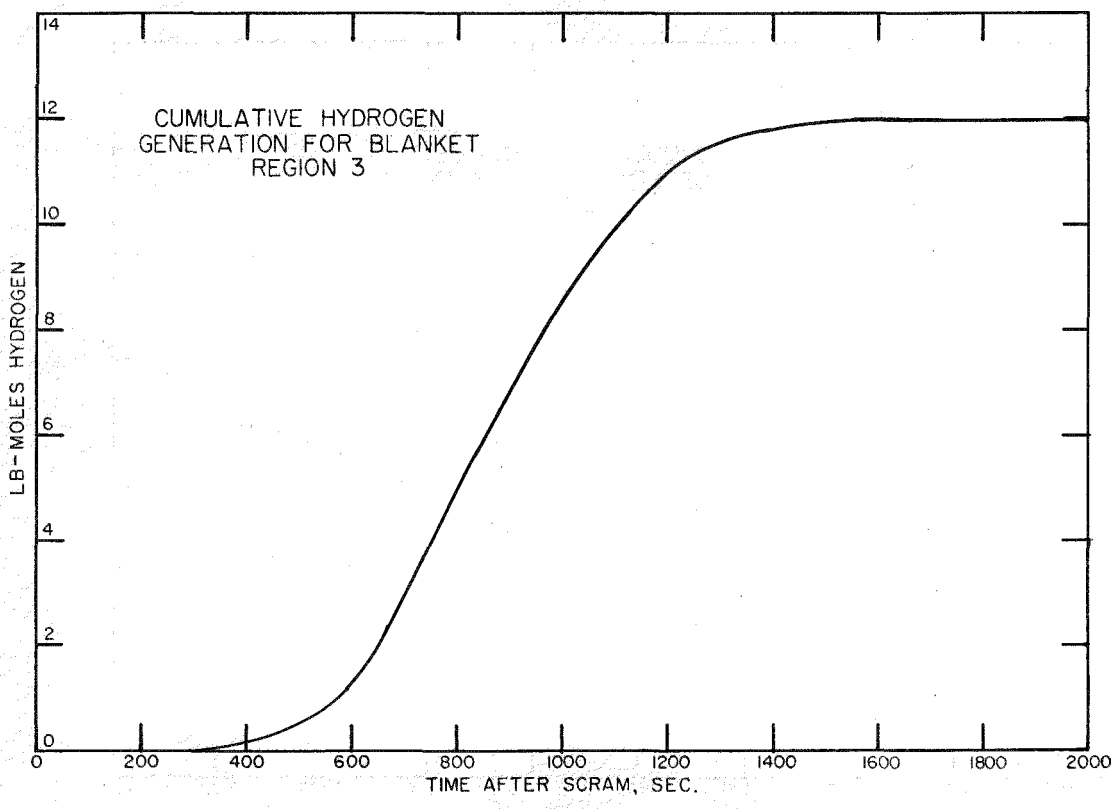

FIGURES 11 AND 12
CUMULATIVE HYDROGEN GENERATION FOR BLANKET REGIONS 2 AND 3

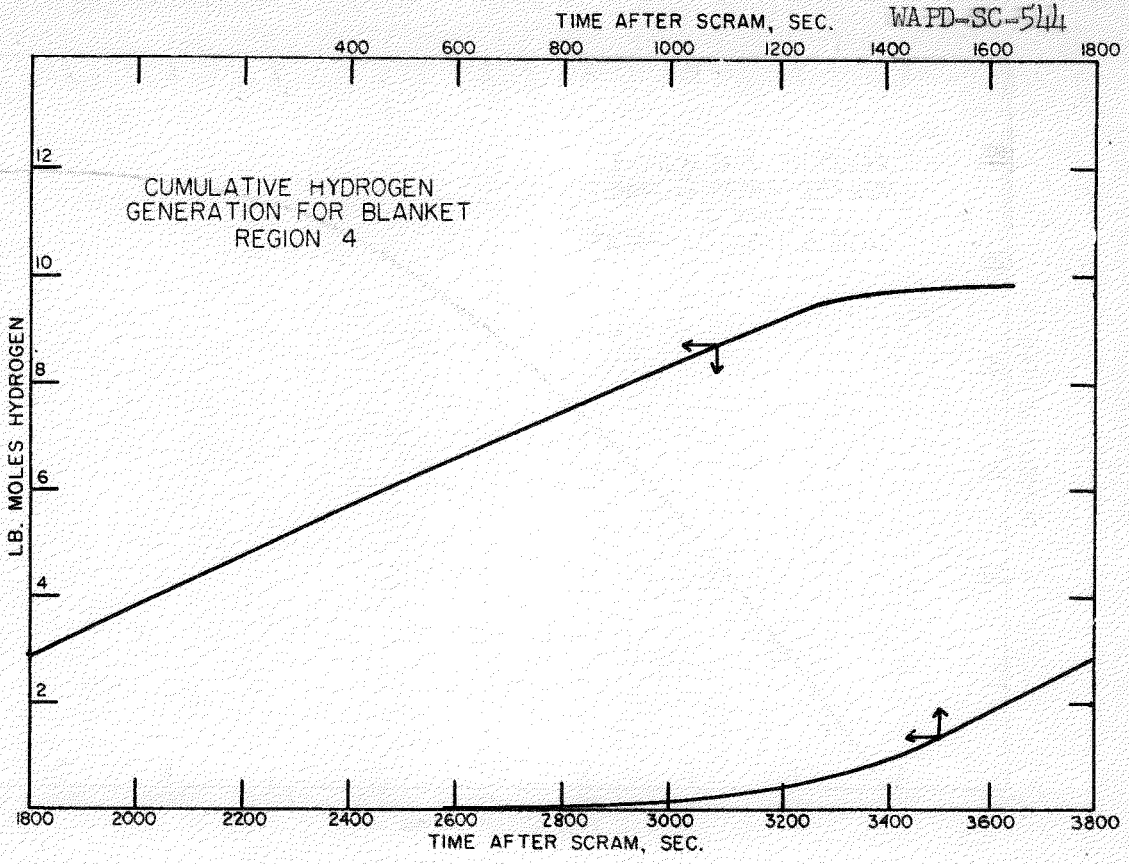

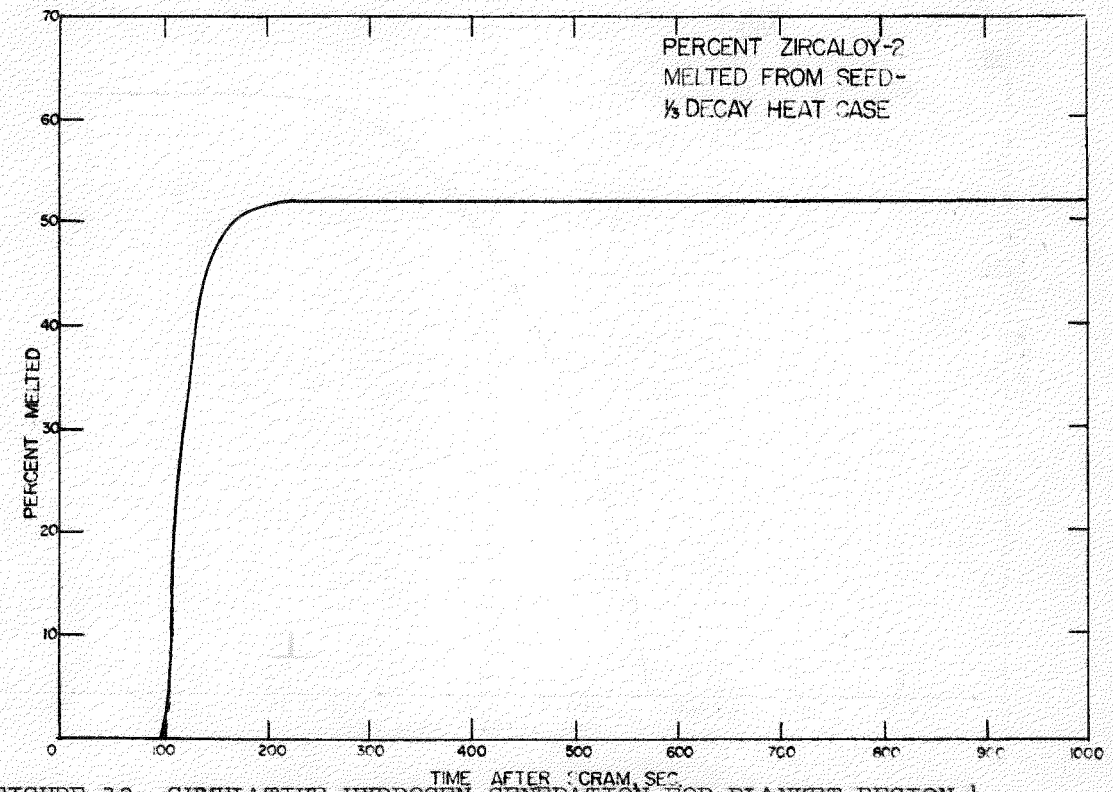

FIGURE 13 CUMULATIVE HYDROGEN GENERATION FOR BLANKET REGION 4

FIGURE 14 PERCENT ZIRCALOY-2 MELTED FROM SEED

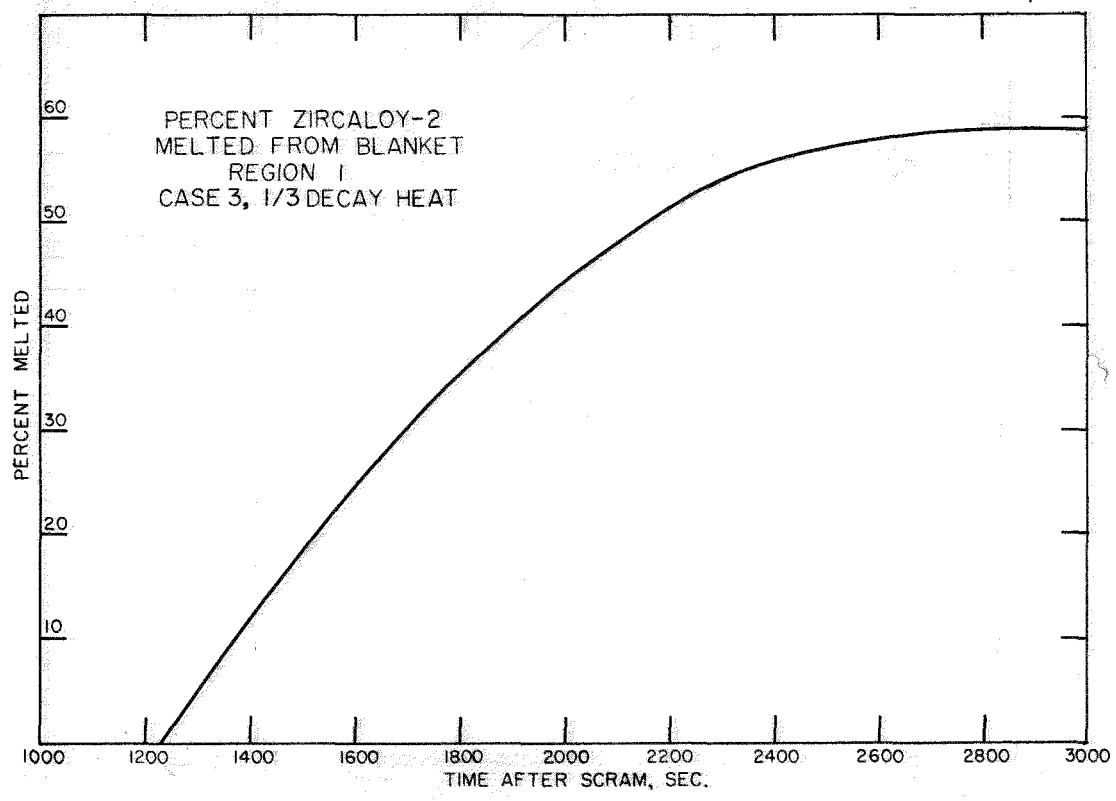

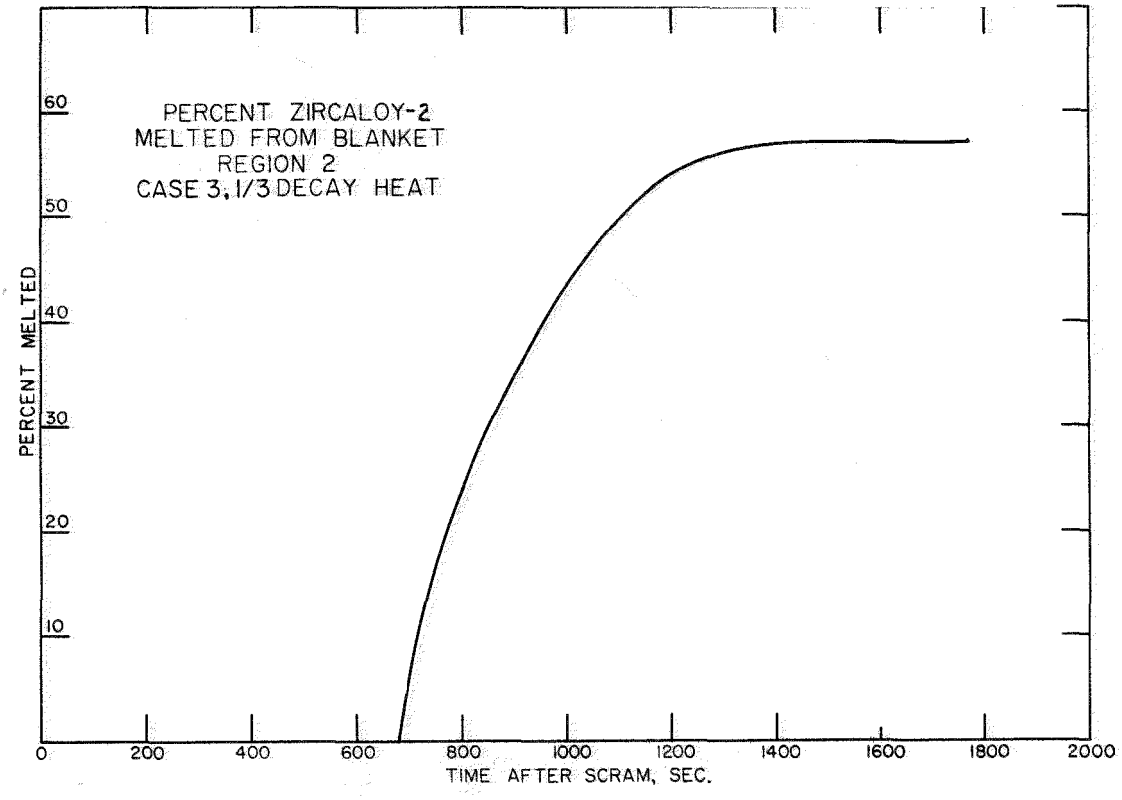

FIGURES 15 AND 16
PERCENT ZIRCALOY-2 MELTED FROM BLANKET REGIONS 1 AND 2

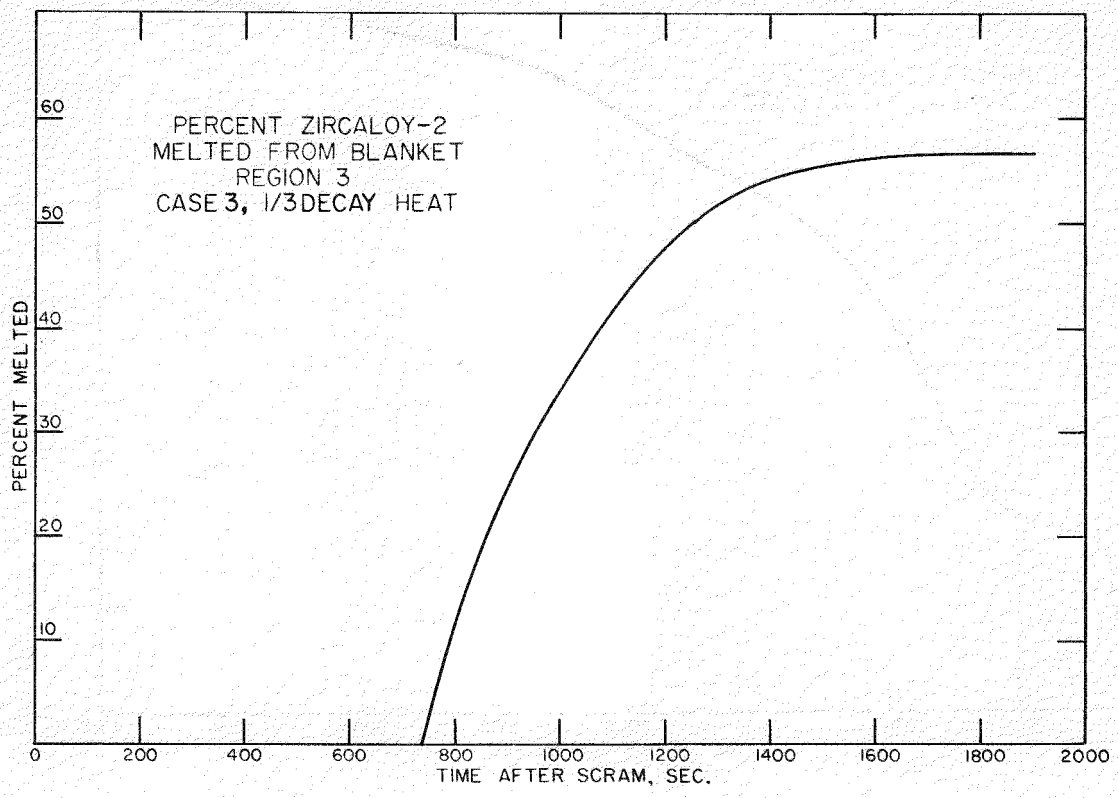

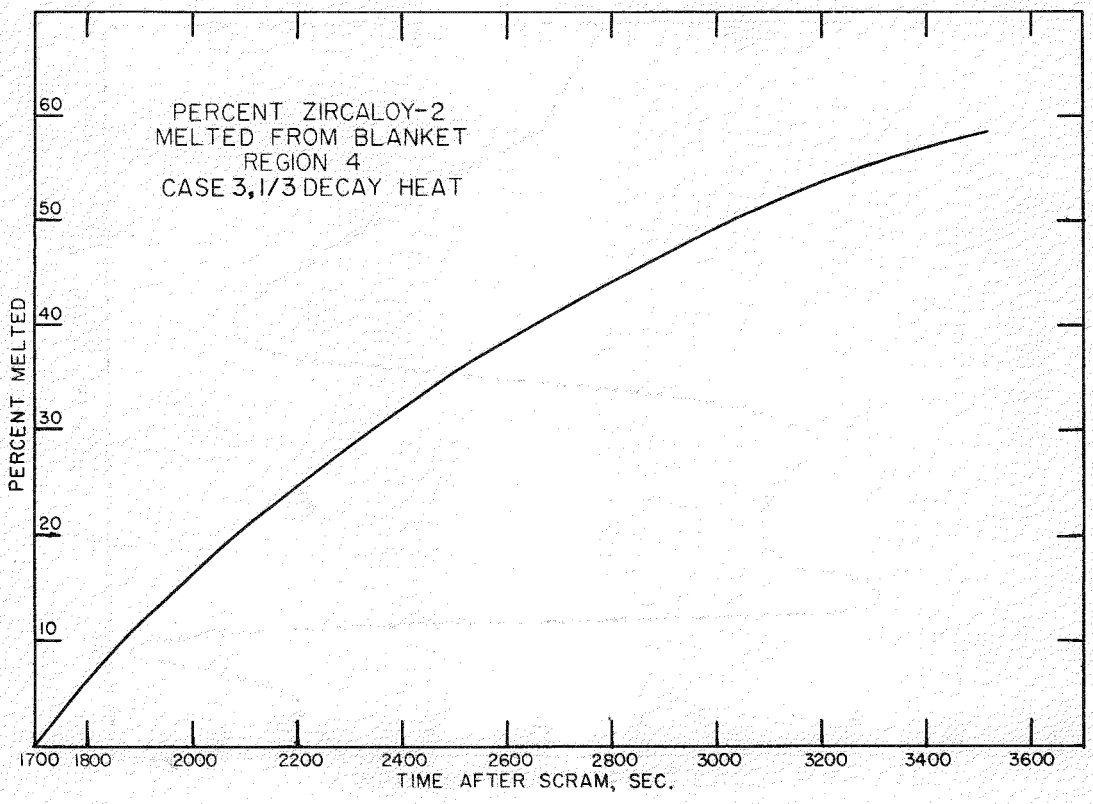

FIGURES 17 AND 18
PERCENT ZIRCALOY-2 MELTED FROM BLANKET REGIONS 3 AND 4

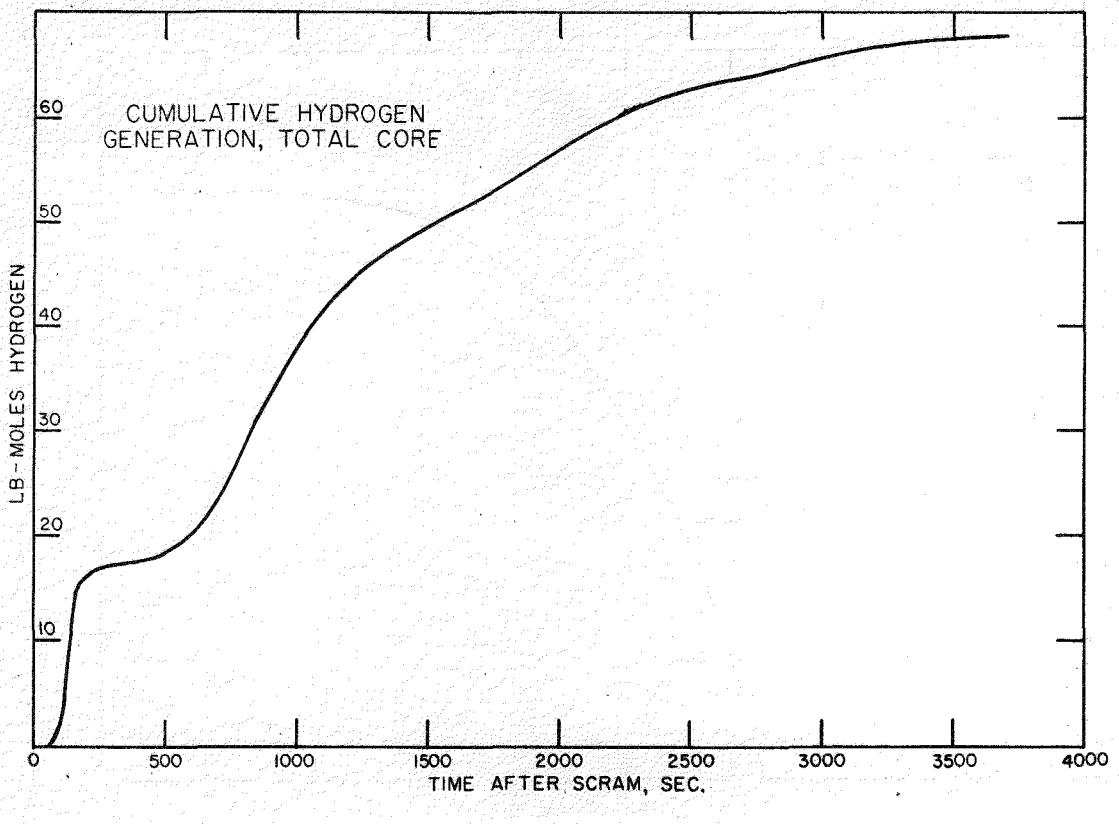

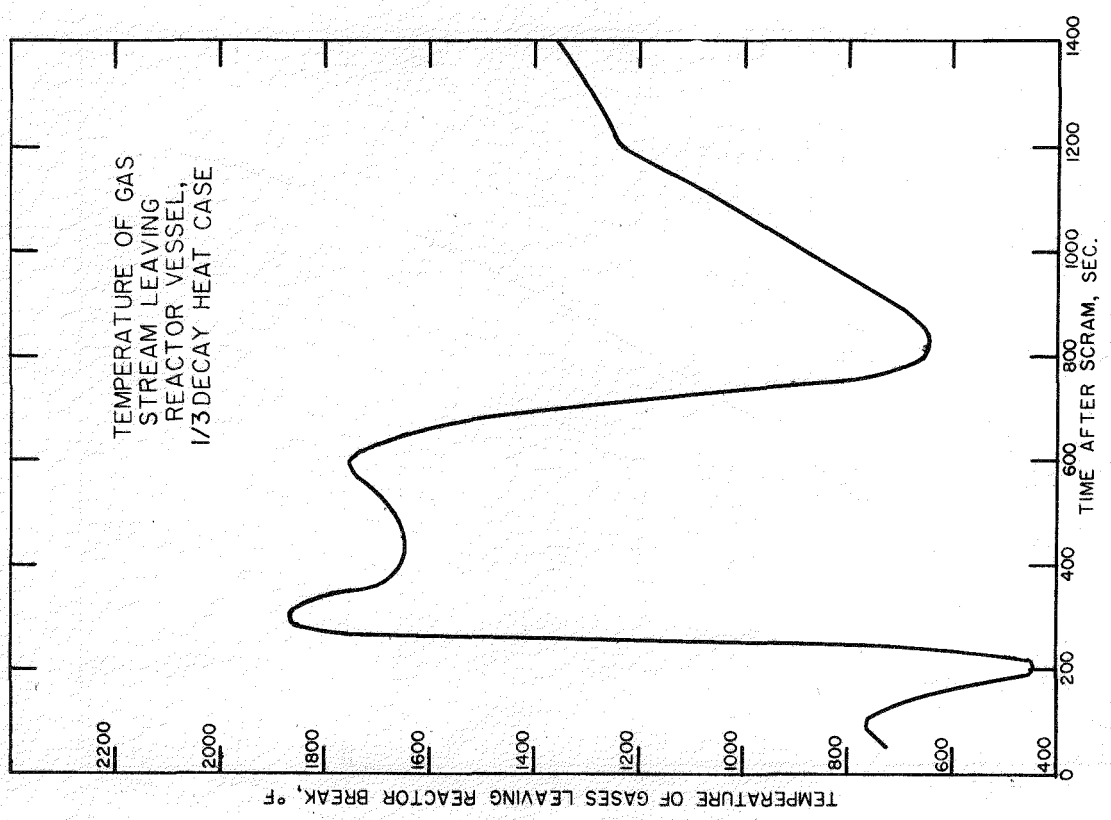

FIGURE 19 CUMULATIVE HYDROGEN GENERATION, TOTAL CORE

FIGURE 20 TEMPERATURE OF GAS STREAM LEAVING REACTOR VESSEL

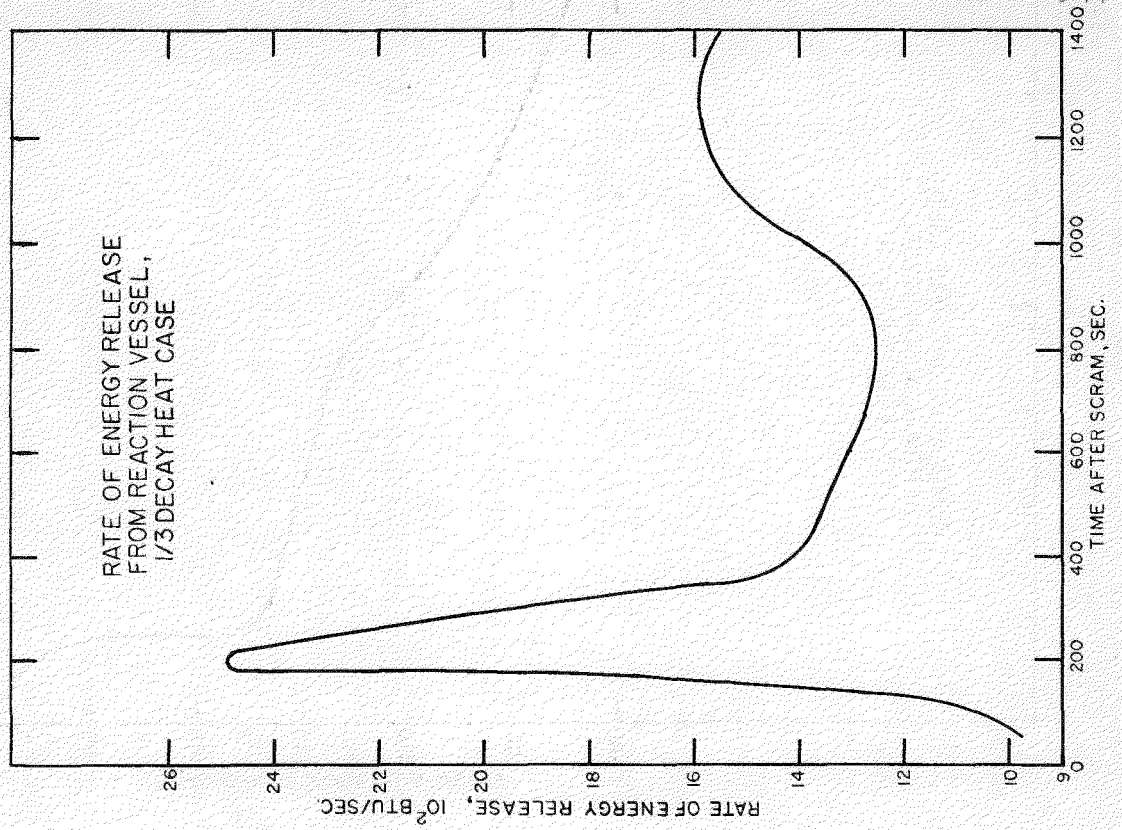

FIGURE 21 RATE OF ENERGY RELEASE FROM REACTOR VESSEL

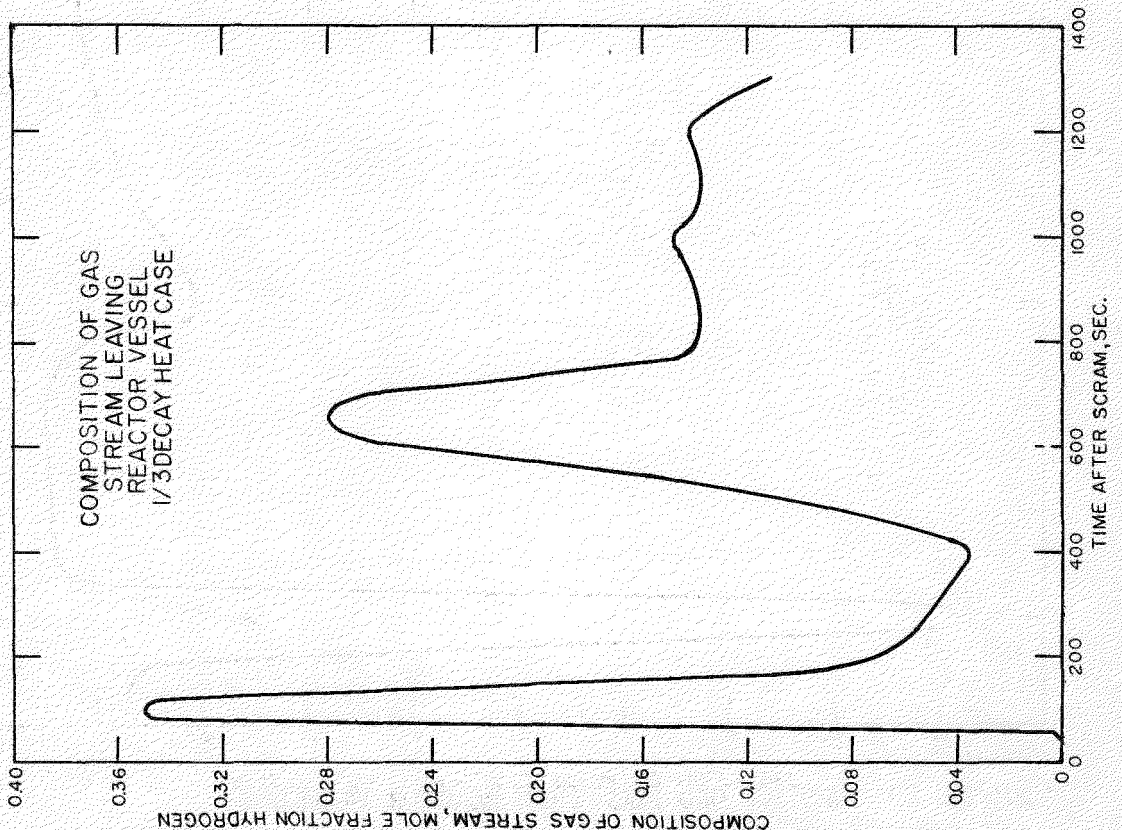

FIGURE 22 COMPOSITION OF GAS STREAM LEAVING REACTOR VESSEL

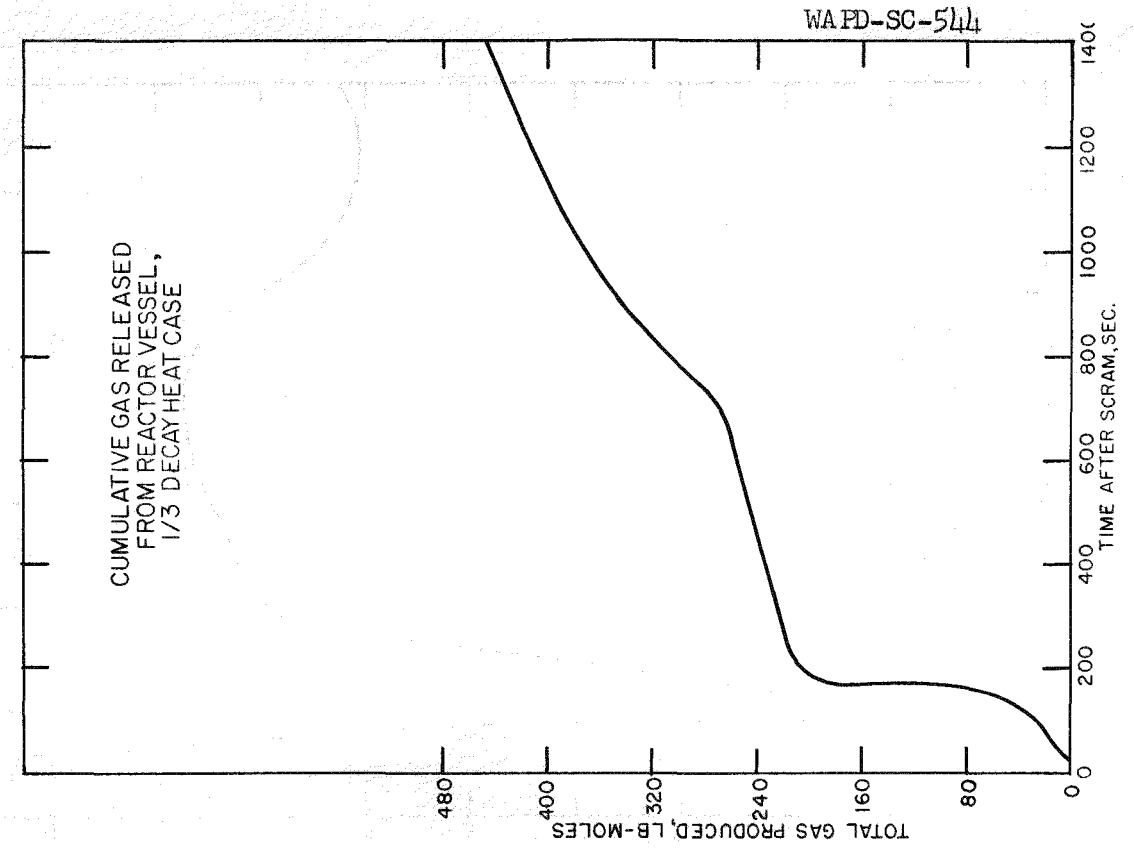

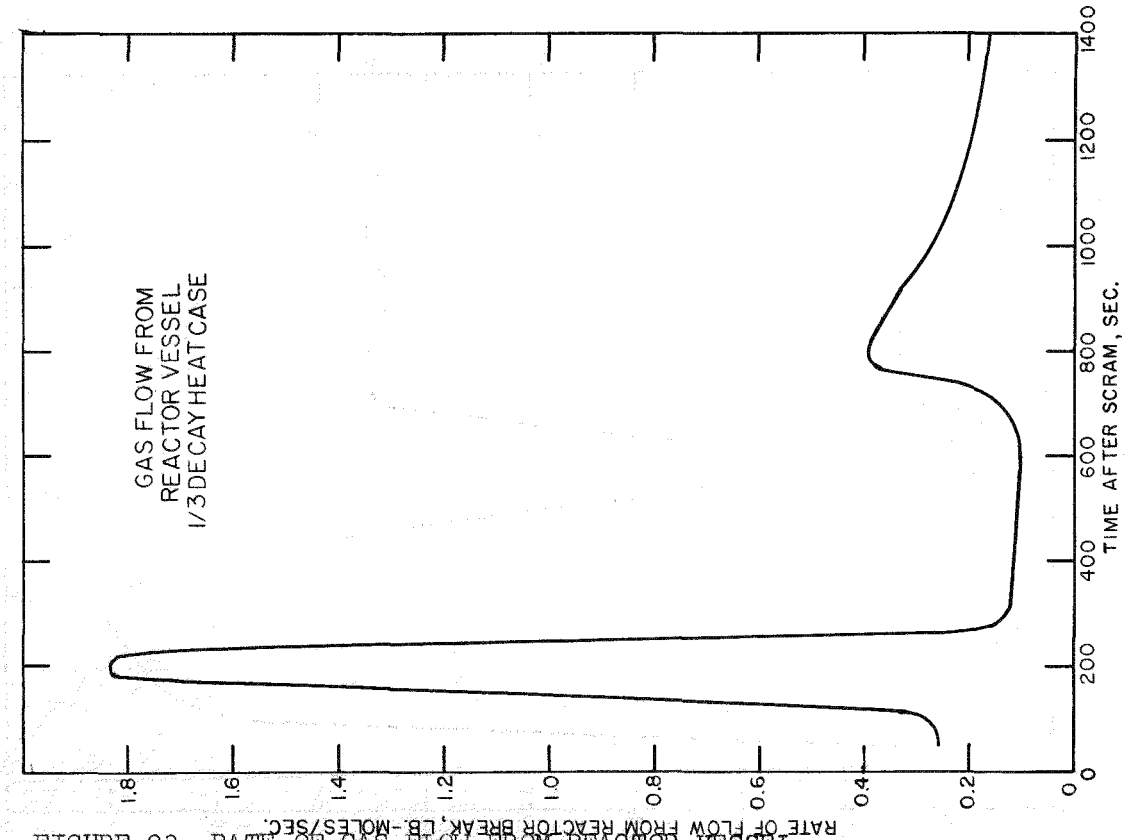

FIGURE 23 RATE OF GAS FLOW FROM REACTOR VESSEL

FIGURE 24 CUMULATIVE GAS RELEASED FROM REACTOR VESSEL

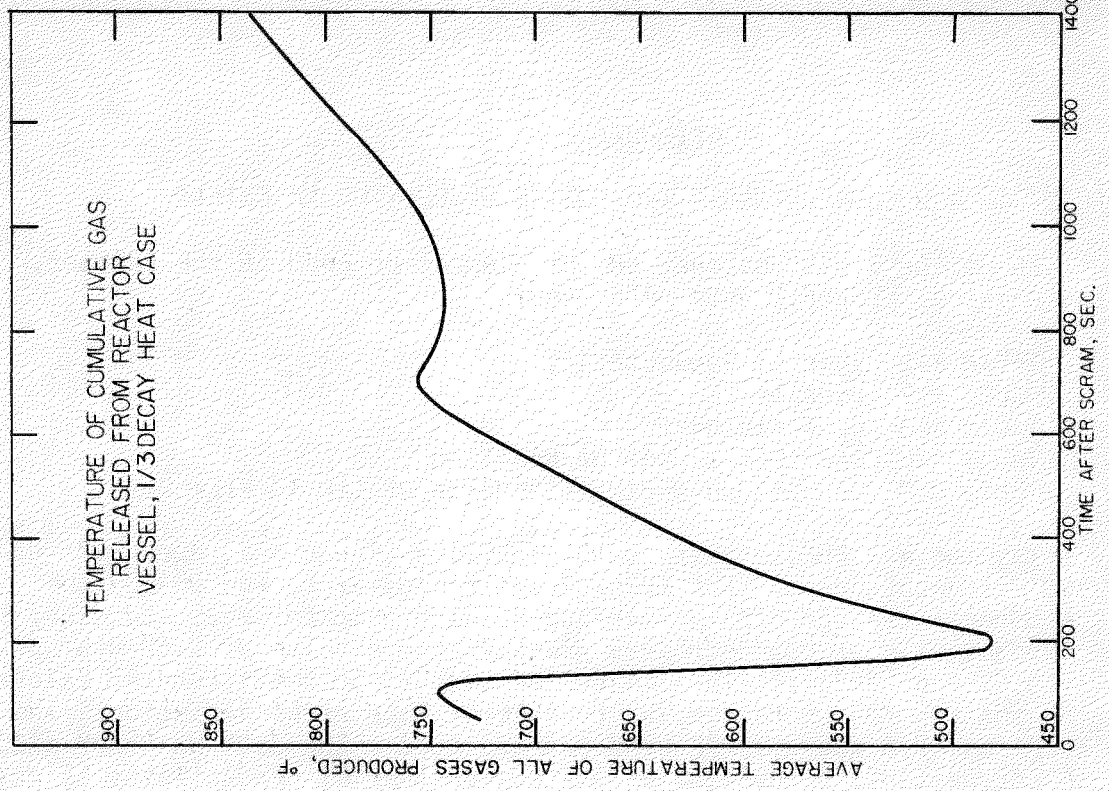

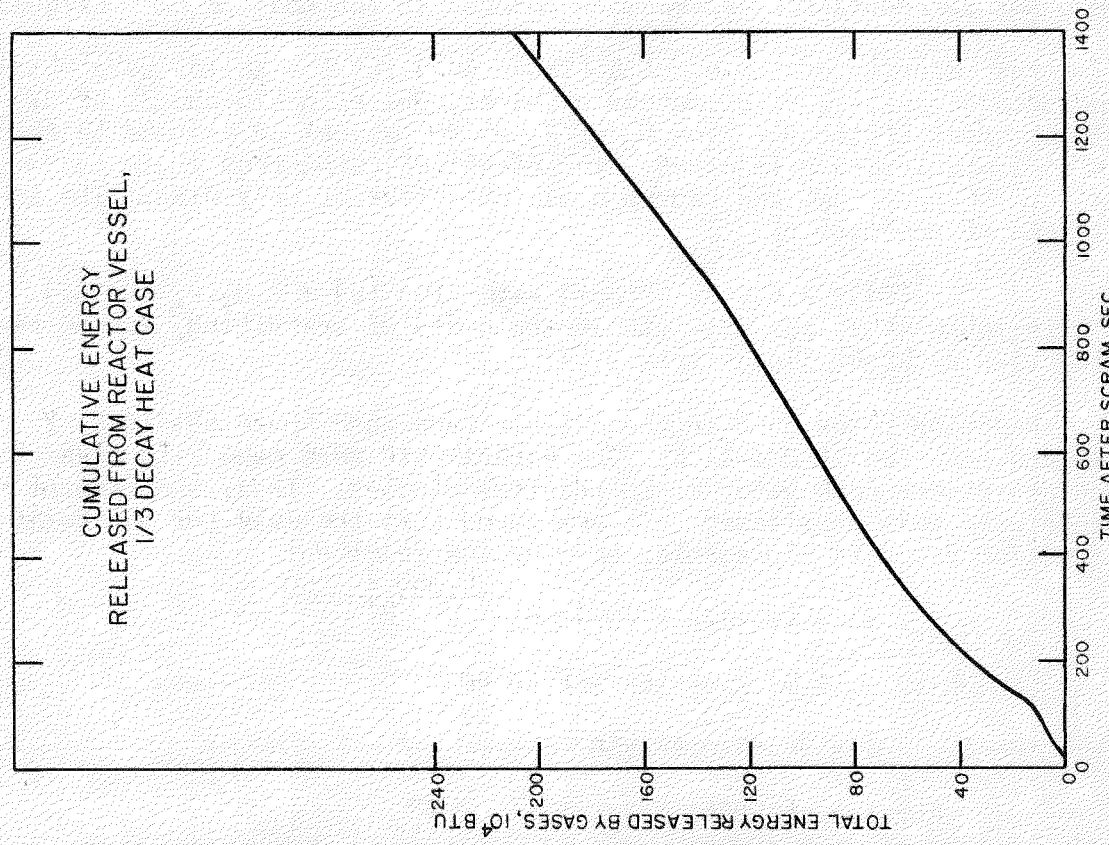

FIGURE 25 CUMULATIVE ENERGY RELEASED FROM REACTOR VESSEL

FIGURE 26 TEMPERATURE OF CUMULATIVE GAS RELEASED FROM REACTOR VESSEL

APPENDIX A

PHYSICAL AND THERMODYNAMIC PROPERTIES OF REACTOR MATERIALS

In making a heat balance on the blanket or seed in the reactor, the following physical property data were used:

Table A-1 Thermal Conductivity
Table A-2 Density
Table A-3 Specific Heat
Table A-4 Isothermal Heat of Reaction
Table A-5 Conditions During Discharge of Liquid From Core

The thermal conductivity data of solids (Table A-1) are given up to about 3300°F in most cases. For ZrO_2, Zr, Zircaloy-2, U, and SS-303 the thermal conductivities generally increase at high temperatures. However, the thermal conductivity of UO_2 decreases greatly from a value of 4.68 Btu/hr-ft^2-°F/ft at 392°F to 0.69 at 3272°F. This makes the conduction heat-transfer calculations on the UO_2 rods more complex because of this great variation. The values of Zircaloy-2 above 752°F were extrapolated using data on other alloys of Zr. A correction for porosity of the UO_2 on thermal conductivity is given in the table.

The density data in Table A-2 are given for room temperature. These data were not corrected for temperature changes in the heat balance calculations.

The majority of the C_p data (Table A-3) for the solids were obtained from the data of Kelley, U. S. Bureau of Mines, Bulletin 476 and J. Ward, Battelle Memorial Institute. The C_p of H_2 at 50 psi can be assumed to be the same as at 1 atm within 0.1% error. The effect of going from 1 atm to 50 psi pressure on the C_p of H_2O gas causes a maximum error of only 0.5%. The isothermal heat of reaction of

$$Zr\ (c) + 2\ H_2O(g,\ 50\ psi) \longrightarrow ZrO_2\ (c) + 2\ H_2(g,\ 50\ psi)$$

is given in Table A-4. The data (including heats of transition) can be represented by a straight line within 0.5%.

Reaction rates used in the calculations were those obtained by Battelle and reported in BMI-1154. The experiments were made with steam as the reactant rather than water as in previous studies. Thus, the present assumed conditions were well duplicated. It was found that the data for the solid phase reaction could be represented best by the relation:

$$v^2 = (0.1132 \times 10^6)\, t\, e^{\frac{-34{,}000 \pm 1440}{RT}}$$

with v = ml hydrogen per sq cm

T = degrees Kelvin

and t = seconds

Reaction rates for the reaction of water (and steam) with molten Zircaloy-2 could not be correlated in any reasonable manner with temperature. It was concluded that the conditions within the PWR were best represented by the experiments reported in Aerojet-General Progress Report AGC-AE-22, September 14, 1956. For a 0.2-in. (5000 microns) diameter droplet, the Aerojet tests showed that 12 w/o of the Zircaloy-2 would be reacted. This value was used in predicting the amount of reaction which would occur for the Zircaloy-2 which melted from the reactor core and dropped to the bottom of the reactor vessel.

A tabulation of conditions in the reactor, during the blow-down following a pipe rupture equivalent in area to a 15 in. ID pipe shear, is given in Table A-5. This table, obtained from WAPD-SC-549, shows that for saturation conditions, an appreciable fraction of the mixture is liquid. However, after 15 seconds when the water level reaches the top of the core, the remaining liquid may be near the bottom of the tank or may vaporize on cooling the vessel walls of the shell. Hence, most of this remaining water may not be available for cooling the core after the first 15 seconds following a break and loss of coolant.

TABLE A-1 THERMAL CONDUCTIVITIES OF SOLIDS, Btu/hr-ft^2-°F/ft

Temperature °C	Temperature °F	UO_2 5% Porosity 10.4 Density	UO_2 5% Porosity 10.4 Density	ZrO_2 (1)(2) 0% Porosity 6.1 Density	Zr(3)	Zircaloy-2(3)	U(3)(4)	SS-303(6)
20	68	(1)	(5)		12.2	8.44	14.5	
100	212	5.50	5.26	1.13	11.5	8.09	15.0	8.71
200	392	4.45	4.68	1.13	10.8	7.98	16.3	9.19
300	572				10.4	8.03	17.6	10.2
400	752	3.24	3.70	1.19	10.3	8.15	19.1	11.4
500	932				10.4	(8.17)	20.8	12.3
600	1112	2.45	2.89	1.21	10.3	(8.26)	22.8	13.3
700	1292				10.7	(8.35)	24.3	14.3
800	1472	2.08	2.25	1.27	(11.2)	(8.5)	27.5	15.5
900	1652	1.91					30.2	
1000	1832		1.79	1.32	(12.2)	(8.7)	33.5	16.5
1200	2192		1.39	1.38	(13.5)	(8.9)	(39.7)	
1400	2552		1.10	1.41	(14.7)	(9.1)	(46.5)	
1600	2912		0.867	(1.44)	(16.3)	(9.3)	(53.5)	
1800	3272		0.694	(1.48)	(17.3)	(9.5)	(60.6)	
2000	3632		0.520	(1.52)		(9.8)	(68.5)	
2200	3992		0.405					

(1) J. of Am. Cer. Society, 37, 108 (1954).
(2) Correction for porosity: Multiply values of 0% porosity by (1-fraction porosity).
(3) Deem, Battelle.
(4) k is unstable and generally increases on thermal cycling.
(5) Vasilos, MIT, Unpublished work.
(6) J. App. Phys., 43, 177 (1952).
Note: Values in parentheses are extrapolated.

* * * * * * * * * * *

TABLE A-2 DENSITIES OF SOLIDS AT ROOM TEMPERATURE

Material	Density, lb/cu ft	Source
UO_2	675 (0% porosity)	Jr. of Am. Cer. Soc., 37, 108 (1954)
	641 (5% porosity)	Ditto
ZrO_2 (Hf free)	380 (0% porosity)	"
	330 (13.5% porosity)	"
Zr	405	Boulger
Zircaloy-2	(405)	Estimated
U	1200	Materials and Methods, 5/54

TABLE A-3 SPECIFIC HEAT, C_p, Btu/lb-mole-°F

	T = °K	Range
Solids		
U (α)	$C_p = 3.39 + 8.02 \times 10^{-3} T + 0.70 \times 10^5 \times T^{-2}$	298° to 935°K
U (β)	$C_p = 10.18$	935° to 1045°K
U (γ)	$C_p = 9.20$	1045° to 1300°K
	$C_p = 9.20$ (Extrapolated)	Above 1300°K
	Note: ΔH (Transition $\alpha \rightarrow \beta$) = +700 cal/gm atm (935°K) ΔH (Transition $\beta \rightarrow \gamma$) = +1145 cal/gm atm (1045°K) (The ΔH transition can be neglected)	
UO_2	$C_p = 19.20 + 1.62 \times 10^{-3} T - 3.96 \times 10^5 T^{-2}$	298° to 1500°K
	Extrapolate above equation	Above 1500°K
Zr (α)	$C_p = 6.83 + 1.12 \times 10^{-3} T - 0.87 \times 10^5 T^{-2}$	298° to 1135°K
Zr (β)	$C_p = 7.27$	1135° to 1400°K
	$C_p = 7.27$ (Extrapolated)	1400° to 2125°K
	Note: ΔH (Transition $\alpha \rightarrow \beta$) = +920 cal/gm atm (1135°K) (The ΔH transition can be neglected since its value is only about 1% of the ΔH reaction of $Zr + 2H_2O$.)	
ZrO_2 (α)	$C_p = 16.64 + 1.80 \times 10^{-3} T - 3.36 \times 10^5 T^{-2}$	298° to 1478°K
ZrO_2 (β)	$C_p = 17.80$	1478° to 1850°K
	$C_p = 17.80$ (Extrapolated)	1850° to 2950°K
	Note: ΔH (Transition $\alpha \rightarrow \beta$) = +1420 cal/gm-mole (This ΔH can be neglected)	
Zircaloy-2	Assume same as Zr α and β .	
Gas		
H_2 (Ideal gas, 1 atm, 50 psi)	$C_p = 6.52 + 0.78 \times 10^{-3} T + 0.12 \times 10^5 T^{-2}$	298° to 3000°K
H_2O (Ideal gas, 1 atm)	$C_p = 7.17 + 2.56 \times 10^{-3} T + 0.08 \times 10^5 T^{-2}$	298° to 2500°K
H_2O (50 psi)	As an estimate the above C_p at 1 atm pressure can be used with a maximum error of 0.5%.	

TABLE A-4 ISOTHERMAL HEAT OF REACTION

$$Zr(c) + 2H_2O(g) \longrightarrow ZrO_2(c) + 2H_2(g)$$

Values at 50 psi and Reactants and Products at the Same Temperature as Given Below:

°K	H_T, Calories/gm mole
298	-145,900
600	-144,120
1000	-141,880
1135 ($Zr\ \alpha$)	-141,180
1135 ($Zr\ \beta$)	-142,130
1200	-141,750
1300	-141,260
1400	-140,720
1478 ($ZrO_2\ \alpha$)	-140,360
1478 ($ZrO_2\ \beta$)	-138,910
1500	-138,820
1600	-138,470
1700	-138,160
1800	-137,780
1900	-137,490
2000	-137,180

The above data can be approximately represented within an error of 0.6% by the following equation:

$$H_T = -147,600 + 5.34T \quad (T = °K)$$

Note: The effect of pressure on the C_p of H_2 and H_2O was neglected but introduces an error of less than 0.5%.

TABLE A-5 CONDITIONS DURING DISCHARGE OF FLUID FROM CORE FOR A 15-INCH BREAK

Time, sec	Water and Steam Remaining in Reactor, lbs	Upstream Pressure, psia	Temp., °F	Rate of Flow, lbs/sec	Average Vapor-Liquid Density, lbs/cu ft
0 (at scram)	108,300	930	535	5400	46.8
1	101,500	893	531	5150	44.8
2	94,700	880	529	5000	41.8
3	88,000	866	527	4850	38.8
4	81,400	850	525	4700	36.0
5	75,000	830	523	4500	33.1
6	68,800	810	520	4350	30.4
7	62,700	786	516	4150	27.7
8	56,600	760	512	3900	25.0
9	51,200	730	509	3700	22.6
10	45,600	708	504	3550	20.1
11	40,400	662	497	3250	17.8
12	35,700	622	493	3025	15.7
13	31,200	578	482	2750	13.8
14	27,200	534	474	2500	12.0
15	23,300	487	464	2250	10.3
16	19,600	434	453	2000	8.65
17	16,400	389	442	1800	7.23
18	14,000	350	431	1600	6.18
19	11,100	300	417	1400	4.90
20	8,900	250	401	1200	3.93
21	7,000	200	382	950	3.08
22	5,400	150	358	750	2.38
23	4,300	100	328	500	1.90

APPENDIX B

REACTOR BLOWDOWN AND ADDITION OF COOLING WATER

During normal operation of the reactor, cooling water is flowing from the bottom inlet pipes, through the flow baffle, through the fuel assemblies, and then out of the reactor via the 15 in. ID outlet nozzles. If a rupture should occur in the 15 in. ID bottom inlet piping, the primary coolant water would drain out through the opening. When the primary system pressure is reduced to 1600 psi, safety shutdown of the reactor (scram) would automatically occur. When the pressure is reduced to 500 psi, safety injection water can be injected through the top 15 in ID (exit) coolant pipes into the reactor vessel. The maximum safety injection rate is 3000 gpm.* The question arises as to the distribution of this water over the core and the level of water in the core.

Two calculations were made:

(1) To determine the extent to which the water supplied would develop a full head to the top of the core and maintain a full flow of water downward through the assemblies.

(2) To determine the trajectories of the jets of water issuing from the holes in the hold-down barrel. This provides an estimate of the distribution of the injection water to the assemblies.

B-1. Flow of Water to Completely Cover Core

At low injection rates, the liquid head in a fuel assembly is dependent upon the water flow in that assembly. By making use of the pressure drop characteristics of the fuel elements, the flow of water required to completely cover the core was calculated and is tabulated below in Table B-1.

TABLE B-1, FLOW OF WATER TO COVER CORE

Region	No. of Assemblies	Water Flow gpm	Water Flow/Assembly gpm
1	21	755	35.7
2	24	1,870	77.8
3	40	2,500	62.5
4	28	670	18.1
Seed	32	5,680	182
	Total	11,475 gpm	

* See WAPD-PWR-970, "Description of the Shippingport Atomic Power Station", for details concerning the Safety Injection System design and operation.

This shows that the maximum injection rate of 3000 gpm will not provide a positive full flow through all assemblies in the core. Since it is considered unreasonable to supply 12000 gpm to the core, other means of achieving a satisfactory distribution were provided, as discussed in the next section.

B-2. Trajectory of the Injection Water from the Hold-Down Barrel

As indicated in the introduction of this report and discussed more completely in WAPD-PWR-970*, the cooling water injected into the reactor enters the reactor via the two rows of holes in the hold-down barrel. The lower row includes 32 holes of 1-1/8 in. diameter located 6 in. below the centerline of the outlet nozzles. Each of the holes in the lower row is located to direct a stream of water to a single control rod shroud.

The upper row includes 32 holes, 1-3/4 in. in diameter and located 12 in. above the first row. The holes in the upper row are located to avoid interference of the jets from the upper and lower holes.

If no control rods or shrouds were present, and the maximum expected amount of water, 3000 gpm, is injected, water from the lower holes would strike the upper grid plate 48 in. from the hold-down barrel (nearly the center of the reactor); at the same time water from the upper holes would strike the upper grid plate 43 in. from the hold-down barrel. However, the control rod shrouds are at a maximum distance of 19 in. from the hold-down barrel. Hence, the jets of water from both rows of holes will strike the shrouds before falling to the upper grid plate. At the minimum injection rate of 1500 gpm the jets from the lower row of holes will reach the seed; but the jets from the upper row will fall short of the more remote seed assemblies, just reaching the blanket assemblies in region 3.

In either case, about half of the water striking the shrouds is expected to splash off to the adjacent assemblies in regions 2 and 3, and possibly farther. If evenly distributed, the amounts flowing through each assembly of the seed and regions 2 and 3 would be in excess of the amount required for cooling by a factor of at least 4. This factor provides a margin to cover any non-uniformity of distribution of the injection water to the assemblies.

---

* See previous page.

APPENDIX C

HEAT-TRANSFER COEFFICIENTS

To make a heat balance on the reactor core, it was necessary to have heat-transfer coefficients for the steam and steam-water mixtures passing through the channels in the blanket fuel bundles and the seed plate assemblies. During the normal operation of the reactor, the heat generated is removed by cooling water flowing up through the reactor. The problem of estimating the heat-transfer coefficients between the single-phase water and seed plates and blanket is a relatively straight-forward calculation. The equation of Dittus and Boelter (McAdams, Heat Transmission, 3rd edition, p. 219) can be used employing a suitable equivalent or hydraulic radius for the noncircular channels. Coefficients, based on this equation, are used in the thermal and hydraulic design of the PWR core.

For the present problem, if a 15 in. break occurs in the bottom inlet piping, the water (and steam) would flow out this opening. During the first 26 second period after the break occurred, the fluid would discharge from the core as given in Table A-5. A portion of the discharging fluid would flow through the blanket and seed channels and provide some cooling for the reactor core. At the time of the break (zero seconds), the fluid in the channels would be entirely liquid water. After about 15 seconds the fluid would be a mixture of about one-fifth water and four-fifts steam. The per cent of water in the mixture would continue to decrease as further time elapsed.

The problem is first to determine or estimate a suitable heat-transfer coefficient for the varying steam-water mixture during the first few seconds after the break occurs for the transient condition when the water begins to "uncover" the core. The only comparable data available for two-phase heat-transfer coefficients are given by McAdams (Heat Transmission, 3rd ed., p. 397, Fig. 14-24). He correlates the heat-transfer coefficient, h, Btu/hr-sq ft-^{o}F, with the volumetric ratio, air/water, for various liquid water rates. In the reactor during the first 15 seconds period, the average ratio of steam/water is slightly less than 1/1. From the correlation, the h is estimated for this condition as about 800 Btu/hr-sq ft-^{o}F. This value is somewhat conservative since steam-water mixture should give higher h values than air-water mixtures. Also, the cross-sectional areas for flow in the core are much smaller than that of the tubes used in McAdams. Smaller areas should give greater turbulence and, hence, higher h values. Constant values for h of 500 and 1000 were used for the analysis reported in Appendix F. Using the value of 1000 should be reasonable and that of 500 provides a check of the sensitivity of the resulting temperature distribution to the input values chosen.

During Phase III (26 seconds after "scram" to meltdown assuming water addition to the core) calculations were made assuming the fluid in the blanket and seed channels was all gas phase consisting of steam and the hydrogen produced by chemical reaction. The heat-transfer coefficient used is the standard equation of McAdams (p. 219) for heat transfer to liquids or gases as follows:

$$\frac{hD_g}{k_g} = (0.76)\ (0.023) \left(\frac{D_g W_g}{A_g \mu_g}\right)^{0.8} \left(\frac{C_g \mu_g}{k_g}\right)^{0.4}$$

The nomenclature is as in Appendix G. The factor of 0.76 was used since passage having cross sections other than circular give h values about 24% below those for circular passages (McAdams, p. 248).

APPENDIX D

DECAY HEAT FLUX DISTRIBUTION

The decay heat generation (after shutdown) varies with position in the core in approximately the same proportion as the heat generation during normal reactor operation. Both axial and radial variations occur. Also, the variations in the blanket and seed regions differ somewhat from each other.

Axial variations, over the length of the fuel elements, are discussed further in Appendices F and I, where analytical approximations are used for computational purposes. For purposes of these calculations, peak-to-average ratios of 2.00 in the seed and 1.77 in the blanket were chosen.

Radial variations likewise occur. The 7 blanket rods placed end-to-end in the core are assumed to constitute one long rod with the axial flux variation as mentioned above. To be conservative, this rod is assumed to have heat fluxes 1.44 times the average, thus applying an over-all peaking factor of 2.55. Similarly, a radial factor of 1.15 was used for the seed, or an over-all peaking factor of 2.30 for the seed. The average heat generation by regions (per rod or per plate) were based on PWR operating parameters.

APPENDIX E

INITIAL TEMPERATURE GRADIENTS AT SCRAM

The radial temperature gradients in the blanket rod in region 2 before scram were calculated and the data are shown in Table E-1. These temperatures are for the hottest portion of the blanket or the hottest rod. The peak heat flux from the outside of the clad surface used was 348,000 Btu/hr-ft^2. It is assumed all of this heat is generated in the UO_2 rod.

Starting with the T_s or surface temperatures which occur in normal operation of PWR, the radial temperature drop of the Zircaloy cladding was calculated at the 77 cm point longitudinally in the rod. The usual equations for steady-state heat transfer through a hollow cylinder were used. This calculation was repeated for different heat fluxes. Then the temperature drop through the helium gap was calculated. The heat transferred by radiation was only about 1% of the heat transferred by conduction and was neglected. Using the equation for heat generation in cylinders, temperatures were calculated for the interior of the UO_2 rods. The thermal conductivity varied greatly and allowance was made for this. The longitudinal heat transfer was about 1% of the radial and, hence, was neglected. The temperatures in this table are those used in Phase I when the reactor is scrammed and the decay heat is being generated.

TABLE E-1. RADIAL TEMPERATURE GRADIENT IN BLANKET ROD BEFORE SCRAM

Distance Z, cm	Local Average Thermal Flux	T_s	Thermal Flux/1.77	Clad ΔT, °F	He gap ΔT, °F	T_s UO_2, °F	Zones of Equal Cross Sec. Area (1) I °F	II °F	III °F	IV °F	V(2) °F
150	0.18	599	0.102	11	30	640	655	672	700	721	754
137	0.4	600	0.226	24	67	691	730	770	812	861	942
117	1.2	607	0.68	71	203	881	998	1146	1311	1519	1902
90	1.52	629	0.86	89	256	974	1131	1333	1568	1879	2483
77	1.77	630	1.0	104	298	1032	1223	1472	1775	2186	3062
60	1.68	620	0.95	99	283	1002	1178	1409	1684	2051	2802
40	1.36	594	0.77	80	230	904	1038	1207	1402	1661	2131
7	0.6	540	0.34	35	101	676	727	787	851	926	1053
0	0.75	540	0.42	44	125	709	773	849	931	1029	1198

(1)

Diameter of UO_2 section, in.	Zone
0.3555	I
0.3192	II
0.2764	III
0.2257	IV
0.1596	V

(2) Center-line temperature.

APPENDIX F

ANALYSIS OF TEMPERATURE DISTRIBUTION IN A BLANKET ROD DURING THE FIRST 15 SECONDS AFTER "SCRAM", (PHASE I)

The study of the temperature distributions in a blanket rod at any time has been broken up into three fairly natural divisions. The first part, called Phase I and considered in this Appendix F, is concerned with the temperature distribution in the rod during the time that the core is covered with water. It is estimated that this condition will persist for about 15 seconds after scram, assuming a 15 in. break occurs. Appendix G is concerned with the temperature distribution in the rod during such time as there might be no water added to the core, (Phase II). Appendix H is concerned with the temperature distribution in the event that water is added to the core, (Phase III).

Certain assumptions were made in order to obtain an analytic solution for the temperature distribution in the rod during the first 15 seconds. In each of these assumptions an effort was made to state the assumption in such a way as to lead to a conservative (i.e., high) estimate of the temperature distribution at the end of 15 seconds.

The assumptions that were made are given as follows:

(1) The initial temperature distribution at scram (0 seconds) was that given in Appendix E. These temperatures were calculated on the basis of an average heat generation in the hottest rod of blanket region 2 of 348,000 Btu/hr-ft^2 at scram. This includes a peaking factor of 1.44 and is for the case where the reactor was at a power of 74.4 Mw net electrical output.

In order to simplify the mathematical expression of the solution, this temperature distribution was approximated by a relation of the form

$$T(r, z, 0) = A + \left[1 + D \cos\left(\frac{2\pi z}{L}\right)\right] \sum a_n J_o(\lambda n r),$$

where A and D are given by 563.28 and 0.70123 respectively and a_n are determined for each case. The cases are given in Table F-1.

(2) The heat of the chemical reaction is negligible for this time interval and was neglected.

(3) Heat loss by radiation from a tube to adjacent tubes was neglected since it is expected that any two adjacent tubes will be at about the same temperature. In addition, during this first phase, the liquid between the tubes effectively stops any radiation that might be present.

(4) The convective heat transfer coefficient, h, was assumed to be constant. Two values of h, 500 and 1000 Btu/hr-ft^2, were assumed, based on the heat transfer from a rod to boiling water. (See Appendix C) (It was assumed that the water is boiling during the first phase.)

(5) The reactor power generation after "scram" or shutdown was that given in Figure F-1. The average heat generation at full power in the hottest rod of region 2 was 1.227 x 10^7 Btu/hr-ft^3 at scram. No credit was taken for shutdown effects which would result from the formation of steam voids. In this graph, the generation drops to about 10% of full power in the first second and then drops gradually (Figure F-1). The same amount of heat generation would be obtained if full power were continued 1/2 second beyond scram and then decreased instantaneously to about 11.24% of full power where it would begin a gradual decline. Instead of this, it was assumed that power decreases instantaneously at scram to 11.24% of full power. To compensate for this the temperature in the rod was calculated at 14.5 seconds instead of 15 seconds. The variation of heat generation with respect to time for Phase I for times less than 15 seconds was then given by

$$\text{Fraction full power} = 0.1124\ e^{-\lambda t}$$

Where $\lambda = 0.050467$

if t is given in seconds.

The longitudinal or axial variation of the heat generation, during normal operation, and assumed for all times in this transient is shown in Figure F-2.

Again in order to simplify the numerical solution for Phase I, this was approximated by an expression of the form

$$q(z,t) = \left(B + C \cos \frac{2\pi z}{L}\right) e^{-\lambda t}$$

where z is the distance measured from the center of the rod and B and C were chosen so that f (z,t) was conservative. Values chosen were:

$B = 1.65528 \times 10^6$ Btu/hr-ft^3
$C = 8.2764 \times 10^5$ Btu/hr-ft^3 (Figure P-2

This corresponds to a peak/average flux of 1.80 instead of the 1.77 predicted for PWR operation. The use of the higher peaking factor does not introduce an error but makes the calculations slightly more conservative.

(6) In order to obtain an analytic solution for Phase I, it was necessary to consider the conductivity to be constant with respect to temperature and uniform over the rod (including the Zr cladding and the He gap). However, it was determined that the average conductivity of the He gap and the Zr cladding together is about equal to the conductivity of the UO_2 core,

making this assumption more reasonable. Two values were used for conductivity, 1.8 and 2.6 Btu/hr-ft^2 °F/ft. An average value of $C_p\rho$ for the whole rod was taken to be 43.5 Btu/ft^3 °F.

(7) Heat loss at the ends of the rod was assumed zero.

(8) The temperature of the boiling water was given as a function of time in Table 5 of Appendix A. From this table the variation of water temperature with time for Phase I was determined to be $T_s(t) = F - Ge^{\beta t}$ where $F = 548.347$, $G = 13.347$, and $\beta = 0.120075$ if t is in seconds, (Figure F-3).

With these assumptions, the boundary value problem for the first phase was to find the temperature T(r, z, t) from the relations:

$$\text{I} \begin{cases} C_p\rho \dfrac{\partial T}{\partial t} = k\nabla^2 T + q(r, z, t) \\ k\left(\dfrac{\partial T}{\partial r}\right)_{r = a} = -h\left[T(a, z, t) - T_s(t)\right] \\ k\left(\dfrac{\partial T}{\partial z}\right)_{z = \pm \frac{L}{2}} = 0 \\ T(r, z, 0) = T_o(r, z) \end{cases}$$

where

C_p = average specific heat of rod.

ρ = average density of rod.

k = average conductivity of rod, (given in assumption 6).

T = temperature of rod.

t = time.

T_o = temperature of rod at time 0, (given in assumption 1).

L = total length of rod.

a = radius of the rod.

$$\nabla^2 T = \frac{\partial^2 T}{\partial z^2} + \frac{\partial^2 T}{\partial r^2} + \frac{1}{r}\frac{\partial T}{\partial r}$$

q(z, t) = heat generation (given in assumption 5).

h = convection coefficient (given in assumption 4).

T_s = steam-water coolant temperature (given in assumption 8).

The solution of this problem was obtained in three stages:

(1) First, let $T(r, z, t) = T^*(r, z, t) + U(r, z, t)$
where T^* is to be chosen in such a way that

(2) $C_p\rho \frac{\partial T^*}{\partial t} = k \nabla^2 T^* + \left(B + C \cos \frac{2\pi z}{L}\right) e^{-\lambda t}$, if $T^*(r,z,t)$ is defined by

(3) $$T^*(r, z, t) = \frac{B}{C_p\rho} e^{-\lambda t} + \cos \frac{2\pi z}{L} \; e^{-\lambda t} \sum a_n J_o(\lambda_n r)$$

where λ_n is the nth solution of

(4) $$-k \left\{ \frac{d}{dr} \left[J_o(\lambda_n r) \right] \right\}_{r = a} = h J_o(\lambda_n a)$$

and a_n is given by

(5) $$a_n = \frac{2C \, ah/k}{\left(k\lambda_n^2 + \frac{4\pi^2}{L^2} k - \lambda C_p\rho\right)\left(\frac{a^2h^2}{k^2} + a^2 \lambda_n^2\right) J_o(\lambda_n \alpha)}$$

We have that U satisfies the system:

II
$$\begin{cases} C_p\rho \frac{\partial U}{\partial t} = k \nabla^2 U \\ k\left(\frac{\partial U}{\partial r}\right)_{r = a} = -h \left[U(a, z, t) - \frac{B}{C_p\rho\lambda} e^{-\lambda t} - T_s(t) \right] \\ \left(\frac{\partial U}{\partial z}\right)_{z = \pm L/2} = 0 \\ U(r, z, o) = T_o(r, z) + \frac{B}{C_p\rho\lambda} - \cos \frac{2\pi z}{L} \sum a_n J_o(\lambda r) = U_o(r, z) \end{cases}$$

Let $U(r, z, t) = U^*(r, z, t) + V(r, z, t)$
where

(6) $$U^*(r, z, t) = \sum_n \left[b_n + \frac{\left[A - T_s(o)\right] \frac{2ah}{k}}{\frac{a^2h^2}{k^2} + a^2\lambda_n^2 J(\lambda_n a)} \right] \exp \left[\frac{-k\lambda_n^2 t}{C_p\rho} \right] J_o(\lambda_n r)$$
$$+ \cos \frac{2\pi z}{L} \sum_n (-a_n + Db_n) \exp \left[\frac{kt}{C_p\rho} \left(\lambda_n^2 + \frac{4\pi^2}{L^2} \right) \right] J_o(\lambda_n r)$$

where b_n are determined from the equation

(7) $T_o(r,z) = A + (1 + D \cos \frac{2\pi z}{L}) \sum_n b_n J_o(\lambda_n r)$ with λ_n subject to Equation 4.

V is then the solution of the following set of equations:

III
$$\begin{cases} C_p \rho \dfrac{\partial V}{\partial t} = k \nabla^2 V \\ k \left(\dfrac{\partial V}{\partial r}\right)_{r = a} = -h \left[V(a,z,t) - \varphi(t)\right] \text{ where } \varphi(t) = \dfrac{B}{C_p \rho \mathcal{H}} e^{-\mathcal{H}t} + T_s(t) \\ \left(\dfrac{\partial V}{\partial z}\right)_{z = \pm L/2} = 0 \\ V(r,z,o) = 0 \end{cases}$$

The function

(8) $V(r,z,t) = \int_o^t \varphi'(t-\tau)\, V^*(r,z,\tau)\, d\tau + \varphi(o)$

Will be a solution of system III if $V^*(r,z,t)$ is a solution of

IV
$$\begin{cases} C_p \rho \dfrac{\partial V^*}{\partial t} = k \nabla^2 V^* \\ k \left(\dfrac{\partial V^*}{\partial r}\right)_{r = a} = -h \left[V^*(a,z,t) - 1\right] \\ V^*(r,z,o) = o \\ \left(\dfrac{\partial V^*}{\partial z}\right)_{z = \pm L/2} = o \end{cases}$$

This gives

(9) $V^*(r,z,t) = 1 - \sum_n \alpha_n J_o(\lambda_n r)\, e^{-\frac{k \lambda_n^2 t}{C_p \rho}}$

where

(10) $\alpha_n = \dfrac{2ah/k}{\left(\dfrac{a^2h^2}{k^2} + a^2\lambda_n^2\right) J_o(\lambda_n a)}$

Summarizing these results we have that

$$(11)\quad T(r,z,t) = T^*(r,z,t) + U^*(r,z,t) + \int_0^t \varphi'(t-\tau)\, V^*(r,z,t)\, d\tau + \varphi(o)$$

Now, if we let $T_s(t) = F - Ge^{\beta t}$ (see assumption 8) the integral can be evaluated. Adding the results and collecting terms then gives finally:

$$(12)\quad T(r,z,t) = F - Ge^{\beta t} + \cos\frac{2\pi z}{L}\exp(-\mu t)\sum_n a_n J_o(\lambda_n r)$$

$$+ \sum_n \left[b_n + (A - F + G)\,\alpha_n\right] \exp\left(-\frac{k\lambda_n^2 t}{C_p\rho}\right) J_o(\lambda_n r)$$

$$+ \cos\frac{2\pi z}{L}\sum_n (-a_n + Db_n)\exp\left[\frac{kt}{C_p\rho}\left(\lambda_n^2 + \frac{4\pi^2}{L^2}\right)\right] J_o(\lambda_n r)$$

$$+ \sum_n \alpha_n J_o(\lambda_n r)\left\{\frac{B}{C_p\rho\mu - k\lambda_n^2}\left[\exp\left(-\frac{k\lambda_n^2 t}{C_p\rho}\right) - \exp(-\mu t)\right]\right.$$

$$\left. - \frac{GB}{\beta + \frac{k\lambda_n^2}{C_p\rho}}\left[\exp\left(-\frac{k\lambda_n^2}{C_p\rho}\right) - \exp(\beta t)\right]\right\}$$

Where a_n, b_n, α_n are given by Equations 5, 7, and 10 respectively, λ_n is given by Equation 4. F, G, β are given in assumption 8; μ, B, and C are given in assumption 5; A and D are given in assumption 1; and k and $C_p\rho$ are given in assumption 6.

Calculations were made with Equation 12 for the following cases:

Case	1	2	3
Diameter Rod, (in)	0.413	0.413	0.413
Thermal conductivity, (Btu/hr-ft^2°F/ft)	2.6	2.6	1.8
h,(Btu/hr-ft^3°F	500	1000	1000
$C_p\rho$, (Btu/ft^3°F)	43.5	43.5	43.5
Time after scram, (sec)	15	15	15

Some temperatures calculated from Equation 12 for these conditions at different points in the rod are as follows: Water Temperature at this time is 472°F.

TABLE F-1

TEMPERATURES AT VARIOUS POSITIONS OF BLANKET ROD AT 15 SECONDS AFTER SCRAM

Axial Distance from Center of Rod, ft.	Radial Distance from Axis of Rod, in.	Case 1 Temperature, °F	Case 2 Temperature, °F	Case 3 Temperature, °F
0 (center of rod) (max temp)	0(center)	682	618	720
	0.413/4	646	584	661
	0.413/2 (surface)	547	501	511
1.5	0	618	574	641
	0.413/4	594	553	602
	0.413/2	525	495	499
3 (end of rod)	0	554	531	563
	0.413/4	542	523	544
	0.413/2	503	488	488

These data are plotted in Figures F-4(a), F-4(b), and F-4(c). These temperatures are to form the basis for choosing initial temperatures for the second part (Phase II). To reduce the magnitude of the Phase II and Phase III calculations, it was necessary to assume that the temperature of the rod is independent of the radius of the rod. This seems justified in view of the rather small temperature gradient from the center to the outside of the rod found in the above three cases. This maximum gradient was 209°F in case 3. However, it was desirable to use a temperature averaged over the radius of the rod as a basis for choosing the initial temperature for Phase II.

The average chosen was as follows:

$$(13)\quad \bar{T}(z, 14.5) = 2\pi \int_0^a r\, T(r, z, 14.5)\, dr \Big/ 2\pi \int_0^a r\, dr$$

which gives for the three cases considered the averaged temperature $\bar{T}$,

$$(14)\ \text{Case 1.}\quad \bar{T}(z, 14.5) = 570.52 + 41.64 \cos\left(\frac{2\pi z}{L}\right)$$

$$(15)\ \text{Case 2.}\quad \bar{T}(z, 14.5) = 533.61 + 22.82 \cos\left(\frac{2\pi z}{L}\right)$$

$$(16)\ \text{Case 3.}\quad \bar{T}(z, 14.5) = 567.64 + 42.35 \cos\left(\frac{2\pi z}{L}\right)$$

For the initial temperatures of Phase II considered in Appendix G, it was decided to use the temperatures of Case 1 for an h value of 500 and k of 2.6.

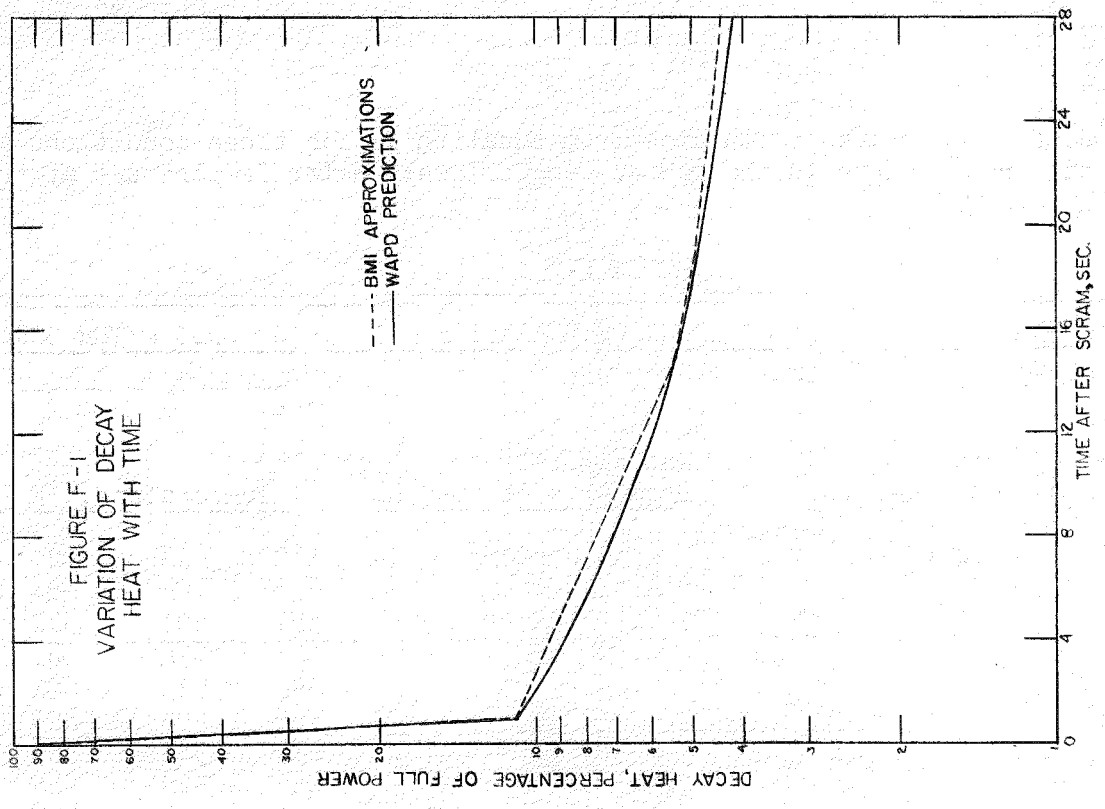

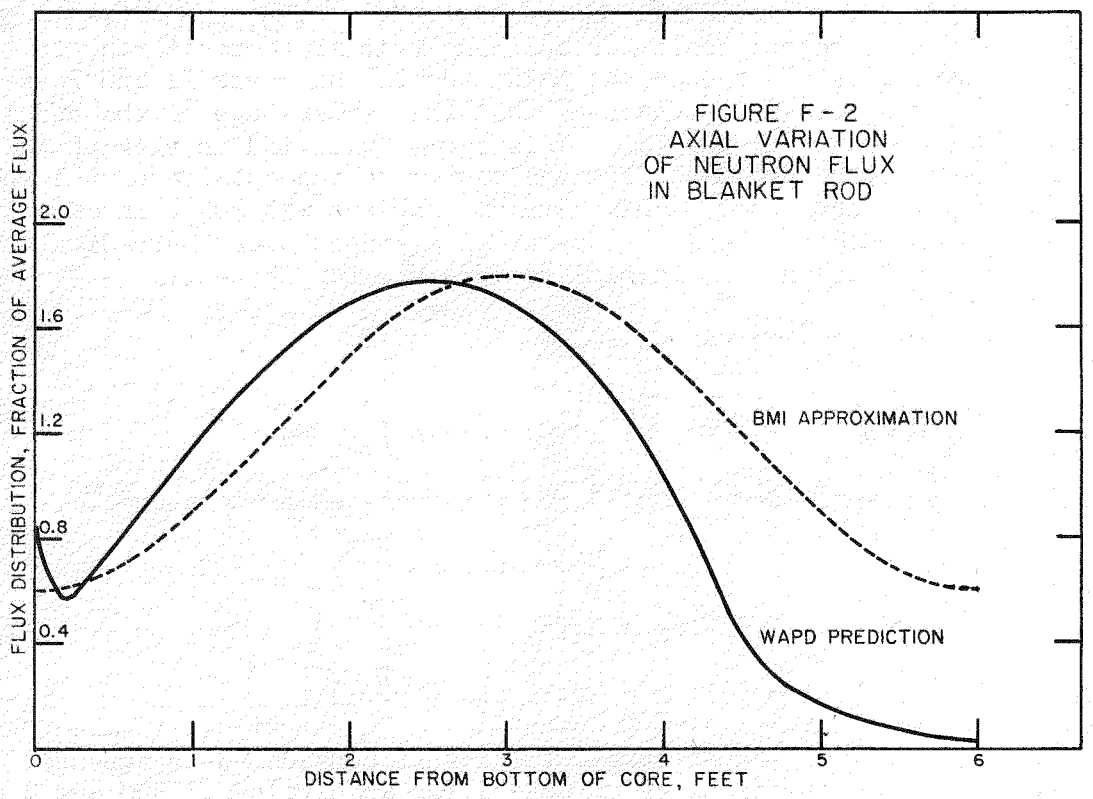

FIGURE F-1 VARIATION OF DECAY HEAT WITH TIME

FIGURE F-2 AXIAL VARIATION OF NEUTRON FLUX IN BLANKET ROD

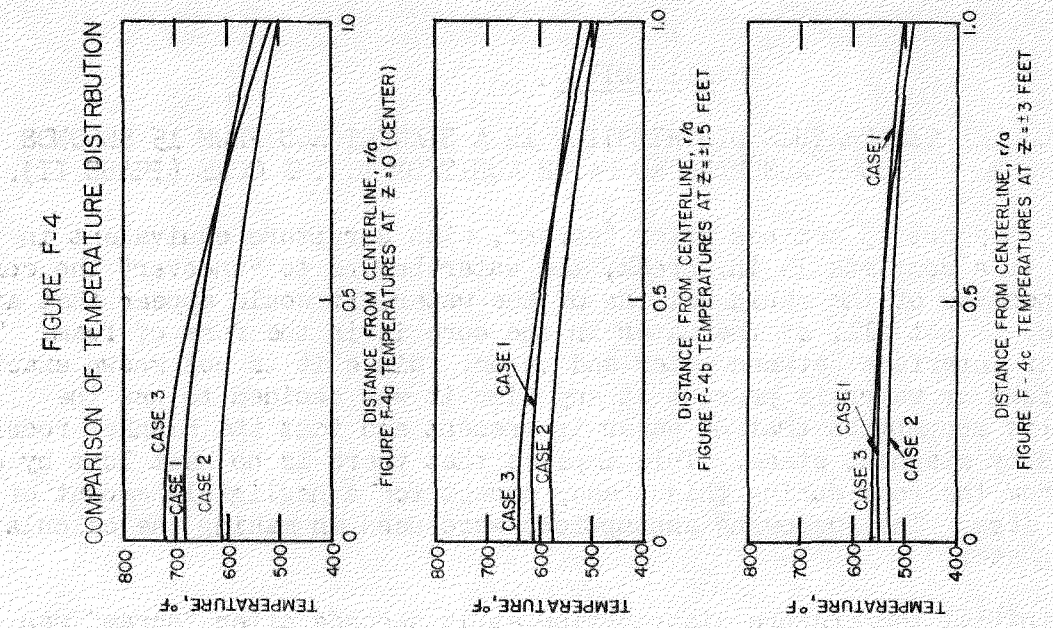

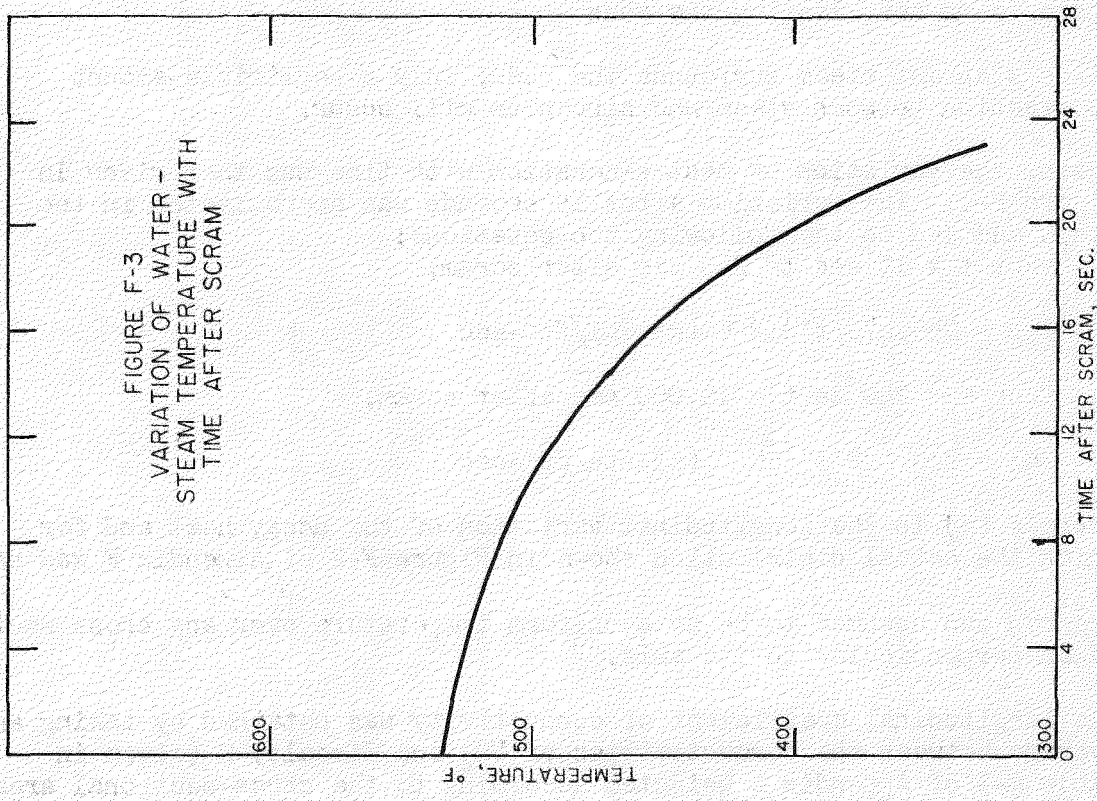

FIGURE F-3 VARIATION OF WATER-STEAM TEMPERATURE WITH TIME AFTER SCRAM

FIGURE F-4 COMPARISON OF TEMPERATURE DISTRIBUTION

APPENDIX G

ANALYSIS OF THE TEMPERATURE DISTRIBUTION IN A BLANKET ROD FROM 15 SECONDS AFTER SCRAM TO MELTDOWN ASSUMING NO WATER ADDITION TO THE CORE (PHASE II).

At about 15 seconds after "scram", with a rupture equivalent in flow area to a complete 15 in. break, the water begins to "uncover" the core. However, because of the rapid boiling of the water, it would appear that at least some, if not all, of the water in the core is in the form of foam. There is no clear interface between water and vapor. Since it is not known exactly how much foam or water is present at any time it was decided to use the conservative assumption that no water is present and that the blanket rods are surrounded by stagnant steam. This implies that there is no heat lost by convection from the rods during this phase, except for a negligible amount of radiation loss. The following assumptions were used in making the calculations for this phase:

(1) The initial temperature distribution at 15 seconds after "scram" was given by Equation F-14 of Appendix F.

$$T\ (z,\ 15) = 570.2 + 41.64 \cos\left(\frac{2\pi z}{L}\right)$$

(2) There is no heat lost by the rods.

(3) Since stagnant steam surrounds the rods, only a negligible amount of reaction between steam and zirconium will occur.

(4) Again, the variation of heat generation with time was that given in Figure F-1. The variation after 15 seconds was approximated in two steps and led to the following two equations:

For t = 15 sec to 240 sec after scram,

$$q_d = 455.475\ t^{-1/3}\ f\ (z)\ \text{Btu/ft}^3\text{-sec.}$$

For t = 240 to t = 10,000 sec after scram,

$$q_d = 288.482\ t^{-1/4}\ f\ (z)\ \text{Btu/ft}^3\text{-sec}$$

where f (z) is the longitudinal variation of the decay heat and for which the actual distribution shown in Figure F-2 of Appendix F was used.

(5) The rod was assumed to be at a uniform temperature over any cross section taken perpendicular to its axis.

(6) The longitudinal coefficient of conductivity was obtained by taking an average between the conductivities of UO_2 and Zircaloy-2 (given in Table A-1 of Appendix A weighted according to the cross-sectional areas

of each material in the blanket rod. (The conductivity or helium is assumed zero). A quadratic equation was fitted to the resulting data giving conductivity as a function of rod temperature. This relation is:

$$k = 1.9150 \times 10^{-3} - 7.3208 \times 10^{-7}\, T_a + 1.6963 \times 10^{-10}\, T_a^2$$

where k is given as Btu/sec-ft^2-F/ft and T_a is the rod temperature at any point in °F.

(7) The heat capacity of the rod ($C_p\rho$) was found from Tables A-2 and A-3 of Appendix A by the same method as that used to obtain thermal conductivity. The expression used for $C_p\rho$ was:

$$C_p\rho = 41.369 + 1.559 \times 10^{-3}\,(T_a + 459.688) - 2.237 \times 10^{6}\,(T_a + 459.688)^{-2}$$

Where $C_p\rho$ is in Btu/ft^3-F and T_a is in °F. (It should be noted that in obtaining this equation the value of C_p of 7.27 was used for Zircaloy-2 below 1583°F as well as above. This leads to less than a 1% error in calculating $C_p\rho$ for temperatures under 1583° F and has the advantage of permitting a single equation to be used for $C_p\rho$ over the whole range of temperatures.)

The differential equation used for Phase II was:

$$\frac{\partial}{\partial t}\left[C_p\rho\, T_a\right] = \frac{\partial}{\partial z}\left[k\,\frac{\partial T_a}{\partial z}\right] + q_d\,(z,\,t) \qquad \text{(G-1)}$$

Since by assumption (7), $C_p\rho$ is a function of T only we can write

$$\frac{\partial\left[C_p\rho\right]}{\partial t} = \frac{\partial\left[C_p\rho\right]}{\partial T_a}\,\frac{\partial T_a}{\partial t} \quad \text{and equation (G-1) becomes:}$$

$$\left[T_a\,\frac{\partial(C_p\rho)}{\partial T_a} + C_p\rho\right]\frac{\partial T_a}{\partial t} = \frac{\partial}{\partial z}\left[k\,\frac{\partial T_a}{\partial z}\right] + q_d(z,t) \qquad \text{(G-2)}$$

The boundary value problem made up of Equation (G-2) and assumptions 1-7 was solved by numerical methods. The rod was divided into 30 equal segments between points z = 0, 0.2, 0.4, ...6.0 feet.

The differential equation, Equation (G-2), was replaced by the difference equation:

$$\left\{T_a\,\frac{\partial\left[C_p\rho\right]}{\partial T_a} + C_p\rho\right\}\frac{T_a\,(z_i,\,t_i + \Delta t) - T_a\,(z_i,\,t_i)}{\Delta z} = \qquad \text{(G-3)}$$

$$= \frac{k(z_i + \Delta z,\, t_i) - k(z_i,\, t_i)}{\Delta z} \cdot \frac{T_a(z_i + \Delta z,\, t_i) - T_a(z_i,\, t_i)}{\Delta z}$$

$$= k(z_i,\, t_i)\,\frac{T_a\,(z_i + \Delta z,\, t_i) - 2T_a(z_i,\, t_i) + T_a\,(z_i - \Delta z,\, t_i)}{\Delta z^2}$$

$$+ q_d\,(z_i,\, t_i)$$

simplifying and solving for $T_a\ (z_i,\ t_i + \Delta t)$ gives:

$$T_a\ (z_i,\ t_i + \Delta t) = \frac{t}{T_a\left[\frac{\partial\ C_p\ \rho}{\partial\ T_a}\right] + C_p\rho}\left\{\begin{array}{l} \dfrac{k(z_i+\Delta z, t_i)}{(\Delta z)^2}\left[T_a(z_i+\Delta z, t_i) - T_a(z_i, t_i)\right] \\ + \dfrac{k(z_i, t_i)}{(\Delta z)^2}\left[T_a(z_i, t_i) - T_a(z_i-\Delta z, t_i)\right] \\ + q_d\ (z_i, t_i) \\ + T_a\ (z_i, t_i) \end{array}\right\} \qquad \text{(G-4)}$$

In this equation:

$k(z,t)$ = the average conductivity of rod (given in assumption 6)

Δz = distance between chosen points of the rod = 0.2 feet

Δt = interval in time

$T_a(z,t)$ = Temperature of the rod at point z, time t.

$q_d(z,t)$ = decay heat generation (given in assumption 4).

$$T_a\ \frac{\partial[C_p\rho]}{\partial T_a} + C_p\rho = 39.648 + 3.183 \times 10^{-3}(T_a + 459.688) + \frac{2.237 \times 10^6 (T_a - 459.688)}{(T_a + 459.688)^3}$$

(This expression is derived from the equation for $C_p\rho$ given in assumption 7)

Using equation G-4, the temperatures in the rod at the selected points as a function of time were calculated on the IBM 650 Electronic computer in the following manner:

Beginning at the point (z_o, t_o), $(z_o = 0, t_o = 15$ sec), Equation G-4 was used to calculate the temperature at the point $(z_o,\ t_o + \Delta t)$. (Here, the points (z_o, t_o), $(z_o,\ t_o + \Delta t)$ are points in the space-time region.) Then temperatures at the points $(z_i,\ t_o + t)$, $(i = 1,2,\ldots 30)$, were calculated in order. When the temperature at the point $(z_{30}, t + \Delta t)$ was found, the temperatures at the next time were calculated, beginning again with the first point and using the temperatures calculated for time $t_o + \Delta t$. This process was then repeated as long as necessary. In this way, beginning with the initial temperature and moving forward step wise with respect to time, the temperatures at the points of the rod were determined as functions of time.

It should be pointed out that in calculating the temperature at the point $(z_o, t_i + \Delta t)$, use was made of temperatures at the points (z_i, t_i) and (z_{-1}, t_i). However, since the point (z_o, t_o) is at one end of the rod the point (z_{-1}, t_o) lies outside the rod. A fictitious temperature was assigned to the point in the following manner. Since it was assumed that the rod was everywhere insulated, it follows that the gradient at the point (z_o, t_i) is zero. This can be approximated either by setting the temperatures at (z_o, t_i) and (z, t_i) equal to one another or by setting the temperature at the point (z_{-1}, t_i) equal to the temperature at the point (z_o, t_i). It was decided to use the latter method since it was easier to fit into the automatic machine method of calculation used. The same relation holds at the other end of the rod between points (z_{29}, t_i), (z_{30}, t_i), and the fictitious point (z_{31}, t_i).

Some system had to be used in choosing the size of Δt in going from one time to the next Instead of choosing Δt constant for all time, it was decided to choose a Δt_{i+1} at time t_i such that the largest rod temperature change in going from time t_{i-1} to t_i would have been less than 30°F, had Δt_{i+1} been used. This insured that the temperature changes were not significantly greater than 30°F during any time interval. Again, this method was chosen as corresponding better to the capabilities of the computing machine.

With the foregoing assumptions, calculations were run until the hottest spot on the rod reached the melting point of zirconium. This occurred at 18 min 31 sec after scram at a point 3.4 ft from the top of the rod.

Figure G-1 shows the temperature distribution in the rod at 15 sec, 5 min, 10 min, 15 min, and 18 min 31 sec after scram.

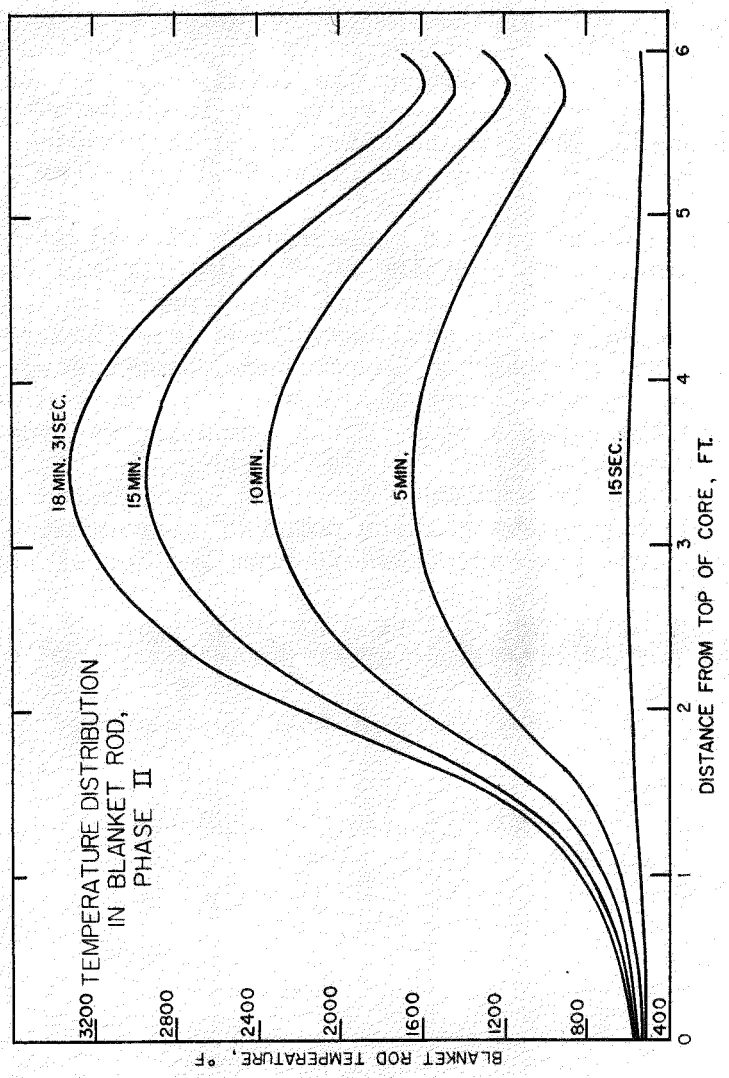

FIGURE G-1
TEMPERATURE DISTRIBUTION IN BLANKET ROD, PHASE II

APPENDIX H

ANALYSIS OF THE TEMPERATURE DISTRIBUTION IN A BLANKET ROD FROM 26 SEC AFTER "SCRAM" TO MELTDOWN ASSUMING WATER ADDED TO THE CORE (PHASE III)

In this phase it is assumed that a certain amount of water, in the form of steam, is added to the core. The corresponding heating effects of a $Zr-H_2O$ reaction (if it occurs) are taken into account, as well as the cooling effects of steam convection. By varying the rate of water (or steam) supply to the core (from an unspecified source) the minimum water requirements for core cooling are determined.

Beginning at about 26 seconds after Scram during Phase II, it is possible to inject water into the core and start Phase III. With the exception of areas around the water inlets, the water will begin filling the interstices between the assemblies. As the water hits the hot jacket surrounding the assemblies, some of it will evaporate, and the steam will pass through the assemblies, entering at the top and leaving at the bottom. It is assumed that decay heat generation in the outer row of rods in a blanket assembly is available for evaporation of the water in the interstices. This amounts to about 1/3 of the total decay heat generated by the assembly. Since there will be a certain amount of heat transfer between the steam and the rod and since there will be steam available for reaction when the rod becomes hot enough, these effects must be taken into account in the calculation of temperatures in the rod. This results in a much more complicated problem, which will now be discussed.

The following nomenclature will be used through this Appendix:

z = distance from top of core (feet)

t = time after scram (sec)

$T_a(z,t)$ = temperature of blanket rod (^oF)

$T_g(z,t)$ = temperature of gas stream (^oF)

A_g = cross-sectional area of steam channel (ft^2)

A = cross-sectional area of rod (ft^2)

$C_p\rho(T_a)$ = average heat capacity of the rod ($Btu/ft^3 - {}^oF$)

$C_g(T_g)$ = heat capacity of the gas (Btu/lb mole-^oF)

$C_s(T_g)$ = heat capacity of steam (Btu/lb mole-^oF)

$C_{H_2}(T_g)$ = heat capacity of hydrogen (Btu/lb mole-^oF)

$\rho_g(T_g)$ = density of gas (lb mole/ft^3)

$q_d(z,t)$ = decay heat generation (Btu/ft^3-sec)

y = amount of Zirconium reacted (lb moles/ft^2)

$y'(T_a,y)$ = rate of Zr-H_2O reaction (lb moles/ft^2-sec)

$\Delta H_r(T_a)$ = heat of reaction (Btu/lb mole)

$q_r(T_a,y) = \Delta H_r y'$ = rate of reaction heat generation (Btu/ft^2-sec)

k = average longitudinal thermal conductivity (Btu/ft^2-^oF/ft)

$W_i(t)$ = inlet velocity of gas stream (moles/sec)

$W_g(W_i,T_a)$ = velocity of gas stream (moles/sec)

M = mole fraction of hydrogen in gas stream (moles/mole)

h = heat transfer coefficient blanket rod to gas stream (Btu/ft^2-sec^oF)

The following are the equations for this problem:

Heat balance for the blanket rod

$$1)\ \frac{\partial}{\partial t}\left[AC_p\rho T_a\right] = \frac{\partial\left[k\,T_a/\partial z\right]}{\partial z} - 2\pi ah(T_a-T_g) + 4\pi ay'(T_g C_s - T_a C_{H_2}) + Aq_d + 2\pi aq_r$$

Heat balance for the gas stream

$$2)\ \frac{\partial}{\partial t}\left[A_g C_g \rho_g T_g\right] = \frac{\partial}{\partial z}\left[C_g W_g T_g\right] + 2\pi ah\,(T_a-T_g) - 4\pi ay'(T_g C_s - T_a C_{H_2})$$

Material balance for the gas stream

$$3)\ \frac{\partial}{\partial t}\left[A_g C_g M\right] = 4\pi ay' - \frac{\partial}{\partial z}\left[W_g M\right]$$

$$4)\ A_g\,\frac{\partial \rho_g}{\partial t} = -\frac{\partial W_g}{\partial z}$$

Combining Equations (3) and (4) gives

(5) $$A_g \rho_g \frac{\partial M}{\partial t} = 4\pi a y' = W_g \frac{\partial M}{\partial z}$$

Combining Equations (2) and (4) gives

(6) $$A_g \rho_g \frac{\partial [C_g T_g]}{\partial t} = 2\pi a h \left[T_a - T_g\right] - W_g \frac{\partial [C_g T_g]}{\partial z} = 4\pi a y' \left[T_g C_s - T_a C_{H_2}\right]$$

Now

(7) $$C_g = C_s (1-M) + M C_{H_2}$$

so that

$$\frac{\partial [C_g T_g]}{\partial t} = C_g \frac{\partial T_g}{\partial t} + T_g \left[(C_{H_2} - C_s) \frac{\partial M}{\partial t} + (1-M) \frac{\partial C_s}{\partial t} + M \frac{\partial C_{H_2}}{\partial t}\right]$$

$$\frac{\partial [C_g T_g]}{\partial z} = C_g \frac{\partial T_g}{\partial z} + T_g \left[(C_{H_2} - C_s) \frac{\partial M}{\partial z} + (1-M) \frac{\partial C_s}{\partial z} + M \frac{\partial C_{H_2}}{\partial z}\right]$$

(8) Substituting these expressions in (6) and using (5) gives

$$A_g \rho_g \left[C_g \frac{\partial T_g}{\partial t} + T_g (1-M) \frac{\partial C_s}{\partial t} + T_g M \frac{\partial C_{H_2}}{\partial t}\right] = 2\pi a h (T_a - T_g) - 4\pi a y' T_g (C_{H_2} - C_s)$$
$$- 4\pi a y' (T_g C_s - T_a C_{H_2}) - W_g \left[C_g \frac{\partial T_g}{\partial z} + T_g (1-M) \frac{\partial C_s}{\partial z} + T_g M \frac{\partial C_{H_2}}{\partial z}\right]$$

Now since C_s and C_{H_2} are functions of T_g only we can write

$$\frac{\partial C_s}{\partial z} = \frac{\partial C_s}{\partial T_g} \cdot \frac{\partial T_g}{\partial z}\ ; \quad \frac{\partial C_{H_2}}{\partial z} = \frac{\partial C_{H_2}}{\partial T_g} \cdot \frac{\partial T_g}{\partial z}$$

Substituting these expressions in Equation (8) and using Equation (7) gives

(9) $$A_g \rho_g \left[(C_s + T_g \frac{\partial C_s}{\partial T_g})(1-M) + M(C_{H_2} + T_g \frac{\partial C_{H_2}}{\partial T_g})\right] \frac{\partial T_g}{\partial t} = \left[2\pi a h + 4\pi a y' C_{H_2}\right] (T_a - T_g)$$
$$- W_g \left[(1-M)\ C_s + T_g \frac{\partial C_s}{\partial T_g}\right.$$
$$\left. + M(C_{H_2} + T_g \frac{\partial C_{H_2}}{\partial T_g})\right] \frac{\partial T_g}{\partial z}$$

We now define the function $\psi(T_g,M)$ as

$$\psi(T_g,M) = (1-M)\left(C_s+T_g\frac{\partial C_s}{\partial T_g}\right)+ M\left(C_{H_2}+T_g\frac{\partial C_{H_2}}{\partial T_g}\right)$$

Substituting this expression in Equation (9) gives finally

$$\psi A_g\rho_g\frac{\partial T_g}{\partial t} = 2\pi a(T_a-T_g)(h-2y'C_{H_2}) - W_g\psi\frac{\partial T_g}{\partial z} \tag{10}$$

Again, since $C_p\rho$ is a function of Ta only, we can write Equation (1) as:

$$\left(Ta\frac{\partial C_p\rho}{\partial T_a}+C_p\rho\right)\frac{\partial T_a}{\partial t} = \frac{\partial\left[K\frac{\partial T_a}{\partial z}\right]}{\partial z} + Aq_d+2\pi aq_r-2\pi ah(T_g-T_g)+4\pi ay'(T_gC_s-T_aC_{H_2}) \tag{11}$$

Further, since ρ_g is a function of T_g only we rewrite Equation (4) as

$$\frac{\partial W_g}{\partial z} = -A_g\frac{\partial\rho_g}{\partial T_g}\frac{\partial T_g}{\partial t} \tag{12}$$

Phase III was solved by numerical methods in a manner similar to that used for Phase II. The rod was again divided into thirty equal segments. Equations (11), (10), (5), and (12) were then approximated by the following equations:

$$\left(T_a\frac{\partial\left[C_p\rho\right]}{\partial T_a}+T_a\right)\left[\frac{T_a(z_i,t_i+\Delta t)-T_a(z_i,t_i)}{\Delta t}\right] \tag{13}$$

$$=\left[\frac{k(z_i+\Delta z_i,t_i)-k(z_i,t_i)}{\Delta z}\right]\left[\frac{T_a(z_i+\Delta z_i,T_i)-T_a(z_i,t_i)}{\Delta z}\right]+\frac{2\pi a}{A}q_r(z_i,t_i)$$

$$-\frac{2\pi ah}{A}\left[T_a(z_i,t_i)-T_g(z_i,t_i)\right]+k(z_i,t_i)\left[\frac{T_a(z_i+\Delta z,t_i)-2T_a(z_i,t_i)+T_a(z_i-\Delta z,t_i)}{(\Delta z)^2}\right]$$

$$+4\pi ay'(z_i,t_i)\left[T_g(z_i,t_i)C_s-T_a(z_i,t_i)C_{H_2}\right]+q_d(z_i,t_i)$$

$$A_g\rho_g\left[\frac{T_g(z_i,t_i+\Delta t)-T_g(z_i,t_i)}{\Delta t}\right]= 2\pi a\left[h+2C_{H_2}y'(z_i,t_i)\right]\left[T_a(z_i,t_i)-T_g(z_i,t_i)\right] \tag{14}$$

$$-W_g\psi\left[\frac{T_g(z_i,t_i)-T_g(z_i-\Delta z,t_i)}{\Delta z}\right]$$

$$(15)\qquad A_g\rho_g\left[\frac{M(z_i,t_i+\Delta t)-M(z_i,t_i)}{\Delta t}\right] = 4\pi a y'(z_i,t_i)-W_g(z_i,t_i)\left[\frac{M(z_i,t_i)-M(z_i-\Delta z,t_i)}{\Delta z}\right]$$

$$(16)\qquad \frac{W_g(z_i+\Delta z,t_i)-W_g(z_i,t_i)}{\Delta z} = -A\frac{\partial\rho_g}{\partial T_g}\left[\frac{T_g(z_i,t_i+\Delta t)-T_g(z_i,t_i)}{\Delta t}\right]$$

Now let $z_i+\Delta z = z_{i+1}$, $z_i-\Delta z = z_{i-1}$, $t_i+\Delta t = t_{i+1}$.

solving Equation (13) for $T_a(z_i,t_{i+1})$ and simplifying gives:

$$(17)\quad T_a(z_i,t_{i+1}) = \frac{\Delta t}{T_a\frac{\partial[C_p\rho]}{\partial T_a}+C_p\rho}\left\{\begin{array}{l} R(z_{i+1}t_i)-R(z_i,t_i)-2\pi ah\left[T_a(z_it_i)-T_g(z_it_i)\right] \\ +4\pi ay'\left[C_sT_g(z_i,t_i)-C_{H_2}T_a(z_i,t_i)\right] \\ +q_d(z_i,t_i)+\frac{2\pi aq_r}{A}\quad(z_i,t_i) \end{array}\right\}$$

$$+T_a(z_i,t_i)$$

Where:

$$R(z_i,t_i) = \frac{k(z_i,t_i)}{(\Delta z)^2}\left[T_a(z_{i+1},t_i)-T_a(z_{i-1},t_i)\right]$$

and:

$$R(z_{i+1},t_i) = \frac{k(z_{i+1},t_i)}{(\Delta z)^2}\left[T_a(z_{i+1},t_i)-T_a(z_i,t_i)\right]$$

solving Equation (14) for $T_g(z_i,t_{i+1})$ gives:

$$(18)\qquad T_g(z_iT_{i+1}) = \frac{\Delta t}{A_g\rho_g}\left\{\begin{array}{l} 2\pi a\left[h+2C_{H_2}y'(z_i,t_i)\right]\left[T_a(z_i,t_i)-T_g(z_i,t_i)\right] \\ -\frac{W_g(z_i,t_i)}{\Delta z}\,T_g(z_i,t_i)-T_g(z_{i-1},t_i) \end{array}\right\}+T_g(z_i,t_i)$$

solving Equation (15) for $M(z_i,t_{i+1})$ gives:

$$(19)\quad M(z_i,t_{i+1}) = M(z_i,t_i) + \frac{\Delta t}{A_g \rho_g}\left\{4\pi a y'(z_i,t_i) - \frac{W_g(z_i,t_i)}{\Delta z}\left[M(z_{i+1},t_i)-M(z_i,t_i)\right]\right\}$$

solving equation (16) for $W_g(z_{i+1},t_i)$ gives finally

$$(20)\quad W_g(z_{i+1},t_i) = W_g(z_i,t_i) - \frac{\Delta z}{\Delta t} A_g \frac{\partial \rho_g}{\partial T_g}\left[T_g(z_i,t_{i+1})-T_g(z_i,t_i)\right]$$

Equations (17) through (20) will be used in the solution of Phase III.

Certain additional assumption had to be made in order to complete the definition of the boundary value problem and to permit the calculation of the values of various quantities appearing in the four equations above.

These assumptions follow:

(1) The initial temperature distribution for Phase III at 26 seconds after scram was that calculated in Phase II and is shown in Figure No. 1.

(2) The decay heat generation $q_d(z_i,t_i)$ was the same as in Assumption 4, of Appendix G.

(3) Assumption 5 of Appendix G also was assumed to hold here.

(4) The longitudinal coefficient of thermal conductivity for the rod was the same as that given in Assumption 6 of Appendix G.

(5) The heat capacity of the rod was the same as that given in Assumption 7 of Appendix G.

(6) The reaction rate was given by the following equation which was fitted to the experimental data obtained at Battelle:

$$y'(z_i,t_i) = \frac{1.1829 \times 10^{-4} \exp\left[\frac{-30.800}{T_a + 459.688}\right]}{y(z_i,t_i)}$$

where

$$y'(z_i,t_i) = y(z_i,26) + \int_{26}^{t_i} y'(z_i,t)dt$$

In the numerical calculation, $y(z_i,t_{i+1})$ was obtained from the expression:

$$y(z_i,t_{i+1}) = y(z_i,t_i) + y(z_i,t_i)\Delta t$$

It was assumed that at 21 sec, y = 0.000032 lb moles Zr/ft^2 at all points of the blanket rod.

(7) A_g is 0.00059069 ft^2

(8) In calculating ρ_g the ideal gas law was assumed. The gas pressure was assumed to be 50 psi so that ρ_g is given by

$$\rho_g = \frac{4.66}{T_g + 459.688} \text{ lb-moles/ft}^3$$

A constant of 4.356 was inadvertently used instead of the 4.66 value. This had a negligible effect on the results since the density term is unimportant.

(9) ΔH_r is given in Table A-4 of Appendix A. A linear equation fitted to this data gives ΔH_r as:

$$\Delta H_r = 263{,}135 - 5.34\ T_a \text{ (Btu/lb-mole Zr reacted)}$$

By mistake, the equation used in the calculations was

$\Delta H_r = 268{,}135 + 5.34\ T_a$. This gives a heat of reaction which is high by 15% at 3000°F. This, of course, would then give conservative results.

(10) W_i, in accord with the remarks given at the beginning of this Appendix, was given as:

For 15 sec to 240 sec.

$$W_i = 3.6278 \times 10^{-8}\ t^{-1/3} \text{ lb-moles/sec}$$

For 240 sec to 10,000 sec

$$W_i = 2.2977 \times 10^{-5}\ t^{-1/4} \text{ lb-moles/sec}$$

(11) The equations for C_s and C_{H_2} are given in Table A-3 of Appendix A. These are:

$$C_s = 7.17 + 1.422 \times 10^{-3}\ (T_g + 459.688) + 0.25 \times 10^5\ (T_g + 459.688)^{-2}$$

$$C_{H_2} = 6.52 + 0.433 \times 10^{-3}\ (T_g + 459.688) + 0.389 \times 10^5\ (T_g + 459.688)^{-2}$$

(12) The heat transfer coefficient h was given by the equation:

$$\frac{hD_g}{k_g} = (0.76)(0.023)\left(\frac{D_g W_g}{A_g \mu_g}\right)^{0.8}\left(\frac{C_g \mu_g}{k_g}\right)^{0.4}$$

where D_g is the equivalent Diameter . . (0.0218 ft for this problem), μ_g is the viscosity of the gas stream, and k_g is the thermal conductivity of the gas stream. Since A_g is also a known constant = 0.00059069 ft^2, h can be written as:

$$h = 14.380\, W_g^{0.8} C_g^{0.4}\left(\frac{k_g^{0.6}}{\mu_g^{0.4}}\right)$$

The quantity C_g is obtained from Equation (7) and assumption (11). W_g is obtained from Equation (20).

The quantities k_g and μ_g were obtained from a paper by Bernard W. Gamson (1). In this paper, the reduced conductivity, k_r, and viscosity, μ_r, of a gas mixture are determined as functions of the reduced temperature, T_r, of the mixture and are reproduced here in Table H-1. (The reduced conductivity, viscosity, and temperature of a gas are found by dividing the conductivity, viscosity, and temperature by the respective values of the gas at its critical point). Thus, if the critical temperature of a hydrogen-steam mixture is assumed given by a linear interpolation between the critical temperatures of hydrogen and steam, the reduced temperature of the mixture can be written as:

(21) $$T_r = \frac{T_g + 459.688}{(1165.14)(1-M)+59.76M} = \frac{T_g + 549.688}{1165.14-1105.38M}$$

where the critical temperature of steam is 1165.14°R and that of hydrogen is 59.76°R. The ratio $\frac{k_r^{0.6}}{\mu_r^{0.4}}$ was calculated from the data of Table H-1, and an equation was derived giving this ratio as a function of the reduced temperature. This expression was found to be:

(22) $$k_r^{0.6}/\mu_r^{0.4} = \frac{-0.10532 + 2.7204\, T_r + 0.17840\, T_r^2}{1 + 2.5283\, T_r + 0.07153\, T_r^2}$$

The ratio $k_c^{0.6}/\mu_c^{0.4}$ was correlated with the mole fraction M to give:

(1) Table 1 of "A Generalized Thermal Conductivity Correlation for Gas State" by Bernard W. Gamson, Chemical Engineering Progress, February 1949, p. 156.

TABLE H-1. REDUCED THERMAL CONDUCTIVITIES AND REDUCED VISCOSITIES AT LOW PRESSURES

T_r	k_r (1)	μ_r (1)
0.4	0.100	0.177
0.5	0.145	0.221
0.6	0.193	0.268
0.7	0.242	0.315
0.8	0.290	0.357
1.0	0.385	0.450
1.2	0.488	0.540
1.4	0.577	0.620
1.6	0.662	0.700
2.0	0.839	0.85
2.5	1.02	1.02
3.0	1.19	1.17
4.0	1.51	1.42
5.0	1.81	1.63
6.0	2.10	1.85
8.0	2.60	2.23
10.0	3.10	2.60
20	5.30	4.08
30	7.25	5.37
40	9.0	6.45

(23) $$k_c^{0.6}/\mu_c^{0.4} = 1.6123 - 0.25227M - 0.12494M^2$$

Then $k_g^{0.6}/\mu_g^{0.4}$ is given by:

(24) $$k_g^{0.6}/\mu_g^{0.4} = \frac{k_r^{0.6}}{\mu_r^{0.4}} \cdot \frac{k_c^{0.6}}{\mu_c^{0.4}}$$

Thus, if the mole fraction of hydrogen in the gas stream and the temperature of the gas stream are known, Equations (21) through (24) can be

(1) See footnote previous page.

used to find the ratio $k_g^{0.6}/\mu_g^{0.4}$. Additional assumptions used are:

(13) It was assumed that the ends of the rods were insulated. This is a conservative assumption. Thus, in calculating the temperature of the rod at its two end points the same treatment was used here as that used in Phase II (i.e., assuming a fictitious point outside either end at the same temperature as the first interior point).

(14) The inlet temperature of the gas was assumed to be 281°F at all times. (This is the boiling temperature of water at 50 psia).

(15) The mole fraction of hydrogen at the inlet was 0 (i.e., the gas is pure steam).

The same system was used in Phase III for determining the time increments as was used in Phase II.

Once the calculations were begun, it became apparent that the specific heat of the gas was so small that unless the time increments, Δt, were taken extremely small, the change in the gas temperature and the mole fractions using Equations (18) and (19) would be extremely large. Although it would be possible to perform the calculation in this manner, the calculation would take impossibly long.

Thus, it was necessary to develop different procedures for the calculation of T_g and M. This was done in the following way:

Since ρ_g is small compared to other factors in the equations, it is assumed zero in Equations (14) and (15). The resulting equations are:

$$0 = 2\pi a \left[h + 2C_{H_2} y'(z_i,t_i)\right]\left[T_a(z_i,t_i)-T_g(z_i,t_i)\right] - \frac{W_g(z_i,t_i)\psi\left[T_g(z_i,t_i)-T_g(z_{i-1},t_i)\right]}{\Delta z}$$

$$0 = 4\pi a y'(z_i,t_i) - \frac{W_g(z_i,t_i)}{\Delta z}\left[M(z_i,t_i) - M(z_{i-1},t_i)\right]$$

Solving these equations for $T_g(z_i,t_i)$ and $M(z_i,t_i)$ gives:

$$(25)\quad T_g(z_i,t_i) = \left[S_1 T_a(z_i,t_i) + S_2 T_g(z_{i-1},t_i)\right] /(S_1 + S_2)$$

where $S_1 = 2\pi a\left[h + 2C_{H_2}y'(z_i,t_i)\right]$ and $S_2 = W_g(z_i,t_i)\Psi/\Delta z$

$$(26)\quad M(z_i,t_i) = \frac{4\pi a y'(z_i,t_i)\Delta z}{W_g(z_i,t_i)} + M(z_{i-1},t_i)$$

These equations were used in calculating T_g and M, instead of Equations (19) and (20) and permitted much more rapid completion of the problem.

The calculations were again run until the hottest spot reached the melting point of zirconium. This occurred at 18 min, 43 seconds after scram at a point 4.0 feet from the top of the core.

Figure 2 shows the temperature distribution in the rod at 26 seconds, 5 min, 10 min, 15 min, and at 18 min 43 seconds.

Figure 3 shows the distributions of the temperatures in the gas stream at 26 seconds, 5 min, 10 min, 15 min, and at 18 min 43 seconds.

Figure 4 shows the total amount of hydrogen evolved from scram to time t as a function of t.

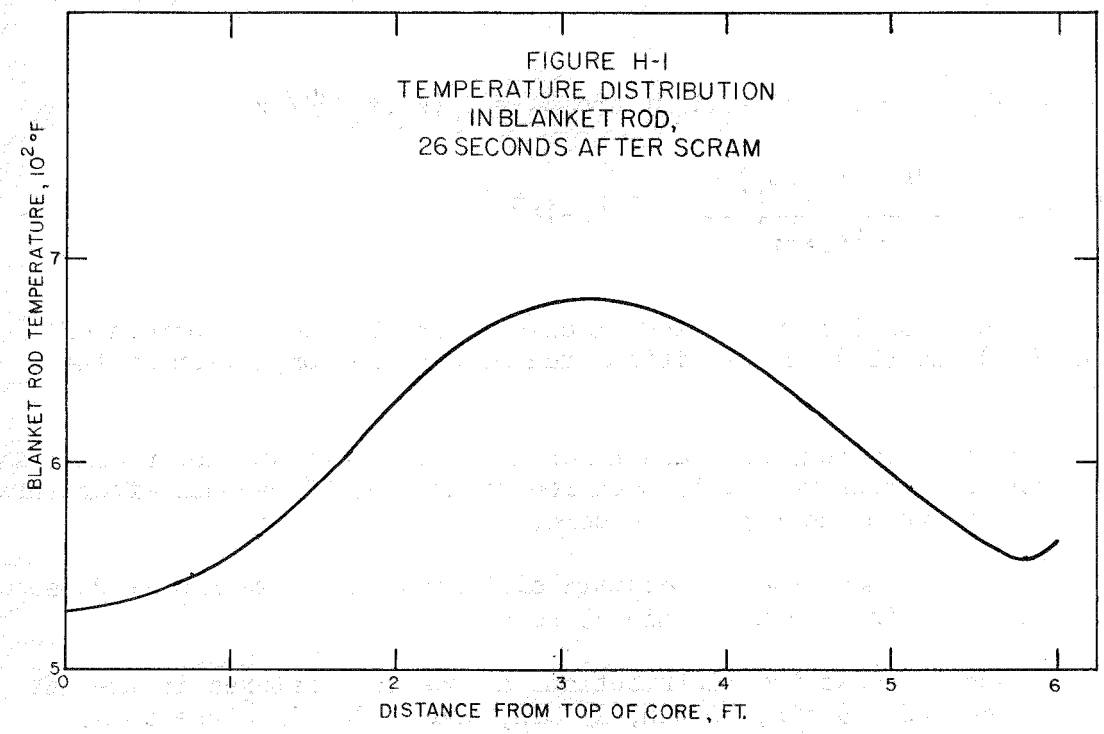

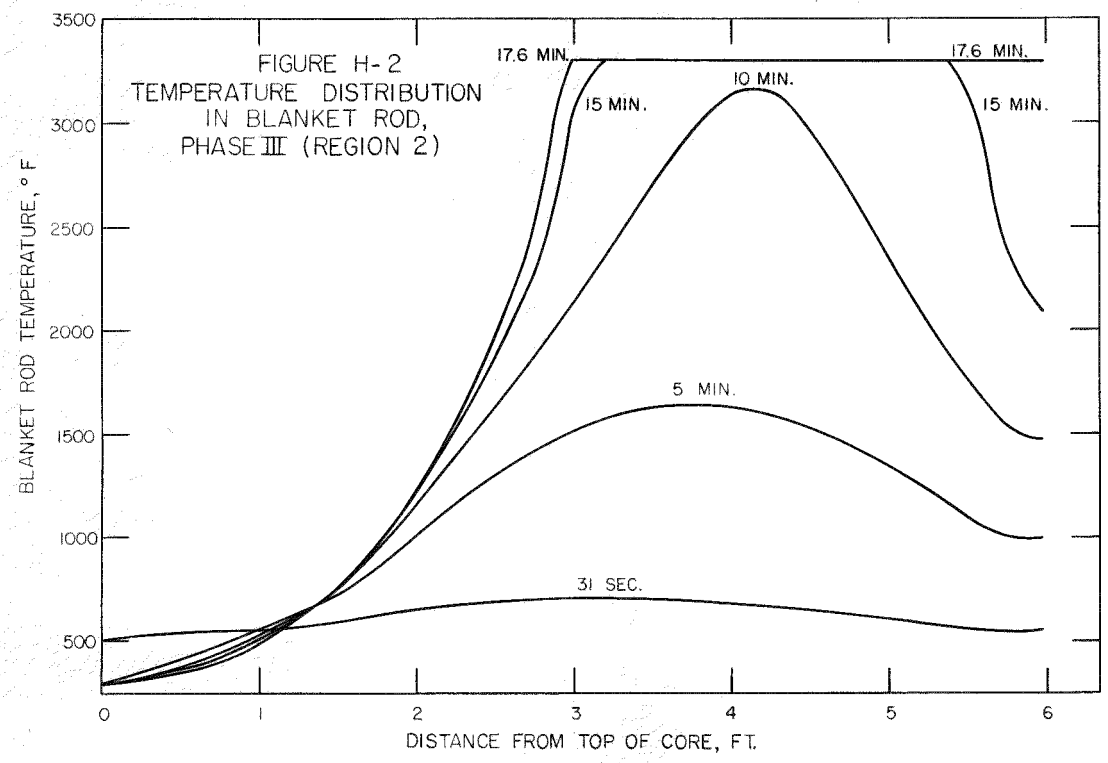

FIGURE H-1 TEMPERATURE DISTRIBUTION IN BLANKET ROD, 26 SECONDS AFTER SCRAM

FIGURE H-2 TEMPERATURE DISTRIBUTION IN BLANKET ROD, PHASE III (REGION 2)

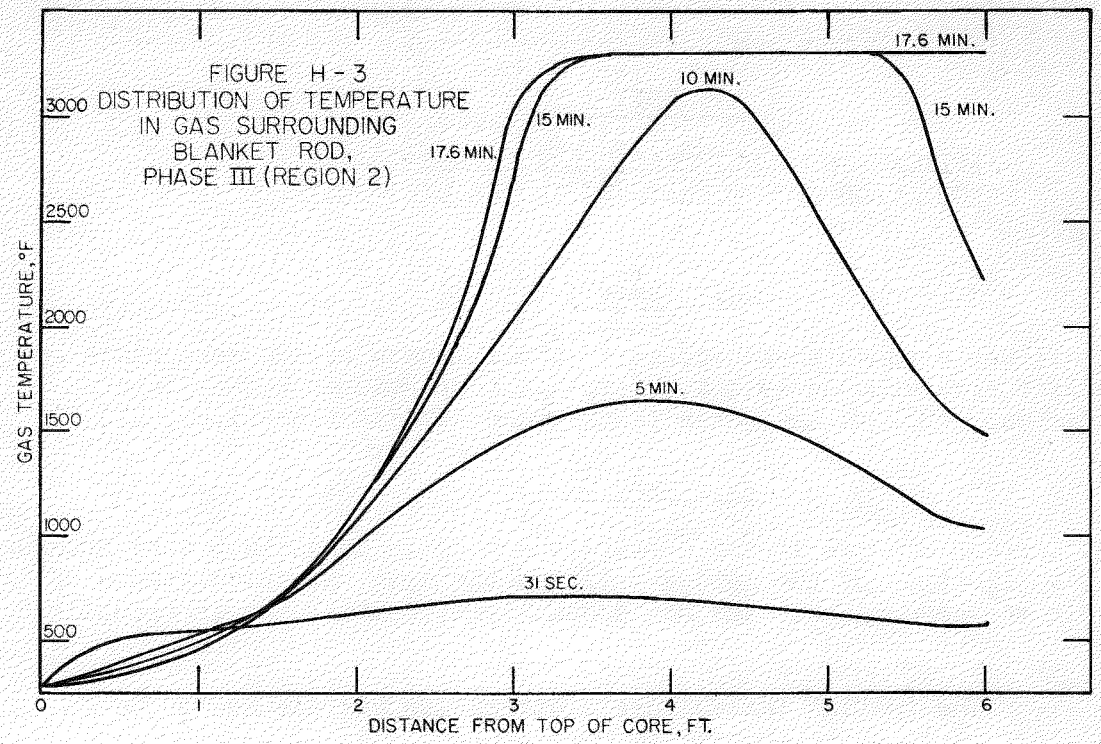

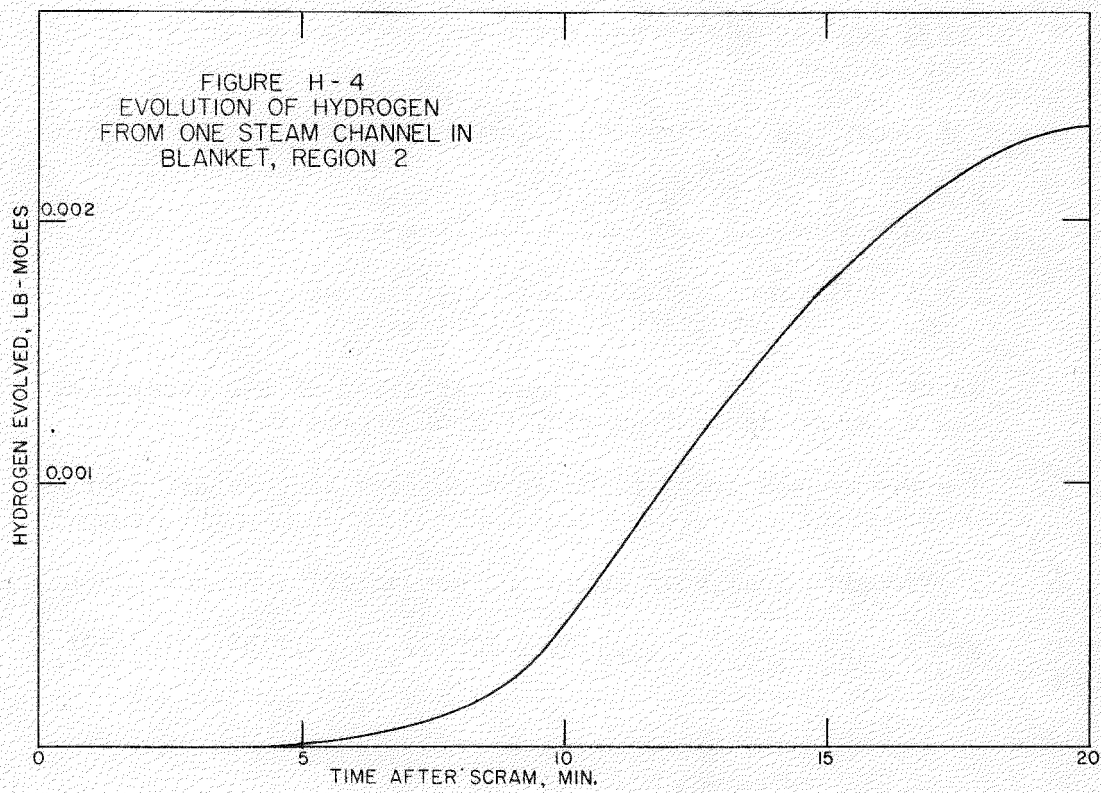

FIGURE H-3 DISTRIBUTION OF TEMPERATURE IN GAS SURROUNDING BLANKET ROD, PHASE III (REGION 2)

FIGURE H-4 EVOLUTION OF HYDROGEN FROM ONE STEAM CHANNEL IN BLANKET (REGION 2)

APPENDIX I

APPLICATION OF MATHEMATICAL ANALYSIS TO THE CALCULATION OF TEMPERATURES IN THE SEED PLATE

A. Phase I

It was assumed that because of the thinness of the seed plate and the large surface area exposed to the water, the temperature in the plate at 15 sec after scram was equal to the water temperature at that time (i.e., 472°F).

B. Phase II

Certain changes in the assumptions made in Appendix G were necessary to permit application of the method outlined there to the calculations of temperatures in the seed plate. The new assumptions, numbered as in Appendix G, are:

1. The initial temperature distribution was assumed to be 472°F at all points of the plate.

2. There was assumed to be no heat lost by the plates (not changed).

3. There was assumed to be only a negligible amount of reaction (not changed).

4. The decay heat generation is now given by:

   For t = 15 sec to 240 sec after "scram",
   $q_d = 1656.463\ t^{-1/3}\ f(z)$ Btu/ft^3-sec)

   For t = 240 sec to 10,000 sec after "scram",
   $q_d = 1049.146\ t^{-1/4}\ f(z)$ Btu/ft^3-sec

   where f(z) is the longitudinal variation of the decay heat and is again taken from Fig. F-2 of Appendix F.

5. The seed was assumed to be at a uniform temperature over any cross-section taken perpendicular to its axis (not changed).

6. The longitudinal coefficient of conductivity is now given by:

   $$k = 2.2352 \times 10^{-3} + (1.3505 \times 10^{-7})T_a + (3.7348 \times 10^{-11})T_a^2$$

7. The heat capacity of the plate is now given by:

$$C_p \rho = 29.927 + 3.3533 \times 10^{-3} (T_g + 459.688) - 0.2022 \times 10^{6} (T_g + 459.688)^{-2} \text{ for } T_a < 1583\text{F and}$$

$$C_p \rho = 32.70 \text{ for } T_a > 1583 \text{ F}$$

These were the only changes necessary in the discussion presented in Appendix G to make it applicable to the calculation of the temperatures in the seed plate if no water is added to the core.

With these modifications the calculations were run again until the hottest spot on the seed plate reached the melting point of zirconium. This occurred at 3 min 25 sec after "scram" at a point 3.8 ft from the top of the seed.

Figure I-1 shows the temperature distribution in the seed plate at 15 sec, 1 min, 1-1/2 min, 2 min, 2-1/2 min, 3 min, and 3 min 25 sec after "scram".

C. Phase III

Again, certain changes were necessary in the assumptions made in Appendix H to permit application of the method outlined there to the calculation of temperatures in the seed plate. These new assumptions, numbered as in Appendix H, are:

1. The initial temperature distribution for Phase III at 26 sec after "scram" was that calculated in Phase II and is shown in Fig. I-2

2. The decay heat generation $q_d(z_i, t_i)$ was the same as given in assumption 4 of part B of this Appendix.

3. Assumption 5 part B of this Appendix also holds here.

4. The longitudinal coefficient of thermal conductivity for the seed plat was the same as that given in assumption 6 of part B of this Appendix.

5. The heat capacity of the seed plate was the same as that given in assumption 7 of part B of this Appendix.

6. The reaction rate was unchanged and is given by:

$$y' = \frac{1.1829 \times 10^{-4} \exp\left(\frac{30,800}{-T_a + 459.688}\right)}{y\,(z_i, t_i)}$$

7. A_g is 0.0010781 ft^2

8. ρ_g was unchanged and is given by:

$$\rho_g = \frac{4.66}{T_g + 459.688} \text{ lb-moles/ft}^3$$

9. ΔH_r was unchanged and is given by:

ΔH_r = 263,230-5.34 T_a Btu/lb-mole Zr reacted.

10. W_i is now given by:

26 to 240 sec after "scram"
$W_i = 1.9860 \times 10^{-4}\ t^{-1/3}$ lb-mole/sec

240 to 10,000 sec after "scram"
$W_i = 1.2579 \times 10^{-4}\ t^{-1/4}$ lb-mole/sec

11. The equations for C_s and C_{H_2} were unchanged. These are again:

$$C_a = 7.17 + 1.422 \times 10^{-3} (T_g + 459.688) + 0.259 \times 10^5 (T_g + 459.688)^{-2}$$

$$C_{H_2} = 6.52 + 0.433 \times 10^{-3} (T_g + 459.688) + 0.389 \times 10^5 (T_g + 459.688)^{-2}$$

12. The equation for the heat transfer coefficient h was unchanged. It is:

$$\frac{hD_g}{k_g} = (0.76)(0.023) \left(\frac{D_g W_g}{A_g \mu_g}\right)^{0.8} \left(\frac{C_g \mu_g}{k_g}\right)^{0.4}$$

However, D_g and A_g are now 0.01116 ft and 0.0010781 ft^2 respectively, so that h is now written:

$$h = 10.159\ W_g^{0.8} C_g^{0.4} \frac{k_g^{0.6}}{\mu_g^{0.4}}$$

C_g was unchanged and is given by

$$C_g = (1-M)\ C_s + M C_{H_2}$$

The quantity $\frac{k_g^{0.6}}{\mu_g^{0.4}}$ was unchanged and is given by equations H-21 through H-24 of Appendix H. Assumptions (13) through (15) were unchanged .

With these modifications, calculations were performed to obtain temperatures in the seed plate from 26 sec after "scram" until the hottest point of the seed plate reached the melting point of zirconium. This occurred at 1 min, 35 sec after scram at a point 4.2 ft from the top of the seed plate.

Figure I-3 shows the temperature distribution in the seed plate at 25 sec, 1 min, 1-1/2 min, 2 min, and at 2 min 25 sec after scram.

Figure I-4 shows distribution of the temperatures in the gas stream at 25 sec, 1 min, 1-1/2 min, 2 min, and at 2 min 25 sec after scram.

Figure I-5 shows the total amount of hydrogen evolved from scram to time t as a function of t.

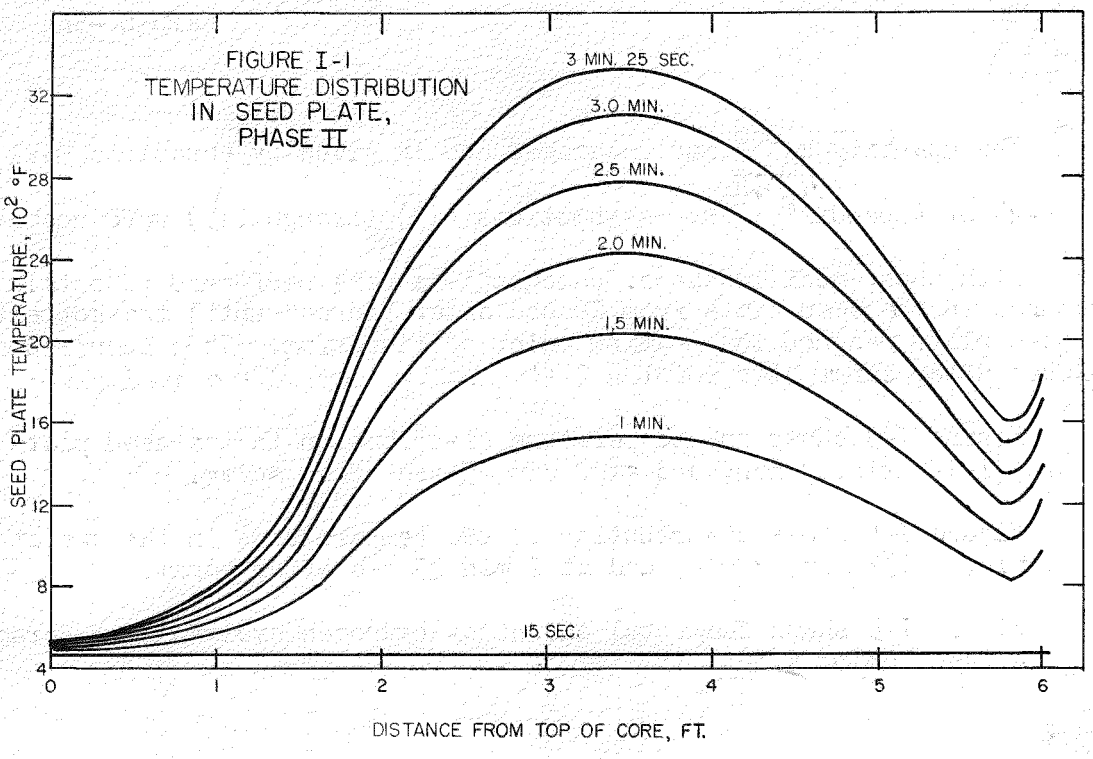

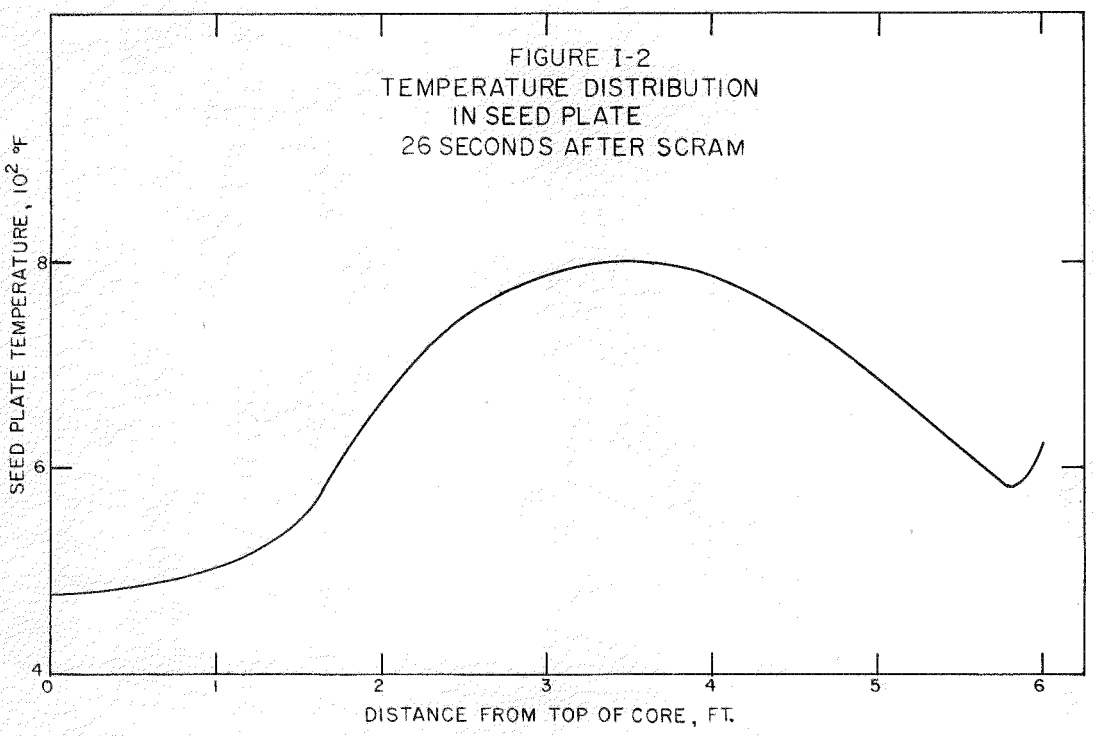

FIGURE I-1 TEMPERATURE DISTRIBUTION IN SEED PLATE, PHASE II

FIGURE I-2 TEMPERATURE DISTRIBUTION IN SEED PLATE 26 SECONDS AFTER SCRAM

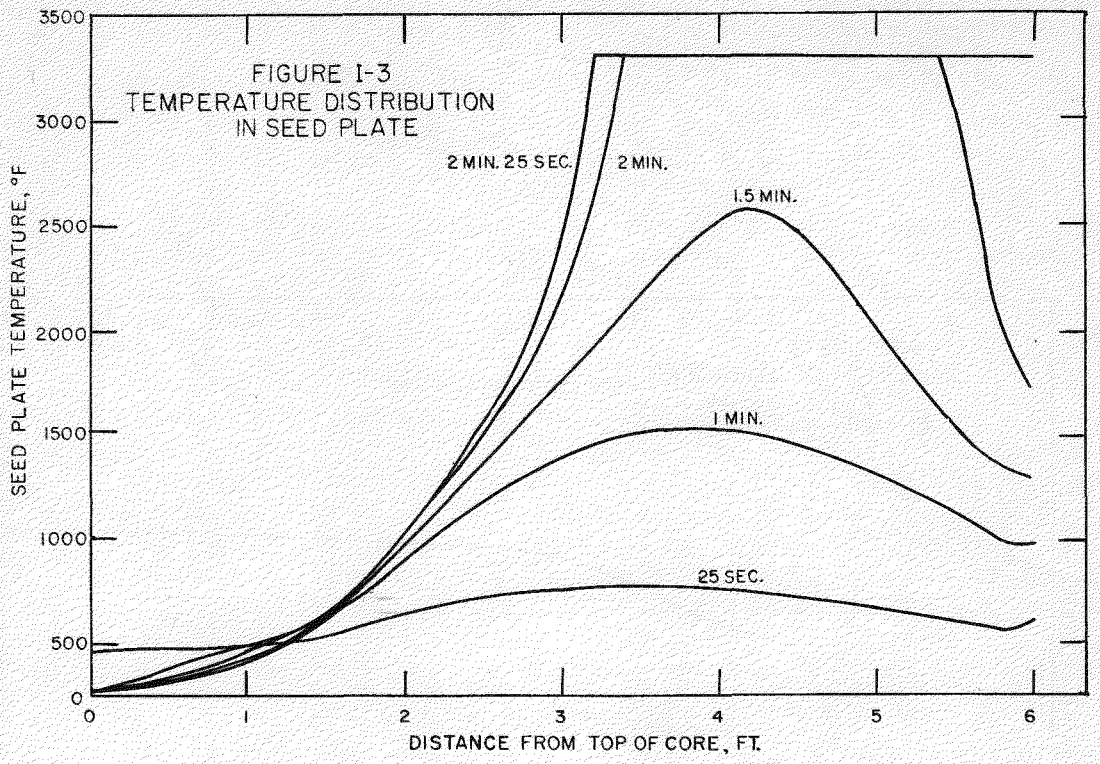

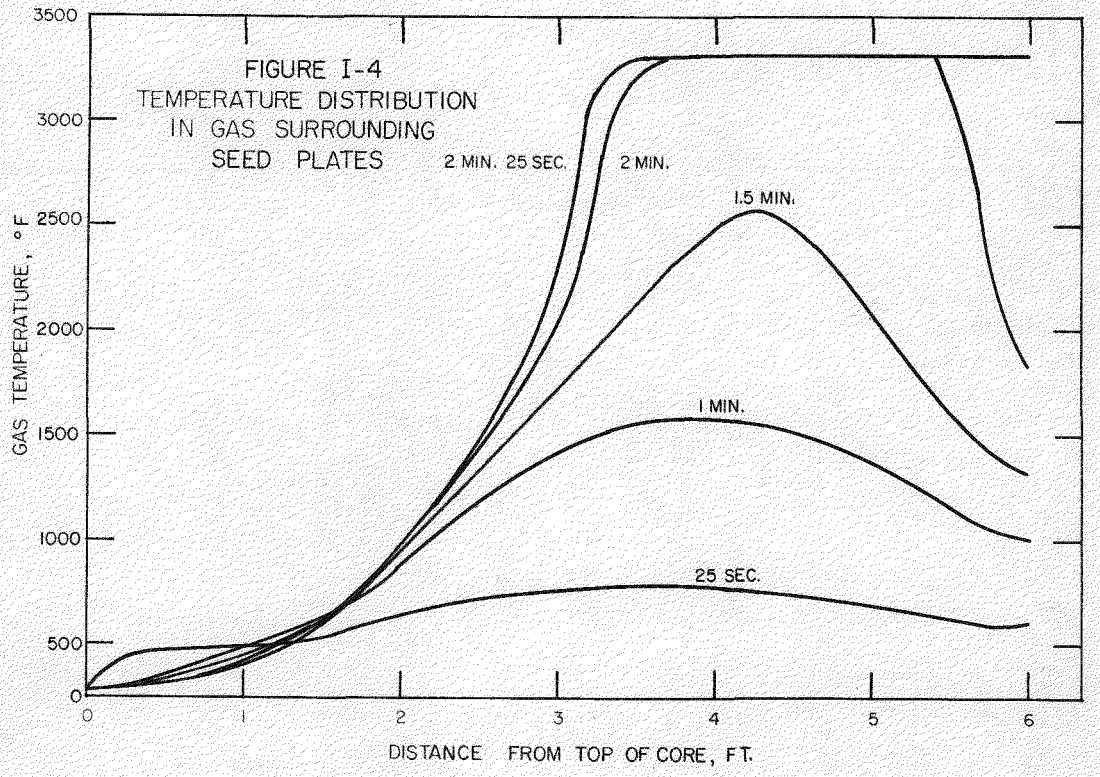

FIGURE I-3 TEMPERATURE DISTRIBUTION IN SEED PLATE, PHASE III

FIGURE I-4 TEMPERATURE DISTRIBUTION IN GAS SURROUNDING SEED PLATES, PHASE III

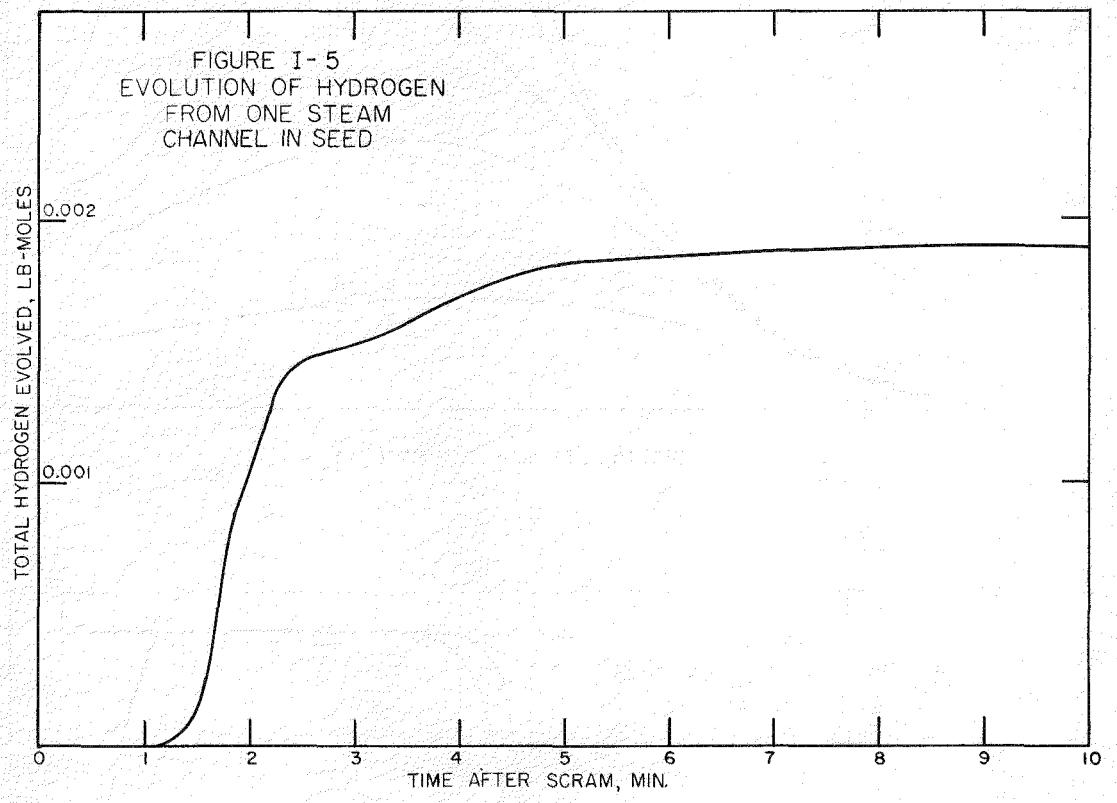

FIGURE I-5
EVOLUTION OF HYDROGEN FROM ONE STEAM CHANNEL IN SEED